On a quantum kinetic linked to the Compton effect - Modelling and 3D simulation of the satellite charge in plasmic environment

Martine Chane-Yook

THESIS

presented at

UNIVERSITY OF PROVENCE, AIX-MARSEILLE I

Ecole doctorale de Mathématiques et Informatique de Marseille

To obtain the title of

DOCTOR

Speciality : Applied Mathematics

Prepared at INRIA Sophia Antipolis, CAIMAN team and at University of Provence

On a kinetic equation linked to the Compton effect. Modelling and 3D simulation of the satellite charge in plasmic environment

by

Martine CHANE-YOOK

Defended on December 1st 2004

JURY

President of the jury	Serge PIPERNO
Reviewer	Kazuo AOKI
Reviewer	Stéphane MISCHLER
Examiner	Sébastien CLERC
Examiner	Olivier GUES
Adviser	Anne NOURI

Acknowledgements

I firstly would like to thank my thesis director, Anne Nouri, for supervising my research work.

I particularly thank Sébastien Clerc for his constant support, his encouragement throughout this research and for supervising my research work.

I am especially grateful to Serge Piperno for following my work daily at INRIA, CAIMAN team.

I gratefully acknowledge the thesis commitee members; Professors Aoki and Mischler for reviewing my manuscript and their constructive comments; Olivier Gues for accepting to belong to my thesis commitee.

Frédéric Poupaud died a few months before defending my thesis. It has been an honour for me to work with him during my thesis. I would like to pay a tribute to him. Many thanks to him for his constant support and his kindness.

Many thanks to Thierry Goudon for his collaboration at the beginning of my thesis.

I would like to thank everybody at ALCATEL SPACE, especially Thierry Dargent.
I also grateful to everybody at INRIA, especially the staff who have been both efficient and friendly. Special thanks to the team CAIMAN members; Nathalie Glinsky-Olivier for her advises. Stéphane Lantéri, Loula Fezoui and Victoritta Dolean for their constant support.

I particularly acknowledge Saïd El Kasmi and Gilles Scarella for their help.

Some friends of CAIMAN team have been with me right from the beginning. That has been the case of Maud Poret, Rudy Hayat, Marc Bernacki, Mondher Ben Jemaa, Hugo Fol and Sabine Barrère.

My deepest gratitude to my best friends Thierry Taïle-Manikom and Fabrice Yode for their constant support and encouragement throughout this thesis.

And finally, I would like to thank my family and my parents for their love and encouragement.

To finish, I would like to thank Patrick for all good things he brings to me in my life.

Contents

Acknowledgements 1

General introduction 7

I On a kinetic equation linked to the Compton effect 15

1 Introduction to the Compton effect 17
- 1.1 A.H. Compton's works . . . 17
- 1.2 Recent works linked to the Compton effect . . . 18
  - 1.2.1 At a physical level . . . 18
  - 1.2.2 At a mathematical level . . . 19

2 The Boltzmann equation 21
- 2.1 Introduction to the Boltzmann equation . . . 21
- 2.2 The Cauchy problem and the asymptotic behaviour of the solutions . . . 25
  - 2.2.1 The classical case in the homogeneous in space case . . . 25
  - 2.2.2 The relativistic non quantum Boltzmann equation . . . 27
    - Global existence for the relativistic Boltzmann equation . 27
    - Existence results and asymptotic behaviour of periodic solutions . . . 29
  - 2.2.3 A quantum relativistic Boltzmann equation . . . 31
  - 2.2.4 A modified Boltzmann equation for Bose-Einstein particles 35

3 Modelling of the studied problem 37
- 3.1 An initial relativistic frame . . . 37
- 3.2 A simplified model linked to the Compton effect . . . 39

4 A priori estimates **45**
4.1 Conservation of the mass 45
4.2 H-theorem 46
4.3 Boundedness of entropy and energy 46
4.4 Mathematical frame 48

5 Main results **49**
5.1 Recent mathematical results 49
5.2 Our results 50
5.3 Proof of Proposition 5.2.1 51

6 Proof of the existence theorem **57**
6.1 Technical bounds on the cross-section h 58
6.2 Existence of a solution to the Cauchy problem 60
6.3 Study of the entropy and boundedness of the energy. 67
6.4 Conclusion. 71

II Modelling and 3D simulation of the satellite charge in plasmic environment **73**

7 The spatial plasma environment **75**
7.1 The plasmas 75
7.1.1 Fundamental quantities in plasma physics 76
The Debye length 76
The Larmor radius 76
7.1.2 Sheath and presheath 77
7.2 The earth magnetosphere 77
7.3 Plasma engines 80

8 Interactions on the surface of a satellite. A first model. **81**
8.1 Physical context and notations 81
8.2 Electrostatic interactions 84
8.3 Reemissions at the surface of the satellite 87
8.3.1 Secondary electron emission 87
8.3.2 Secondary emission for ions 88
8.3.3 Photoemission 88
8.4 Mathematical model of Vlasov-Poisson 88
8.4.1 The system of Vlasov-Poisson 88

8.4.2 Existence and uniqueness results for the Vlasov-Poisson system . . . 90
8.4.3 Dimensionless Vlasov and Poisson equations . . . 90
Dimensionless quantities . . . 90
Passage to the limit in a formal way . . . 92

9 An infinite element method for the resolution of the Laplace equation in an infinite domain 95
9.1 Introduction . . . 95
9.1.1 Variational formulation . . . 96
9.2 Different methods used in problems with infinite domains . . . 97
Robin condition . . . 97
Boundary Element Method (BEM) . . . 98
Infinite element method . . . 98
9.3 A new approach of infinite element . . . 99
9.3.1 Computation of the terms in the elementary stiffness matrix . . . 102
9.4 Numerical results . . . 103
9.4.1 Case of a sphere . . . 104
9.4.2 Case of two sources . . . 107

10 The coupling with the Vlasov equation 111
10.1 The back-trajectories method . . . 111
10.2 Numerical approximation for the ion and the electron currents at the surface of the satellite . . . 114
10.2.1 The ion current . . . 115
10.2.2 The electron current . . . 116

11 Analytical computations of the charge density in the whole space for a sphere 119
11.1 Computations of the electron and ion densities . . . 121
11.1.1 Electron density . . . 121
11.1.2 Trapping case . . . 125
11.1.3 Untrapping case . . . 133
11.2 The Charge density and the asymptotic behaviour . . . 133
11.2.1 Trapping case . . . 135
11.2.2 Untrapping case . . . 137
11.3 Curves . . . 139
11.3.1 Untrapping case . . . 139

11.3.2 Trapping case 140

12 Solution of the stationary Vlasov-Poisson system **143**
12.1 Solution of the Poisson equation 143
12.2 A new approach for the solution of the Poisson equation 144
12.3 Conclusion 148

III General conclusion and perspectives **149**

13 Part 1 **151**
13.1 Description of Bose-Einstein condensates 151
13.2 The first condensate 152
13.3 Bose-Einstein condensates from a mathematical point of view . 152

14 Part 2 **153**

Bibliography **158**

General introduction

The present thesis is made of two parts having together a common point which is the study of kinetic equations. The first part deals with the Compton effect which describes the interaction between photons and electrons. The second part is about the modelling and the simulation of a satellite's charge in the magnetosphere environment. This second part has been realized in partnership with Alcatel space and the research institute INRIA Sophia Antipolis.

First part.

The Compton effect was discovered in 1922 by Arthur Holly Compton. It takes place when high X-ray energy photons collide with electrons. This results in deflections of the particles trajectories. The incident photons emerge with longer wavelength due to some loss of energy during the interactions. These deflections, together with a change of wavelength, are known as the Compton effect.

A.H. Compton found that, due to the scattering of X-rays from free electrons, the wavelength of the scattered rays is measurably longer than that of the incident light. His discovery was of special importance in 1922, when quantum mechanics was debated.

X-rays are particularly used in scientific research field, in industries and in medical field.

Many physicists like G. Cooper ([15]), H. Dreicer ([19]), A.S. Kompaneets ([28]), Ya.B. Zel'Dovich and Levich ([40]) were interested in the Compton effect.
R.E. Caflish and C.D. Levermore ([11]), M. Escobedo and S. Mischler ([23], [22]) studied the Compton effect at a mathematical level.

The first objective of this thesis is to study the Compton effect at a kinetic level. We consider a homogeneous quantum kinetic equation, established by par M. Escobedo, S. Mischler and M.A. Valle ([23]), describing the interaction between the light and an electron bath. We prove existence of solutions to the equation obtained when keeping the highest-order term with respect to the speed of light in the relativistic model. The electrons are assumed to be at nonrelativistic equilibrium, and the scattering of photons by electrons is studied.

The kernel in the collision integral presents a strong singularity at energy zero. As in [22] already, the boundedness of the photons entropy is not sufficient for the photon distribution function to stay in an L^1 frame. Measure solutions for the photon distribution functions are expected. Moreover, the singularity in the collision kernel brings severe restrictions; existence results to the Cauchy problem are obtained for initial data small enough and locally in time. The entropy of the solution is controlled.

First, we recall the context in which the Compton effect has been obtained and the consequences of its discovery in 1922 in the quantum mechanics field. We also recall the results obtained on it by physicists and mathematicians.

Secondly, we introduce the mathematical model. We explain in detail the derivation stated by M. Escobedo, S. Mischler and M.A. Valle ([23]) for a homogeneous quantum kinetic equation describing the Compton effect.

Next, we establish a priori estimates as well as the existence result of an entropy solution for the Cauchy problem.
The main difficulty to state the existence theorem comes from singularities met in the collision kernel. To avoid these singularities, we have determined a necessary condition in order to give a sense to the weak formulation for the Cauchy problem and established an appropriate functional frame to the resolution of the problem.
This work refers to [12].

Second part.

Since satellites have been sent in space, breakdowns have happened frequently. Some studies ([34]) show that the particles coming from the solar wind interact with the surfaces of the satellite, modify the charge of the satellite and

can cause electric discharges which can partially disable the working of the spacecrafts. For example, a breakdown happened in 1997 to the TV satellite Telstar. The satellite was disconnected from the earth for several days.
We also cite the satellite Turksat launched by Alcatel Space in 1996. The breakdown was caused by a resident electrostatic discharge and the consequence was only a cutting-off during one hour for the emissions.
In 1998, the satellite Radio/TV Galaxy *IV* launched by Hughes S & C was hit by an intense flow of protons which caused important damages.

Satellites on the geostationary orbit are in the magnetosphere at an altitude of 36000 km.
The earth is surrounded by a magnetic field extending beyond thousands of km in space, composing the magnetosphere. Like a comet, the magnetosphere resembles a water droplet facing the sun. It is a barrier to the solar wind. Only two zones lead the ionized particles from the sun to the North and the South poles of the magnetosphere.

Satellites in flight are in a mixture of free and charged particles. The magnetosphere is a collisionless plasma. Ions and electrons coming from this plasma interact with the surfaces of the satellite, so that they modify the electrostatic charge of the surfaces.

These particles come firstly from the solar wind. Indeed, the slow particles ejected by the sun accumulate static electricity on the external parts of the satellite. When an electrical discharge happens, incident currents achieve to get into the electronic system, so that the spacecraft is ruined. The fast particles come into the satellite, and directly charge the electronic system.

These particles come secondly from the combustible ejected by plasma engines (which also modify the electrostatic environment around the satellite). These engines release a Xenon gas. The fast particles are ejected to infinity and do not come back to the satellite. However, the slow particles can come back to the surface of the satellite.

Two main phenomena happen : the charge phenomenon which is not dangerous for the device and the electrical discharge phenomenon which is important and dangerous for the satellite because the currents can damage the electronic system and also the solar panels.
In this thesis, we are only interested in the electrostatic charge phenomenon

of a satellite on a geostationnary orbit.

In order to understand these interactions between the plasma and the satellite, we have constructed a numerical model for the simulation of the charge on a satellite on a geostationnary orbit. Ions and electrons must be described following a kinetic approach. The evolution of their distribution functions are ruled by the Vlasov-Poisson system.
O. Chanrion ([13]) studied this problem in a two-dimensional axisymmetric frame.
The second objective of this thesis is to study the Vlasov-Poisson system in a three-dimensional frame.
One particle method for the Vlasov equation resolution is coupled with a finite and an infinite elements method for the Poisson equation resolution.
This work leads to the article [14].

First, we recall the physical context as well as the notations introduced in [13]. Next, we introduce the Vlasov-Poisson system in $3D$.
Secondly, we start to solve the Poisson equation by using the finite elements method with infinite elements on the boundary of the computational domain. As the Debye length is larger than the dimension of the satellite in the magnetospheric plasma, the space charge is neglected.
The current of ions and electrons received by the surfaces of the satellite are obtained by the backtrajectories algorithm, which consists in following back the trajectories of the particles which impact the surface of the satellite. However, the computation of the space charge around the satellite shows that it cannot be neglected. So, we have to take into account the space charge in the resolution of the Poisson equation.

The present thesis is made of two parts having together a common point which is the study of kinetic equations. The first part deals with the Compton effect which describes the interaction between photons and electrons. The second part is about the modelling and the simulation of a satellite charge in the magnetosphere environment. This second part has been realized in partnership with Alcatel space and the research institute INRIA Sophia Antipolis.

First part.

The Compton effect was discovered in 1922 by Arthur Holly Compton. It takes place when high X-ray energy photons collide with electrons. This results in deflections of the particle trajectories. The incident photons emerge

with longer wavelength due to some loss of energy during the interactions. These deflections, together with a change of wavelength, are known as the Compton effect.

A.H. Compton found that, due to the scattering of X-rays from free electrons, the wavelength of the scattered rays is measurably longer than that of the incident light. His discovery was of special importance in 1922, when quantum mechanics was debated.

X-rays are particularly used in scientific research field, in industries and in medical field.

Many physicists like G. Cooper ([15]), H. Dreicer ([19]), A.S. Kompaneets ([28]), Ya.B. Zel'Dovich and Levich ([40]) were interested in the Compton effect.
R.E. Caflish and C.D. Levermore ([11]), M. Escobedo and S. Mischler ([23], [22]) studied the Compton effect at a mathematical level.

The first objective of this thesis is to study the Compton effect at a kinetic level. We consider a homogeneous quantum kinetic equation, established by par M. Escobedo, S. Mischler and M.A. Valle ([23]), describing the interaction between the light and an electron bath. We prove existence of solutions to the equation obtained when keeping the highest-order term with respect to the speed of light in the relativistic model. The electrons are assumed to be at nonrelativistic equilibrium, and the scattering of photons by electrons is studied.

The kernel in the collision integral presents a strong singularity at energy zero. As in [22] already, the boundedness of the photons entropy is not sufficient for the photon distribution function to stay in an L^1 frame. Measure solutions for the photon distribution functions are expected. Moreover, the singularity in the collision kernel brings severe restrictions; existence results to the Cauchy problem are obtained for initial data small enough and locally in time. The entropy of the solution is controlled.

First, we recall the context in which the Compton effect has been obtained and the consequences of its discovery in 1922 in the quantum mechanics field. We also recall the results obtained on it by physicists and mathematicians.

Secondly, we introduce the mathematical model. We explain in detail the derivation stated by M. Escobedo, S. Mischler and M.A. Valle ([23]) for a homogeneous quantum kinetic equation describing the Compton effect.

Next, we establish a priori estimates as well as the existence result of an entropy solution for the Cauchy problem.
The main difficulty to state the existence theorem comes from singularities met in the collision kernel. To avoid these singularities, we have determined a necessary condition in order to give a sense to the weak formulation for the Cauchy problem and established an appropriate functional frame to the resolution of the problem.
This work refers to [12].

Second part.

Since satellites have been sent in space, breakdowns have happened frequently. Some studies ([34]) show that the particles coming from the solar wind interact with the surfaces of the satellite, modify the charge of the satellite and can cause electric discharges which can partially disable the working of the spacecrafts. For example, a breakdown happened in 1994 to the satellite Anik-E1. The breakdown was caused by an internal electrostatic discharge.
We also cite the TV satellite Telstar breakdown happended in 1997. The satellite was disconnected from the earth for several days.
In 1998, the satellite Radio/TV Galaxy IV launched by Hughes S & C was hit by an intense flow of protons which caused important damages.

Satellites in geostationary orbit are in the magnetosphere at an altitude of 36000 km.
The earth is surrounded by a magnetic field extending beyond thousands of km in space, composing the magnetosphere. Like a comet, the magnetosphere resembles a water droplet facing the sun. It is a barrier to the solar wind. Only two zones lead the ionized particles from the sun to the North and the South poles of the magnetosphere.

Satellites in flight are in a mixture of free and charged particles. The magnetosphere is a collisionless plasma. Ions and electrons coming from this plasma interact with the surfaces of the satellite, so that they modify the electrostatic charge of the surfaces.

These particles come firstly from the solar wind. Indeed, the slow particles ejected by the sun accumulate static electricity on the external parts of the satellite. When an electrical discharge happens, incident currents achieve to get into the electronic system, so that the spacecraft is ruined. The fast particles come into the satellite, and directly charge the electronic system.

These particles come secondly from the combustible ejected by plasma engines (which also modify the electrostatic environment around the satellite). These engines release a Xenon gas. The fast particles are ejected to infinity and do not come back to the satellite. However, the slow particles can come back to the surface of the satellite.

Two main phenomena happen : the discharge phenomenon which is a local phenomenon and the charge phenomenon which is a global phenomenon and a consequence of the discharge.
In this thesis, we are only interested in the electrostatic charge phenomenon of a satellite in geostationary orbit.

In order to understand these interactions between the plasma and the satellite, we have constructed a numerical model for the simulation of the satellite charge in geostationary orbit. Ions and electrons must be described following a kinetic approach. The evolution of their distribution functions are ruled by the Vlasov equation which is coupled with the Poisson equation.
O. Chanrion ([13]) studied this problem in a two-dimensional axisymmetric frame.
The second objective of this thesis is to study the Vlasov-Poisson system in a three-dimensional frame in the whole space.
One particle method for the Vlasov equation resolution is coupled with a finite and an infinite element method for the Poisson equation resolution.
This work leads to the article [14].

First, we recall the physical context as well as the notations introduced in [13]. Next, we introduce the Vlasov-Poisson system in a three-dimensional frame.
In geostationary orbit, as the Debye length is larger than the dimension of the satellite, we usually neglect the space charge. So, we start to solve the Laplace equation in the whole space for any geometry of the satellite by using the finite/infinite element method.

The current of ions and electrons received by the surfaces of the satellite are obtained by the back-trajectories algorithm, which consists in following back the trajectories of the particles which impact the surface of the satellite.

In order to understand why we neglect the space charge ρ , we are interested in the charge around a sphere. In this case, we are able to compute an analytical expression of ρ. Its asymptotic behaviour at infinity leads to the asymptotic behaviour of the potential at infinity.

Next, we solve the Vlasov-Poisson system in the whole space by taking into account the asymptotic behaviour of ρ at infinity. The main result is that the space charge can be neglected in the region around the satellite which is called the sheath and ρ is not negligible at infinity, i.e. in the presheath.

Part I

On a kinetic equation linked to the Compton effect

Chapter 1

Introduction to the Compton effect

Contents

1.1 A.H. Compton's works 17

1.2 Recent works linked to the Compton effect 18

1.2.1 At a physical level 18

1.2.2 At a mathematical level 19

1.1 A.H. Compton's works

In 1916, A.H. Compton began his studies in the field of X-rays. He developed a theory on the intensity of X-ray reflection from crystals as a means of studying the arrangement of electrons and atoms. In 1918, he started a study of X-ray scattering. This led, in 1922, to his discovery of the increase of wavelenght of X-rays due to scattering of the incident radiation by free electrons, which implies that the scattered quanta have less energy than the quanta of the orignal beam. This effect, nowadays is known as the Compton effect.
Picture 1.1 illustrates the Compton effect.

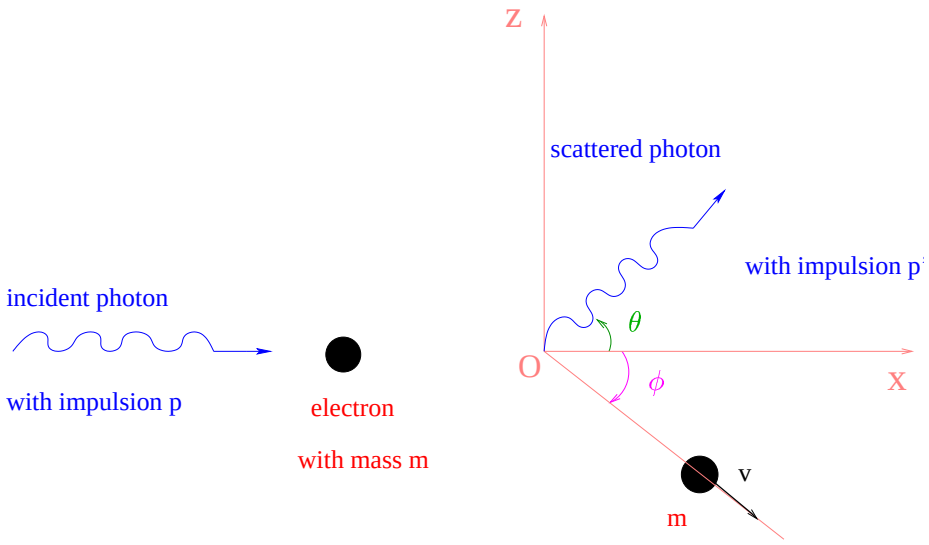

Figure 1.1: The Compton effect

1.2 Recent works linked to the Compton effect

1.2.1 At a physical level

In various astronomical events, such as supernovae, the analysis of time-varying phenomena in highly ionized gases is of importance. In particular, for the problem of nonequilibrium radiation transport in such systems, the Compton scattering with electrons may often be the dominant mechanism for energy transfer. Since the scattering integral for this process is extremely complicated, one often uses a Fokker-Planck approximation. This consists in expanding the collision integral in powers of the energy transfer through second order. It is a valid approximation as long as the energy transfer per Compton scattering is small.
In the limit of low electron temperatures and photon energies, this is not only a valid approximation but is also very convenient, since the resulting equation may be expressed in a simple analytical form. This will be called the non-relativistic limit, though in reality it is correct through second order in v/c and $h\nu/mc^2$. On the basis of an analysis of the energy exchange rate between Maxwellian electrons and Planckian photons, the nonrelativistic approximation is seen to break down for electron temperatures greater than 20 keV. The Fokker-Planck approximation, however, is still valid beyond these limits; the

errors above result mainly from the nonrelativistic development.
G. Cooper in [15] remedies this by deriving the Fokker-Planck equation for an isotropic photon distribution without recourse to a nonrelativistic approximation. He shows that only the average energy exchange per unit time need be known. In the case of arbitrary electron temperatures and photon energies, this quantity must be evaluated numerically since the integrals are far too complicated to be known analytically.

H. Dreicer presented in [19] an extension of the Boltzmann equation for plasmas, including interactions between the electrons and the photons which populate the radiation field. He introduced a simple kinetic theory describing relaxation phenomena. These interactions are handled by means of simple electron-photon collision terms, which can be expected to coincide with the results of a more rigorous theory whenever collective effects become unimportant. Single-photon emission and absorption as well as Compton scattering are treated. The equation derived is specialized to the case of electrons orbiting in a steady magnetic field, and is used to follow the relaxation of a test electron which is interacting with a thermal radiation field via the emission and absorption of cyclotron radiation.

A.S. Kompaneets studied in [28] the role of the Compton effect in the establishement of equilibrium between quanta and electrons in the nonrelativistic approximation.

Ya. B. Zel'Dovich and V. Levich studied in [40] the process of equilibrium of radiation in a totally ionized plasma. By solving the kinetic equation it is shown that in the absence of absorption the photons undergo Bose condensation. The process depends essentially on the form of the initial distribution.

More recently, R.H. Steuwer explained in [38] the Compton effect and its transition to quantum mechanics.

1.2.2 At a mathematical level

R.E. Caflish and C.D. Levermore studied in [11] the Fokker-Planck equation for the Compton scattering in a homogeneous plasma. The entropy function was used to find the equilibrium distributions. When emission-absorption is neglected, this is used to find equilibrium distributions that have the form of a Planckian distribution plus a δ function at zero photon energy. For distribu-

tions below the Planckian distribution and with emission-absorption included, a rate of entropy increase is obtained. Numerical results confirm these conclusions.

More recently, M. Escobedo and S. Mischler stated in [22] existence results for a quantum kinetic equation with a simplified regular and bounded kernel. They studied the asymptotic behaviour of the solutions, and showed that the photon distribution function may condensate at zero energy, asymptotically in time.

Chapter 2

The Boltzmann equation

Contents

2.1 Introduction to the Boltzmann equation 21

2.2 The Cauchy problem and the asymptotic behaviour of the solutions 25

2.2.1 The classical case in the homogeneous in space case 25

2.2.2 The relativistic non quantum Boltzmann equation . 27

2.2.3 A quantum relativistic Boltzmann equation 31

2.2.4 A modified Boltzmann equation for Bose-Einstein particles 35

2.1 Introduction to the Boltzmann equation

In this section, we briefly recall the general properties of the Boltzmann equation introduced by M. Escobedo, S. Mischler and M.A. Valle in [23].

We are interested in a gas composed of identical and indiscernible particles. When two particles with respective impulsions p and p_* in $\mathbb{R}^3$ encounter each other, they collide and get p' and p'_* as new impulsions after the collision. We assume that the collisions are elastic, which means that the total impulsion and the total energy of the system constituted by pair of particles are conserved. More precisely, denoting by $\mathcal{E}(p)$ the energy of one particle with impulsion p,

we assume that

$$\begin{cases} p' + p'_* = p + p_* \\ \mathcal{E}(p') + \mathcal{E}(p'_*) = \mathcal{E}(p) + \mathcal{E}(p_*) \end{cases} \tag{2.1}$$

We denote by $\mathcal{C}$ the set of all 4-upplets of particles $(p, p_*, p', p'_*) \in \mathbb{R}^{12}$ satisfying equations (2.1). The expression of the energy $\mathcal{E}(p)$ of a particle in function of its impulsion p depends on the type of the particle :

$$\begin{cases} \mathcal{E}(p) = \mathcal{E}_{nr}(p) = \dfrac{|p|^2}{2m} \text{ for a non relativistic particle,} \\ \mathcal{E}(p) = \mathcal{E}_r(p) = \gamma\, mc^2;\ \gamma = \sqrt{1 + \dfrac{|p|^2}{c^2 m^2}} \text{ for a relativistic particle,} \\ \mathcal{E}(p) = \mathcal{E}_{ph}(p) = c|p| \text{ for massless particle such as a photon or a neutrino.} \end{cases} \tag{2.2}$$

Here, m stands for the mass of the particle and c for the speed of light. The velocity $v = v(p)$ of a particle with impulsion p is defined by $v(p) = \nabla_p \mathcal{E}(p)$, and therefore

$$\begin{cases} v(p) = v_{nr}(p) = \dfrac{p}{m} \text{ for a non relativistic particle,} \\ v(p) = v_r(p) = \dfrac{p}{m\gamma} \text{ for a relativistic particle,} \\ v(p) = v_{ph}(p) = c\dfrac{p}{|p|} \text{ for a photon.} \end{cases} \tag{2.3}$$

Now, we consider a gas constituted by a very large number (of order the Avogadro number $A \sim 10^{23}/mol$) of a single specie of identical and indiscernible particles. The very large number of particles makes impossible (or irrelevant) the description of the gas by the knowledge of the position and impulsion (x, p) (with x in a domain $\Omega \subset \mathbb{R}^3$ and $p \in \mathbb{R}^3$) of all the particles of the gas. We introduce the gas density distribution $f(t, x, p) \geq 0$ of particles which at time $t \geq 0$ have position $x \in \mathbb{R}^3$ and impulsion $p \in \mathbb{R}^3$. Under the hypothesis of molecular chaos and of low density of the gas, so that particles collide by pairs (no collision between three or more particles occurs). L. Boltzmann established that the evolution of a classical (i.e. not quantum nor relativistic) gas distribution function f must satisfy

$$\begin{cases} \dfrac{\partial f}{\partial t} + v(p).\nabla_x f = Q(f(t, x, .))(p) \\ f(0, .) = f_{in}, \end{cases} \tag{2.4}$$

where $f_{in} \geq 0$ is the initial gas distribution and $Q(f)$ is the so-called Boltzmann collision kernel which describes how particles change their impulsions due to the collisions.

In all the following we make the assumption that the density f only depends on the impulsion. The collision term $Q(f)$ may then be expressed in all the cases described above as :

$$\begin{cases} Q(f)(p) = \int\int\int_{\mathbb{R}^9} W(p, p_*, p', p'_*)\ q(f)\ dp_*\ dp'\ dp'_*, \\ q(f) \equiv q(f)(p, p_*, p', p'_*) = [f' f'_*(1+\tau f)(1+\tau f_*) - f f_*(1+\tau f')(1+\tau f'_*)] \\ \tau \in \{-1, 0, 1\}, \end{cases} \tag{2.5}$$

where as usually, we denote by

$$f = f(p),\ f_* = f(p_*),\ f' = f(p'),\ f'_* = f(p'_*),$$

and W is a non negative measure called transition rate, which may be written as

$$W(p, p_*, p', p'_*) = w(p, p_*, p', p'_*)\delta(p + p_* - p' - p'_*)\delta(\mathcal{E}(p) + \mathcal{E}(p_*) - \mathcal{E}(p') - \mathcal{E}(p'_*)), \tag{2.6}$$

where δ represents the Dirac measure. The quantity $W\ dp'\ dp'_*$ is the transition probability per unit volume and per unit time that two particles with incoming momenta $p,\ p_*$ are scattered with outgoing momenta $p,\ p'_*$.

The character relativistic or not, of the particles is taken into account in the expression of the energy of the particle $\mathcal{E}(p)$ given by (2.3). The quantum effect appears in the expression of the term $q(f)$. The case of classical particles corresponds to the choice $\tau = 0$. The quantum effect is taken into account by choosing $\tau = \pm 1$. It actually corresponds to the values $\tau = \pm\bar{h}$, where $\bar{h}$ is the Planck constant. But for the sake of simplicity we have chosen this constant to be one all along this work. Therefore, one takes $\tau = 1$ in the case of a gas of Bosons and $\tau = -1$ for a gas of Fermions.

The function w is strongly related with the differential cross section σ and is determined by the kind of interactions considered between the particles. Here, we take $w = 1$. Since the particles are indistinguishable, the collisions are reversible and the two interacting particles form a closed physical system,

so that

$$\begin{cases} W(p,p_*,p',p'_*) = W(p_*,p,p',p'_*) = W(p',p'_*,p,p_*) \\ + \text{ Galilean invariance (in the non relativistic case)} \\ \quad + \text{ Lorentz invariance (in the relativistic case).} \end{cases} \tag{2.7}$$

The Boltzmann equation reads then very similarly, formally at least, in all the different contexts : classical, quantum and relativistic. In particular some of the fundamental physically relevant properties of the solutions f may be established formally in all the cases in the same way : conservation of the total number of particles, mean impulse and total energy; existence of an "entropy" which increases along the trajectories (Boltzmann's H-theorem). For any $\Psi = \Psi(p)$, symmetries (2.7) imply the fundamental and elementary identity

$$\int_{\mathbb{R}^3} Q(f)\ \Psi\ dp = \frac{1}{4} \int\int\int\int_{\mathbb{R}^{12}} W(p,p_*,p',p'_*)\ q(f)\ (\Psi+\Psi_*-\Psi'-\Psi'_*)\ dp\ dp_* dp' dp'_*. \tag{2.8}$$

By taking $\Psi(p) = 1,\ p,\ p^2$, the conservation of mass, momentum and energy of a solution f to the Boltzmann equation (2.4) is obtained

$$\frac{d}{dt} \int_{\mathbb{R}^3} f(t,p) \begin{pmatrix} 1 \\ p \\ \mathcal{E}(p) \end{pmatrix} dp = \int_{\mathbb{R}^3} Q(f) \begin{pmatrix} 1 \\ p \\ \mathcal{E}(p) \end{pmatrix} dp = 0, \tag{2.9}$$

so that

$$\int_{\mathbb{R}^3} f(t,p) \begin{pmatrix} 1 \\ p \\ \mathcal{E}(p) \end{pmatrix} dp = \int_{\mathbb{R}^3} f_{in}(p) \begin{pmatrix} 1 \\ p \\ \mathcal{E}(p) \end{pmatrix} dp. \tag{2.10}$$

The entropy functional is defined by

$$H(f) := \int_{\mathbb{R}^3} h(f(p))\ dp, \quad h(f) = \tau^{-1}(1+\tau f)\ln(1+\tau f) - f \ln f. \tag{2.11}$$

Taking in (2.8) $\Psi = h'(f) = \ln(1+\tau f) - \ln f$, we get

$$\int_{\mathbb{R}^3} Q(f)\ h'(f)\ dp = \frac{1}{4}\ D(f), \tag{2.12}$$

with

$$\begin{aligned} D(f) &= \int\int\int\int_{\mathbb{R}^4} W\ e(f)\ dp\ dp_* dp' dp'_*, \\ e(f) &= j(ff_*\ (1+\tau f')(1+\tau f'_*), f'f'_*\ (1+\tau f)(1+\tau f_*), \\ j(s,t) &= (t-s)\ (\ln t - \ln s) \geq 0. \end{aligned} \tag{2.13}$$

We deduce the $H-$theorem : the entropy is increasing along the trajectories, i.e.

$$\frac{d}{dt}H(f(t,.)) = \frac{1}{4}D(f) \geq 0. \tag{2.14}$$

The main qualitative characteristics of f are described by the two properties that are the conservations (2.9) and the increasing entropy (2.14). It is therefore natural to expect that as t tends to ∞ the function f converges to a function f_∞ which realizes the maximum of the entropy $H(f)$ under the momentum constraint (2.10).

2.2 The Cauchy problem and the asymptotic behaviour of the solutions

2.2.1 The classical case in the homogeneous in space case

Let us consider the case $\tau = 0$, i.e. the classical Boltzmann equation, which has been the most studied in the mathematical and physical litterature.
In this section, we recall the main existence and uniqueness results on the homogeneous Boltzmann equation with cutoff ([39]).

The Boltzmann equation writes as

$$\begin{cases} \partial_t F + v.\nabla_x F = Q(F,F), \quad t>0, v \in T^3,\ x \in \mathbb{R}^3, \\ F(x,v,0) = F_0(x,v), \end{cases} \tag{2.15}$$

describing the evolution of a dilute, monoatomic gas confined to a box T with periodic boundary conditions. The collision operator writes as

$$Q(F,F) = \int_{\mathbb{R}^3}\int_0^{2\pi}\int_0^{\pi/2} (F(v')F(v'_1) - F(v)F(v_1))|v-v_1|^\beta h(\theta)\ d\theta\ d\phi\ dv_1, \tag{2.16}$$

in which the physical characteristics of the molecules constituting the gas are given by $0 \leq \beta \leq 1$ and $h(\theta) > 0$.

The exponent β is related to the decay of the intermolecular forces, and with the given range, it corresponds to the so-called hard potentials.

An angular cutoff condition is assumed for the function $h(\theta)$, i.e.

$$\int_0^{\pi/2} h(\theta)\ d\theta \equiv h_0 < \infty. \tag{2.17}$$

The conservation of mass, momentum, energy and the decrease of entropy are recalled here.

$$\begin{aligned}
&\int_{\mathbb{R}^3\times T^3} F(x,v,t)\ dx\ dv = \int_{\mathbb{R}^3\times T^3} F_0(x,v)\ dx\ dv \\
&\int_{\mathbb{R}^3\times T^3} F(x,v,t)v\ dx\ dv = \int_{\mathbb{R}^3\times T^3} F_0(x,v)v\ dx\ dv \\
&\int_{\mathbb{R}^3\times T^3} F(x,v,t)|v|^2\ dx\ dv = \int_{\mathbb{R}^3\times T^3} F_0(x,v)|v|^2\ dx\ dv \\
&\int_{\mathbb{R}^3\times T^3} F(x,v,t)\log F(x,v,t)dxdv \leq \int_{\mathbb{R}^3\times T^3} F_0(x,v)\log F_0(x,v)dxdv
\end{aligned} \tag{2.18}$$

Let the weighted spaces L^q_s be defined by the norm

$$\|f\|_{q,s} = \Big(\int_{\mathbb{R}^3} f(v)^q (1+\|v\|^2)^{qs/2}\ dv \Big)^{1/q},$$

for $q < \infty$, and with the usually modification for $q = \infty$.

The theorem below summarizes some main results on the spatially homogeneous equation.

Theorem 2.2.1
Assume that $\beta \geq 0$. Let $s_1 > 2$, $\beta(1-1/q) \leq s < s_1 - \beta/q$ for $1 < q \leq \infty$, and $s = s_1$ if $q = 1$. Suppose that $F_0 = F_0(v) \in L^1_{s_1} \cap L^s_q$, $F_0 \geq 0$, and $F_0 \log F_0 \in L^1$.

(i) There exists a nonnegative solution $F \in L^\infty([0,\infty[; L^1_{s_1} \cap L^q_s) \cap C^1([0,\infty[; L^1_0)$ of the spatially homogeneous Boltzmann equation with initial data F_0.

This solution satisfies (2.18), and is unique in the class of solutions possessing moments of order higher than 2.
If $q = 1$, *then*

$$F \in C([0,\infty[; L^1_{s_1}) \cap C^1(]0,\infty[; L^1_{s_1}),$$

and

$$\frac{dF}{dt} = Q(F,F) \quad in \quad L^1_{s_1}, \ for\ almost\ every\ t > 0. \tag{2.19}$$

If $1 < q < \infty$ *and* $s > \beta$, *then*

$$F \in C([0,\infty[; L^1_{s_1} \cap L^q_{s'}) \cap C^1(]0,\infty[; L^1_{s_1} \cap L^q_s),$$

and (2.19) holds in $L^1_{s_1} \cap L^s_q$. *Here* $s' < s$.

(ii) If $\beta > 0$ *and* $1 \le q < \infty$, *then for any* $r_1 > 0$, $r > 0$ *and* $t_0 > 0$, *there is a constant* C *depending on* r_1, r, s_1, s *and* t_0 *such that the* L^1*-moment of order* r_1 *and the* L^q*-moment of order* r *both are bounded by* C, *uniformly for all* $t \ge 0$.

(iii) Let ω *be the unique Maxwellian with the same first five moments as* F_0. *Then as* $t \to \infty$, *the solution* F *converges strongly in* $L^1_{s_1}$ *to* ω, *and for* $s > \beta$; $s' < s$, *the same holds in* $L^q_{s'}$.

(iv) If $F_0 \in L^1_{s_1} \cap L^q_s$, *with* $s_1 > 2$ *and* $\beta(1-1/q) < s < s_1 - \beta/q$, *then the solution* F *converges exponentially in time to* ω_0 *in* $L^1_{s_1'} \cap L^q_{s'}$ *for all* $s_1' \le s_1$, *and* $s' < s$. *This means that there is a* $\mu > 0$ *and a constant* C, *depending on* s, s_1, s', s_1', $\gamma \in]0,\mu[$, *and* F_0, *such that*

$$\|F_t - \omega_0\|_{\tilde{q},\tilde{s_1}} \le C\|F_0 - \omega_0\|_{\tilde{q},\tilde{s}} e^{-\gamma t}, \quad for\ all\ t > 0,$$

where $\tilde{q} = 1, q$ *and* $\tilde{s} = s_1, s$.

2.2.2 The relativistic non quantum Boltzmann equation

Global existence for the relativistic Boltzmann equation

The existence of solutions to the relativistic Boltzmann equation in L^1 is proven by M. Dudynski and M. Elkiel-Jezewska in [20].

The relativistic Boltzmann equation writes as ($c = 1$ where c is the speed of light),

$$\left(\partial_t + \frac{\mathbf{p}}{p_0}.\nabla_x\right) f = Q(f,f), \tag{2.20}$$

where

$$\begin{aligned} Q(f,f) &= Q^+(f,f) - Q^-(f,f) \\ Q^+(f,f) &= \frac{1}{p_0}\int_{\mathbb{R}^3} \frac{d^3\mathbf{p}_*}{p_{*0}} \int_{S^2} d\Omega\ f(\mathbf{p}')f(\mathbf{p}'_*)\ B(g,\theta) \\ Q^-(f,f) &= f\ L(f) = f(\mathbf{p})\frac{1}{p_0}\int_{\mathbb{R}^3} \frac{d^3\mathbf{p}_*}{p_{*0}} \int_{S^2} d\Omega\ f(\mathbf{p}_*)\ B(g,\theta), \end{aligned}$$

and $p = (p_0, \mathbf{p})$ with $p_0 = (M^2 + \mathbf{p^2})^{\mathbf{1/2}}$ is the particle energy, M is the particle rest mass.
When two particles with respective impulsions $\mathbf{p}$ and $\mathbf{p}_*$ encounter each other, they collide and get $\mathbf{p}'$ and $\mathbf{p}'_*$ as impulsions after the collision.
Moreover,

$$\cos\theta = 1 - 2(p - p_*)(p - p')(4M^2 - s)^{-1},$$

where θ is the scattering angle in the center of mass system, and

$$d\Omega = d(\cos\theta)\ d\phi.$$

The collision kernel B writes as

$$B(g,\theta) = \frac{g\ s^{1/2}}{2}\ \sigma(g,\theta),$$

where $\sigma(g,\theta)$ is the scattering cross section, $s^{1/2} = |p_* + p|$ is the total energy, and $2g = |p_* - p|$ is the relative momentum value in the center of mass system.

The global existence of solutions to the Cauchy problem (2.20) in $C([0,\infty); L^1(\mathbb{R}^3 \times \mathbb{R}^3))$ is given by the following theorem,

Theorem 2.2.2
Let $f_0 \geq 0$ a.e in $\mathbb{R}^3 \times \mathbb{R}^3$ satisfying

$$\int_{\mathbb{R}^3} d^3\mathbf{x} \int_{\mathbb{R}^3} d^3\mathbf{p}\ (1 + p_0 + |lnf_0|)\ f_0 < C.$$

Then there exists $f \in C([0,\infty); L^1(\mathbb{R}^3 \times \mathbb{R}^3))$ *satisfying*

$$f|_{t=0} = f_0,$$
$$(1+f)^{-1}Q^-(f,f) \in L^\infty(0,\infty; L^1(\mathbb{R}^3 \times B_R)),$$
$$(1+f)^{-1}Q^+(f,f) \in L^1(0,T; L^1(\mathbb{R}^3 \times B_R)),$$
$$L(f) \in L^\infty(0,\infty; L^1(\mathbb{R}^3 \times B_R)),$$

for all R, $T < \infty$. *It is a mild or equivalently a renormalized solution of (2.20). In addition,* f *satisfies*

$$\sup_{t\geq 0} \int_{\mathbb{R}^3} d^3\mathbf{x} \int_{\mathbb{R}^3} d^3\mathbf{p}\ (1 + p_0 + |\ln f|)f < C.$$

Existence results and asymptotic behaviour of periodic solutions

Relativistic kinetic equations have been studied by S. R. Groot, W. A. Van Leeuwen and Ch. G. Weert in ([27]) on a physical level. R.T. Glassey, W.A. Strauss ([26], [25]) and H. Andreasson ([1]) studied it on a mathematical level. Periodic and continuous solutions of the relativistic Boltzmann equation are studied by R.T. Glassey and W.A. Strauss ([26], [25]) for initial periodic data in the space variable and near equilibrium. We recall here the existence and uniqueness results obtained by R.T. Glassey and W.A. Strauss in [26].
A relativistic Maxwellian is characterized as a particle distribution $\mu(p)$ which minimizes the entropy subject to constant mass, momentum and energy. It is an equilibrium solution of (2.20) since $Q(\mu,\mu) = 0$, and it has the form

$$\mu(v) = \exp(a + b \cdot p - c\sqrt{1+|p|^2}), \tag{2.21}$$

where a, b and $c > |p|$ are constants.

We consider a solution $f(t,x,p)$ of (2.20) which has period 2π in each x_i-component and satisfies an initial condition $f(0,x,v) = f_0(x,v)$. We assume that the initial distribution $f_0(x,v)$ is close to a Maxwellian $\mu(p)$. The parameters a, b, c are chosen so that f_0 and μ have the same total mass, energy and momentum,

$$0 = \int\int (f_0 - \mu)\, dx\, d\mu = \int\int p(f_0-\mu)\, dx\, d\mu = \int\int \sqrt{1+|p|^2}\,(f_0-\mu)\, dx\, d\mu,$$

where the integration is over $x \in \Omega = (0,2\pi)^3$ and $p \in \mathbb{R}^3$ (see [26] for more details).

The collision cross section $\sigma(g,\theta)$ is assumed to satisfy

$$\begin{aligned} &c_1\frac{g^{\beta+1}}{1+g}\ \sin^\gamma\theta \le \sigma(g,\theta) \le c_2(g^\beta + g^{-\delta})\sin^\gamma\theta, \\ &\left|\frac{\partial\sigma}{\partial g}\right| \le c_3(g^{\beta'} + g^{-\delta'})\sin^{\gamma'}\theta, \end{aligned} \tag{2.22}$$

where $c_1,\ c_2,\ c_3$ are positive constants,

$$0 \le \delta < \frac{1}{2},\ 0 \le \beta < 2 - 2\delta,$$

$$0 \le \delta' < 4,\ \beta' \ge 0,\ \gamma' > -2,$$

and either

$$\gamma \ge 0 \text{ or } |\gamma| < \min\{2-\beta, \frac{1}{2}-\delta, \frac{1}{3}(2-2\delta-\beta)\}.$$

The following theorem is stated.

Theorem 2.2.3
Let $\sigma(s,\theta)$ satisfy (2.22). Let $f^0(x,v)$ be a nonnegative continuous function which has period 2π in each x_i-component. Assume that $\mu(v)$ is a Maxwellian (2.21) and c_0 is a positive constant such that

$$\sup_x |f^0(x,v) - \mu(v)| \le c_0(1+|v|^2)^{-\alpha/2}\sqrt{\mu(v)}, \tag{2.23}$$

where $\alpha > \frac{1}{2}(3+\beta)$ is fixed. If c_0 is sufficiently small, then there are constants c_1 and $h > 0$ and a unique global continuous solution $f(t,x,v)$ of (2.20) for $0 \le t < \infty$ such that $f(0,x,v) = f^0(x,v)$ and

$$\sup_x |f(t,x,v) - \mu(v)| \le c_1\ e^{-ht}\ (1+|v|^2)^{\alpha/2}\sqrt{\mu(v)}, \tag{2.24}$$

for all $v \in \mathbb{R}^3$ and $t \in [0,\infty)$.

H. Andreasson in ([1]) has stated a theorem concerning the asymptotic behaviour of solutions to the relativistic Boltzmann equation. He has proved strong L^1 convergence to a global Jüttner equilibrium solution for arbitrary initial data, periodic in the space variables, and satisfying the natural bounds of finite energy and entropy.

H. Andreasson applied Arkeryd's or Lions'approaches to obtain L^1 convergence to a local Jüttner equilibrium solution. Arkeryd's method is based on a nonstandard measure theorical analysis of the entropy dissipation term ([2]). Moreover, H. Andreasson has shown that the periodicity in the space variables implies that every local Jüttner solution is a global one.
Here is one of his results.

Theorem 2.2.4
Given a sequence $(t_k)_{k\in\mathbb{N}}$, $t_k \nearrow \infty$, there is a subsequence $(t_{k'})$ and a global Jüttner equilibrium solution

$$J(p) = exp(\alpha - \beta_\mu p^\mu), \quad \alpha \in \mathbb{R}, \ \beta_\mu = (\beta_0, \beta) \in \mathbb{R}^4 \ \textit{with} \ \beta_0 > |\beta|,$$

such that for $T > 0$, $f(. + t_{k'}) \to J$ strongly in $L^1(\Lambda \times \mathbb{R}^3 \times [0,T])$, and for $t > 0$, $f(., t + t_{k'}) \to J$ strongly in $L^1(\Lambda \times \mathbb{R}^3)$.

2.2.3 A quantum relativistic Boltzmann equation

Recall the results stated in [22] and [21]. Consider the equation describing the dynamics of a low energy, homogeneous, isotropic photon gas which interacts via Compton scattering with a low energy electron gas at low temperature $\theta > 0$, assumed to have a Maxwellian distribution of energy $e^{-k/\theta}$. It writes

$$k^2 \frac{\partial f}{\partial t} = \int_0^\infty (f'(1+f)\ B(k',k;\theta) - f(1+f')\ B(k,k';\theta))\ dk'. \tag{2.25}$$

Here $f(t,k) \geq 0$ is the density of photons which at time t have energy $k \geq 0$. f denotes $f(t,k)$ and f' denotes $f(t,k')$.
The cross section $B(k,k';\theta)/k^2$ represents the probability for a given particle at energy state k to be scattered to the energy state k'. B satisfies

$$e^{k/\theta} B(k',k;\theta) = e^{k'/\theta} B(k,k';\theta). \tag{2.26}$$

For the sake of simplicity, we take $\theta = 1$. Let

$$N(f) = \int_0^\infty f(k)\ k^2\ dk \ \text{ and } \ S(f) = \int_0^\infty s(f(t,k),k)\ k^2\ dk \tag{2.27}$$

be the total number of photons and the entropy, where

$$s(x,k) = (1+x)\ln(1+x) - x\ln x - kx.$$

We have the fundamental results,

$$\frac{d}{dt}N(f(t,.)) = 0, \quad \text{and} \quad \frac{d}{dt}S(f(t,.)) \geq 0, \quad t \geq 0. \tag{2.28}$$

Moreover we introduce

$$b(k,k') = B(k',k;1)\ e^k\ k^{-2}\ k'^{-2}.$$

Assumption (2.26) on B implies that b is symmetric. We assume that b satisfies

$$b(k,k') = e^{\eta k}e^{\eta k'}\sigma(k,k'), \tag{2.29}$$

for some function $\eta \in [0,1]$ and some nonnegative, bounded and symmetric function σ. We also need a more restrictive assumption on b, i.e. for some $\sigma_*,\ \sigma^*,\ \nu > 0,\ \gamma \in [0,1]$,

$$\sigma(k,k') \equiv \sigma(k'-k) \quad \text{and} \quad 0 < \sigma_* e^{-\nu|z|^\gamma} \leq \sigma(z) \leq \sigma^*, \quad z \in \mathbb{R}. \tag{2.30}$$

We perform the change of the unknown function $F = k^2 f$.
The equation (2.25) becomes

$$\frac{\partial F}{\partial t} = Q(F,F) = \int_{\mathbb{R}_+} b(k,k')(F'(k^2+F)e^{-k} - F(k'^2+F')e^{-k'})\ dk'. \tag{2.31}$$

Taking into account the a priori bounds given by (2.28), a natural space for the solutions of (2.25) is the set of bounded and nonnegative measures $M^1(\mathbb{R}_+) = (C_b(\mathbb{R}_+))'$.
In the sequel, for a given $0 \leq F \in M^1$ we denote by

$$F = g + G,$$

where $g \in L^1(\mathbb{R}_+)$, G is a singular measure with respect to the Lebesgue measure in $\mathbb{R}_+$.
$Q(F,F)$ is well defined for all nonnegative measures $F \in M^1(\mathbb{R}_+)$.
Equation (2.31) can be written as the following system of equations,

$$\begin{aligned}
\frac{\partial g}{\partial t} &= Q_1(g,G) = Q_1^+(g,G) - Q_1^-(g,G) = (k^2+g)e^{-k}L(F) - gL((k^2+F)e^{-k}),\\
\frac{\partial G}{\partial t} &= Q_2(g,G) = Q_2^+(g,G) - Q_2^-(g,G) = G[L(F)e^{-k} - L((k^2+F)e^{-k})],
\end{aligned} \tag{2.32}$$

with $L(\phi) := \displaystyle\int_{\mathbb{R}_+} b(k,k')\ \phi'\ dk'$.

The initial datum for the Cauchy problem is

$$F(0,.) = g(0,.) + G(0,.) = F_{in} = g_{in} + G_{in}. \tag{2.33}$$

When b is bounded, a natural space to look for solutions is

$$\mathcal{E}_0 = \{F \in M^1(\mathbb{R}_+),\ F \geq 0,\ M((1+k)F) < \infty\}.$$

Where more general cross sections b are considered, the spaces

$$\mathcal{E}_\eta = \{F \in M^1(\mathbb{R}_+),\ F \geq 0,\ Y_\eta(F) := M(e^{\eta k}F) < \infty\}, \quad \eta > 0,$$

are introduced.

Let $M(F) := \displaystyle\int_0^\infty dF(k)$ be the mass of F.

So,

$$\frac{d}{dt}M(F) = 0,$$

i.e.

$$M(F(t,.)) = M(F_{in}) =: m, \quad t \geq 0. \tag{2.34}$$

We define the entropy for a general state $F = g + G$ by

$$H(F) := H(g) - M(kG), \tag{2.35}$$

where $H(g) = \displaystyle\int_0^\infty h(g,k)\ dk$, and

$$h(x,k) = (k^2+x)\ln(k^2+x) - x\ln x - k^2 \ln k^2 - kx.$$

Moreover,

$$\frac{d}{dt}H(F) = \frac{1}{2}D(F), \tag{2.36}$$

where $D(F) \geq 0$ is the dissipation entropy rate. It is defined by :

$$\begin{aligned} D(F) &= 2\int_{\mathbb{R}_+} \left(h'(g,k)\ \frac{\partial g}{\partial t} - k\ \frac{\partial G}{\partial t}\right) dk \\ &= 2\int_{\mathbb{R}_+} (Q_1(g,G)\ h'(g,k) - k\ Q_2(g,G))\ dk \end{aligned}$$

Furthermore, we define the Bose distributions

$$\mathcal{B}_m = g_\mu + \alpha\delta_0, \tag{2.37}$$

where

$$g_\mu(k) = \frac{1}{e^{k+\mu} - 1}, \quad \mu \geq 0.$$

Here, μ and α are defined in the following way. Let $N_\mu = N(g_\mu)$.
If $m \leq N_0$, then $M(g_\mu) = m$ and $\alpha = 0$.
If $m > N_0$, then $\mu = 0$ and $\alpha = m - N_0$.

Remark 2.2.1
A distribution $F \in C([0,\infty); M^1(\mathbb{R}_+))$ is defined in [22] as an entropy solution of the Cauchy problem (2.31)-(2.33) if

$$\int_{\mathbb{R}_+} F(t,k)\phi(t,k)\, dk = \int_{\mathbb{R}_+} F_{in}(k)\phi(0,k)\, dk + \int_0^t \int_{\mathbb{R}_+} Q(F,F)\, \phi\, dk\, ds, \tag{2.38}$$

for all $\phi \in C_c([0,\infty) \times \mathbb{R}_+)$, and satisfies either the entropy inegality

$$\int_{t_1}^{t_2} D(F(s,.))\, ds \leq H(F(t_2,.)) - H(F(t_1,.)), \quad t_2 \geq t_1 \geq 0, \tag{2.39}$$

or the entropy dissipation bound

$$\int_0^\infty D(F(t,.))\, dt \leq H(\mathcal{B}_m) - H(F_{in}). \tag{2.40}$$

M. Escobedo and S. Mischler have established the three following theorems ([22]).

Theorem 2.2.5
Assume that b satisfies (2.29) with $\eta = 0$. Then for any initial datum $F_{in} = g_{in} + G_{in} \in \mathcal{E}_0$, there exists a unique entropy solution to (2.31),(2.33) and (2.39), $F = g + G \in C([0,\infty), \mathcal{E}_0)$. Moreover, F satisfies (2.34) and is such that

$$supp\ G(t,.) \subset supp\ G_{in}. \tag{2.41}$$

In particular, if $F_{in} = g_{in} \in L^1(\mathbb{R}_+)$ then $G(t,.) = 0$ for every $t \geq 0$ and thus $F(t,.) = g(t,.) \in L^1(\mathbb{R}_+)$ for every $t \geq 0$.

Theorem 2.2.6
Assume that b satisfies (2.30). Then, for all initial datum $F_{in} = g_{in} + G_{in} \in \mathcal{E}_{\theta'}$ *with* $\theta' > 0$, *there exists a unique global entropy solution to equation (2.31)-(2.33) and (2.39),* $F = g + G \in C([0,T), \mathcal{E}_\theta) \cap L^1(0,T; \mathcal{E}_{\eta+\theta})$ *for all* $T > 0$ *and all* $0 < \theta < min(\theta', \eta, 1-\eta)$. *Moreover, it satisfies (2.41).*

Theorem 2.2.7
Assume that b satisfies (2.29) for some $\eta \in [0,1)$ *and that the initial datum has the special shape*

$$F_{in} = g_{in} + \alpha_{in}\delta_0, \quad with \;\; 0 \le g_{in} \le g_0 \;\; and \;\; \alpha_{in} \ge 0.$$

Then there exists an entropy solution $F = g + \alpha\delta_0 \in C([0,T), \mathcal{E}_1)$ *to (2.31),(2.33) and (2.40). Moreover, F satisfies (2.34) and*

$$0 \le \alpha(t) \le \alpha_{in}, \quad 0 \le g(t,.) \le g_0, \quad t \ge 0.$$

The asymptotic behaviour of these global solutions are also considered. The main result is the following.

Theorem 2.2.8
Assume that b is positive and that F_{in} *satisfies the assumptions of one of the existence Theorems 2.2.5, 2.2.6, or 2.2.7. Let* $m = M(F_{in})$, $\mathcal{B}_m = g_\mu + \alpha\delta_0$ *the Bose distribution of mass m defined in (2.37) and* $F \in C([0,\infty); M^1)$ *the corresponding solution to (2.31). Then,*

$$\begin{aligned} &F(t,.) \underset{t\to\infty}{\rightharpoonup} \mathcal{B}_m \;\; weakly \;\; * \;\; in \;\; (C_c(\mathbb{R}_+))', \\ &\lim_{t\to\infty} \|g(t,.) - g_\mu\|_{L^1((k_0,\infty))} = 0, \quad k_0 > 0. \end{aligned} \tag{2.42}$$

Moreover, if $m \le N_0$ *or* $0 \le g_{in} \le g_0$, k_0 *can be taken as* 0 .

2.2.4 A modified Boltzmann equation for Bose-Einstein particles

In [31], X. Lu studies a homogeneous quantum Boltzmann equation for Bosons under a cutoff assumption on the collision kernel. His frame is isotropic.

He proves a global existence and uniqueness result for L^1 conservative entropy solutions. Moreover, their asymptotic behavior in time is considered. In the low temperature case, some velocity concentration appears in infinite time. In the high temperature case, there is a weak L^1 convergence of the solution to the equilibrium state with the same mass and energy as the initial datum.

Chapter 3

Modelling of the studied problem

Contents

3.1 An initial relativistic frame 37

3.2 A simplified model linked to the Compton effect 39

3.1 An initial relativistic frame

As considered in [22], the following quantum relativistic homogeneous equation describes the evolution of the photon distribution function in the interaction of photons with a gas of electrons via Compton scattering. The gas of electrons is of low energy with mass m. Photons are weakly dense and at low temperature. This equation is written as

$$\frac{\partial f}{\partial t}(t,P) = Q(f,g)(P), \quad t>0, \ P \in I\!R^4, \tag{3.1}$$

with

$$\begin{aligned} Q(f,g)(P) = \frac{8c}{p^0} \int_{I\!R^4}\int_{I\!R^4}\int_{I\!R^4} & s\sigma(s,\theta)\ q(f,g)\ \delta_{\{P+P_*-P'-P'_*=0\}} \\ & \chi_2(P_*^0)\ \chi_1(P'^0)\ \chi_2(P_*'^0)\ dP'\ dP'_*\ dP_*. \end{aligned} \tag{3.2}$$

P and P' (resp. P_* and P'_*) are the momentum of the photons (resp. electrons) before and after a collision.

A particle is determined by the pair $(X, P) \in I\!R^4 \times I\!R^4$ of position $X = (t, x)$ and momentum $P = (P^0, p)$. Let

$$P^0 \equiv p^0 := |p|,\ P'^0 \equiv p'^0 := |p'|,\ P^0_* \equiv p^0_* := \sqrt{|p_*|^2 + m^2c^2},$$

and

$$P'^0_* \equiv p'^0_* := \sqrt{|p'_*|^2 + m^2c^2}.$$

Denote by $s = (P + P_*)^2 := (P^0 + P^0_*)^2 - |p + p_*|^2$, and by θ the scattering angle, given by

$$\cos\theta \ = \ \frac{(P_* - P).(P'_* - P')}{(P_* - P)^2}.$$

The nonnegative scalar function $f(t, p)$ is the distribution function of photons. $g(p)$ is the distribution function of electrons assumed to be at non relativistic equilibrium, i.e.

$$g(p) = \exp(-\frac{|p|^2}{2c}).$$

c denotes the speed of light.

The functions $\chi_1(P'^0)$, $\chi_2(P^0_*)$ and $\chi_2(P'^0_*)$ are defined by

$$\chi_1(P'^0) = \frac{1}{2p'^0}\delta_{\{P'^0 = p'^0\}},\quad \chi_2(P^0_*) = \frac{1}{2p^0_*}\delta_{\{P^0_* = p^0_*\}},\quad \chi_2(P'^0_*) = \frac{1}{2p'^0_*}\delta_{\{P'^0_* = p'^0_*\}},$$

and

$$q(f, g) = g(p'_*)f(p')(1 + \hbar f(p)) - f(p)g(p_*)(1 + \hbar f(p')), \tag{3.3}$$

where $\hbar$ is the Planck constant.
Here and below, the following notations are used for any function f,

$$f' = f(t, p'),\quad f_* = f(t, p_*),\quad f'_* = f(t, p'_*).$$

In equation (3.1), emission and absorption of photons have not been taken into account, so that the transitions are produced exclusively by the Compton scattering.
In order to simplify the formulas, m and $\hbar$ are taken equal to 1.

3.2 A simplified model linked to the Compton effect

M. Escobedo, S. Mischler and M.A Valle have shown in [22] how to obtain the final expression of the collision operator $Q(f,g)(p)$. We will explain later how to obtain the expression of the collision integral in (3.1).
In order to simplify the model, we only keep the highest-order term with respect to the speed of light c in the collision integral $Q(f,g)(P)$. The cross section $\sigma(s,\theta)$ is given by the Klein Nishina formula ([27]). An equivalent when $c \to \infty$ is given in the following lemma.

Lemma 3.2.1

$$\sigma(s,\theta) \sim \frac{1}{2} r_0^2 (1+\cos^2\theta), \qquad c \to \infty. \tag{3.4}$$

Here, e is the charge of the electron and $r_0 = \dfrac{e^2}{4\pi m c^2}$.

Proof of the lemma.

The proof refers to [27]. We here give the main steps of the proof.
The cross section $\sigma(s,\theta)$ is given by the Klein-Nishina formula

$$\sigma(s,\theta) = \frac{1}{2} r_0^2 (1-\xi)\Big(1 + \frac{1}{4}\frac{\xi^2(1-x)^2}{1-\frac{1}{2}\xi(1-x)} + \Big[\frac{1-(1-\frac{1}{2}\xi)(1-x)}{1-\frac{1}{2}\xi(1-x)}\Big]^2\Big),$$

with

$$x = 1 + \frac{2st}{(s-m^2)^2},\ \xi = \frac{(P+P_*)^2 - m^2c^2}{(P+P_*)^2},\ t = (P-P')^2.$$

As

$$\xi = \frac{s-m^2c^2}{s} = \frac{2|p|\sqrt{|p_*|^2+m^2c^2} - 2(p,p_*)}{m^2c^2 + 2|p|\sqrt{|p_*|^2+m^2c^2} - 2(p,p_*)},$$

then

$$\xi \underset{c\to\infty}{\sim} \frac{2|p|}{mc}.$$

Furthermore,

$$\cos\theta = 1 + \frac{(P+P_*).(P'-P'_*-P+P_*)}{(P-P_*)^2},$$

and by taking a reference frame where $p' = 0$ (see [32] for more details), we obtain

$$\frac{(P+P_*).(P'-P'_*-P+P_*)}{(P-P_*)^2} = \frac{2st}{(s-m^2)^2}.$$

So,

$$\cos\theta = x.$$

Let

$$L := (1-\xi)\Big(1+\frac{1}{4}\frac{\xi^2(1-x)^2}{1-\frac{1}{2}\xi(1-x)} + \Big[\frac{1-(1-\frac{1}{2}\xi)(1-x)}{1-\frac{1}{2}\xi(1-x)}\Big]^2\Big).$$

L can be written as

$$L = 1 + x^2 + C_1(x)\xi + C_2(x)\xi^2 + C_3(x)\xi^3,$$

with

$$\begin{aligned} C_1(x) &= x(1-x^2) - (1+x^2), \\ C_2(x) &= \frac{1}{4}\{(1-x)[1+(1+x)(1+3x)] - 4x(1+x)\}, \\ C_3(x) &= \frac{1}{8}(1-x)^2\{(1-x)[1+2x(1+x)] - 2[1+(1+x)(1+3x)]\}. \end{aligned}$$

When $c \to \infty$, $\xi \to 0$ and $L \to 1 + x^2 = 1 + \cos^2\theta$.
Finally

$$\sigma(s,\theta) \underset{c\to\infty}{\sim} \frac{1}{2} r_0^2 (1+\cos^2\theta).$$

□

Lemma 3.2.2
The collision integral writes as

$$Q(f)(p) = c \int_{I\!R^3} \frac{\sigma(s,\theta)}{|p||p'|}\, e^{|p'|}\, q(f) \Big(\int_{I\!R^3}\int_{I\!R^3} \delta_\Sigma \ \exp(-\frac{|p_*|^2}{2c})\, dp_*\, dp'_* \Big)\, dp',$$

with

$$q(f) = e^{-|p|} f(p')(1+f(p)) - e^{-|p'|} f(p)(1+f(p')).$$

Proof.

Replacing $\chi_1(P'^0)$, $\chi_2(P_*^0)$ et $\chi_2(P_*'^0)$ by their expressions, $Q(f,g)$ writes as

$$Q(f,g)(P) = \frac{c}{p^0}\int_{\mathbb{R}^4}\int_{\mathbb{R}^4}\int_{\mathbb{R}^4} s\sigma(s,\theta)\ q(f,g)\ \delta_{\{P+P_*-P'-P'_*=0\}} \\ \delta_{\{P_*^0=p_*^0\}}\delta_{\{P'^0=p'^0\}}\delta_{\{P'^0_*=p'^0_*\}}\ \frac{dP'}{p'^0}\ \frac{dP'_*}{p'_*}\ \frac{dP_*}{p_*}.$$

Considering the inner integrations with respect to P_*^0, P'^0 and $P_*'^0$ in the former expression $Q(f,g)$,

$$Q(f,g)(p) = c\int_{\mathbb{R}^3}\int_{\mathbb{R}^3}\int_{\mathbb{R}^3} \frac{s}{p^0p'^0p_*^0p_*'^0}\ \sigma(s,\theta)\ q(f,g)\times$$

$$\times\ \delta_\Sigma\ dp'dp'_*dp_*,$$

where Σ is the manifold of 4-uplets (p,p_*,p',p'_*) such that,

$$\begin{aligned} p+p_* &= p'+p'_*, \\ c|p|+\frac{|p_*|^2}{2} &= c|p'|+\frac{|p'_*|^2}{2}. \end{aligned}$$

By taking the highest-order term with respect to c, we obtain

$$Q(f,g)(p) = c\int_{\mathbb{R}^3}\int_{\mathbb{R}^3}\int_{\mathbb{R}^3} \frac{s}{p^0p'^0p_*^0p_*'^0}\ \sigma(s,\theta)\ q(f,g)\ \delta_\Sigma\ dp'dp'_*dp_*,$$

To simplify the model, only the highest-order terms with respect to c are kept in $Q(f,g)(p)$. The term $\dfrac{s}{p^0p'^0p_*^0p_*'^0}$ is equivalent to $\dfrac{1}{|p||p'|}$, when $c\to\infty$. Indeed,

$$\frac{s}{p^0p'^0p_*^0p_*'^0} = \frac{1}{|p||p'|}\frac{s}{\sqrt{|p'_*|^2+c^2}\sqrt{|p_*|^2+c^2}}.$$

When $c\to\infty$,

$$\frac{s}{\sqrt{|p'_*|^2+c^2}\sqrt{|p_*|^2+c^2}}\to 1.$$

Together with (3.4), this implies that the collision operator can be approximated by

$$Q(f,g)(p) = c\int_{\mathbb{R}^3}\int_{\mathbb{R}^3}\int_{\mathbb{R}^3} \frac{\sigma(s,\theta)}{|p||p'|}\ q(f,g)\ \delta_\Sigma\ dp'dp'_*dp_*,$$

where

$$q(f,g) = g(p'_*)f(p')(1+f(p)) - f(p)g(p_*)(1+f(p')).$$

Then, the collision integral becomes

$$Q(f)(p) = c \int_{I\!R^3} \frac{\sigma(s,\theta)}{|p||p'|}\, e^{|p'|}\, q(f) \left(\int_{I\!R^3}\int_{I\!R^3} \delta_\Sigma \, \exp(-\frac{|p_*|^2}{2c})\, dp_*\, dp'_* \right) dp',$$

with

$$q(f) = e^{-|p|} f(p')(1+f(p)) - e^{-|p'|} f(p)(1+f(p')).$$

□

The collision operator can be simplified in the following way.

Lemma 3.2.3
Denote by

$$S(p,p') = \int_{I\!R^3}\int_{I\!R^3} \delta_\Sigma \, \exp(-\frac{|p_*|^2}{2c})\, dp_*\, dp'_*, \quad A = |p'|-|p|+\frac{|p-p'|^2}{2c}, \quad w = p'-p.$$

Then

$$S(p,p') = \frac{2\pi c^2}{|w|} \, \exp(-\frac{A^2 c}{2|w|^2}).$$

Proof.

We start by writing the following expression

$$|p| + \frac{|p_*|^2}{2c} - |p'| - \frac{|p+p_*-p'|^2}{2c} = -(A - \frac{1}{c}(p_*, w)).$$

$S(p,p')$ writes as

$$S(p,p') \;=\; \int_{I\!R^3} \left(\int_{I\!R^3} \delta_{\{p'_*=p+p_*-p'\}} \, \delta_{\{|p|+\frac{|p_*|^2}{2c}=|p'|+\frac{|p'_*|^2}{2c}\}} \, dp'_* \right) \exp(-\frac{|p_*|^2}{2c})\, dp_*,$$

And so,

$$\begin{aligned} S(p,p') &= \int_{I\!R^3} \delta_{\{|p|+\frac{|p_*|^2}{2c}=|p'|+\frac{|p+p_*-p'|^2}{2c}\}} \, \exp(-\frac{|p_*|^2}{2c})\, dp_* \\ &= \int_{I\!R^3} \delta_{\{A-\frac{1}{c}(p_*,w)=0\}} \, \exp(-\frac{|p_*|^2}{2c})\, dp_*. \end{aligned}$$

The change of variables in polar coordinates leads to

$$S(p,p') = \int_0^\infty \Big(\int_{S^2} \delta_{\{A-\frac{|p_*|}{c}(\Omega_*,w)=0\}}\ d\Omega_* \Big)\ \exp(-\frac{|p_*|^2}{2c})\ |p_*|^2\ d|p_*|.$$

Let us evaluate the term $\int_{S^2} \delta_{\{A-\frac{|p_*|}{c}(\Omega_*,w)=0\}}\ d\Omega_*$.

Since

$$\Omega_* = \begin{pmatrix} \cos\beta\sin\varphi \\ \sin\beta\sin\varphi \\ \cos\varphi \end{pmatrix}, \qquad \beta\in[0,2\pi],\ \varphi\in[0,\pi],$$

it holds that

$$\int_{S^2} \delta_{\{A-\frac{|p_*|}{c}(\Omega_*,w)=0\}}\ d\Omega_* = 2\pi \int_0^\pi \delta_{\{A-\frac{|p_*||w|}{c}\cos\varphi=0\}} \sin\varphi\ d\varphi.$$

By the change of variables $y=\cos\varphi$, we obtain

$$\int_{S^2} \delta_{\{A-\frac{|p_*|}{c}(\Omega_*,w)=0\}}\ d\Omega_* \ = \ -2\pi \int_{-1}^1 \delta_{\{A-\frac{|p_*||w|}{c}y=0\}}\ dy.$$

Since

$$\delta_{\{b-ax=0\}} = -\frac{1}{a}\delta_{\{x=\frac{b}{a}\}},$$

$$\begin{aligned}\int_{S^2} \delta_{\{A-\frac{|p_*|}{c}(\Omega_*,w)=0\}}\ d\Omega_* &= \frac{2\pi c}{|p_*||w|}\int_{-1}^1 \delta_{\{y=\frac{Ac}{|p_*||w|}\}}\ dy \\ &= \frac{2\pi c}{|p_*||w|} H\Big(1-\frac{A^2c}{|p_*|^2|w|^2}\Big).\end{aligned}$$

Finally,

$$\begin{aligned}S(p,p') &= \int_0^\infty \frac{2\pi c}{|p_*||w|}\ \exp(-\frac{|p_*|^2}{2c}) H\Big(1-\frac{A^2c}{|p_*|^2|w|^2}\Big)|p_*|^2\ d|p_*| \\ &= \int_{\frac{|A|c}{|w|}}^\infty \frac{2\pi c}{|w|}|p_*|\ \exp(-\frac{|p_*|^2}{2c})\ d|p_*| \\ &= \frac{2\pi c^2}{|w|}\ \exp(-\frac{A^2c}{2|w|^2}).\end{aligned}$$

□

Assume that the photon distribution function is isotropic. Denote by $k = |p|$, $k' = |p'|$, $F(t,k) = k^2 f(t,k)$. The collision operator is then

$$Q(F)(t,k) = \int_0^\infty b(k,k')[F'(k^2+F)e^{-k} - F(k'^2+F')e^{-k'}]\ dk',$$

with

$$b(k,k') = \frac{2c^3 r_0^2 \pi^2}{k\ k'} \int_0^\pi (1+\cos^2\theta)\ \frac{\sin\theta}{|w|}\ \exp(-\frac{A^2 c}{2|w|^2} + k')\ d\theta, \tag{3.5}$$

and

$$A = k' - k + \frac{|w|^2}{2c}, \quad |w|^2 = k^2 + k'^2 - 2kk'\cos\theta.$$

The aim of chapters 4, 5 and 6 is to prove the existence of a solution F to the Cauchy problem

$$\begin{cases} \dfrac{\partial F}{\partial t}(t,k) = Q(F)(t,k), \quad t \in [0,T],\ k \geq 0, \\ F(0,k) = F_0(k), \end{cases} \tag{3.6}$$

where the initial datum F_0 is given.

Chapter 4

A priori estimates

Contents

4.1 **Conservation of the mass** 45

4.2 ***H*-theorem** 46

4.3 **Boundedness of entropy and energy** 46

4.4 **Mathematical frame** 48

The following a priori estimates for (3.6) hold.

4.1 Conservation of the mass

Proposition 4.1.1
Let $M(F)(t) = \int_0^\infty F(t,k)\,dk$ *be the total number of photons at time* t. *Then,*

$$\frac{d}{dt}M(F)(t) = 0. \tag{4.1}$$

Proof.

Proposition 4.1.1 follows from an integration of (3.6) with respect to k and the change of the variable k by k'.

4.2 H-theorem

Proposition 4.2.1
The entropy, defined by

$$H(F)(t) = \int_0^\infty [(k^2+F(t,k))\ln(k^2+F(t,k)) - F(t,k)\ln F(t,k) - k^2\ln k^2 - kF(t,k)]\, dk,$$

is a non-decreasing function of time.

Proof.

Multiply equation (3.6) by $ln\Big(\dfrac{(k^2+F)e^{-k}}{F}\Big)$,
so that

$$2\,\frac{d}{dt}H(F) = \int_0^\infty \int_0^\infty b(k,k')\; j(F(k'^2+F')e^{-k'}, F'(k^2+F)e^{-k})\; dk'\; dk.$$

Here,

$$j(u,v) = (v-u)(\ln v - \ln u) \;\text{ if }\; u>0,\; v>0,$$
$$j(u,v) = 0 \;\text{ if }\; u=v=0,$$
$$j(u,v) = +\infty \;\text{ elsewhere.}$$

The nonnegativity of b and j implies the result. □
Nevertheless, $H(F)$ is used to control the energy as we can verify below.

4.3 Boundedness of entropy and energy

Proposition 4.3.1
There exists a constant $C > 0$ such that for any solution F to (3.6), the following inequalities hold,

$$M(kF) \le C(1 + M(F) - H(F)), \tag{4.2}$$

$$|H(F)| \le CM((1+k)F). \tag{4.3}$$

Proof.
A proof of Proposition 4.3.1 is given in [23]. We recall here the main steps of (4.2).

The proof of (4.3) is similar.
The entropy $H(F)$ writes as

$$H(F) = \int_0^{+\infty} [(k^2+F)\ln(k^2+F) - F\ln F - k^2\ln k^2]\, dk - M(kF),$$

i.e.

$$M(kF) = H_0(F) - H(F)$$

with

$$H_0(F) := \int_0^{+\infty} [(k^2+F)\ln(k^2+F) - F\ln F - k^2\ln k^2]\, dk.$$

We use the following lemma ([23]).

Lemma 4.3.1
(i) For every $s \in (0,1)$ and $k > 0$,

$$0 \le (s+k^2)\ln(s+k^2) - k^2\ln k^2 \le s(1+\ln(1+k^2)). \tag{4.4}$$

(ii) There exists a positive constant C_1 such that, for all $s \ge 1$ and $k > 1$,

$$0 \le (s+k^2)\ln(s+k^2) - s\ln s - k^2\ln k^2 \le 2s(C_1+\ln(1+k^2)). \tag{4.5}$$

(iii) For all $\delta \in (0,1)$, there exists a positive constant C_δ such that, for all $s \ge 1$ and $k \in (0,1)$,

$$0 \le (s+k^2)\ln(s+k^2) - s\ln s \le \delta_s + C_\delta. \tag{4.6}$$

Thanks to Lemma 4.3.1,

$$\begin{aligned}
&\int_0^{+\infty} [(F+k^2)\ln(F+k^2) - k^2\ln k^2]\, dk - \int_0^{+\infty} F\ln F\ \mathbb{1}_{\{F\ge 1\}}\, dk \\
&= \int_0^{+\infty} [(F+k^2)\ln(F+k^2) - k^2\ln k^2 - F\ln F]\ \mathbb{1}_{\{F\ge 1,\ k>1\}}\, dk \\
&+ \int_0^{+\infty} [(F+k^2)\ln(F+k^2) - k^2\ln k^2 - F\ln F]\ \mathbb{1}_{\{F\ge 1,\ 0<k\le 1\}}\, dk \\
&+ \int_0^{+\infty} [(F+k^2)\ln(F+k^2) - k^2\ln k^2]\ \mathbb{1}_{\{0<F<1\}}\, dk \\
&\le C\int_0^{+\infty} F\ [1+\ln(1+k^2)]\, dk + C.
\end{aligned}$$

Because of the monotonicity of the functions $s \to -s \ln s$ and $-\ln s$,

$$
\begin{aligned}
-\int_0^{+\infty} F \ln F \ \mathbb{1}_{\{0 \le F \le 1\}} \, dk &= -\int_0^1 F \ln F \ \mathbb{1}_{\{0 \le F \le 1\}} \, dk \\
&\quad - \int_1^{+\infty} F \ln F \ \mathbb{1}_{\{0 \le F \le \exp(-\sqrt{k})\}} \, dk \\
&\quad - \int_1^{+\infty} F \ln F \ \mathbb{1}_{\{\exp(-\sqrt{k}) \le F \le 1\}} \, dk \\
&\le C_1 + C_2 + M(F) + \frac{1}{4} \int_0^{+\infty} kF \, dk,
\end{aligned}
$$

where

$$
C_2 = \int_1^{+\infty} \exp(-\sqrt{k}) \ \sqrt{k} \, dk < +\infty.
$$

Finally, we obtain (4.2). □

4.4 Mathematical frame

This work is devoted to prove an existence result for the quantum kinetic equation (3.6) describing the Compton effect. Its kernel is kept singular as it is derived when keeping the highest-order term with respect to the speed of light in the relativistic model. Like in [22] already, the boundedness of the photon entropy is not sufficient to stay in an L^1 frame. Indeed, a solution of the Cauchy problem is obtained as a limit of an approximated sequence of this problem. The boundedness of mass $M(F)$, energy $M(kF)$ and entropy $H(F)$ are not sufficient for the limit of this sequence to stay in L^1 frame. Measure solutions for the photon distribution function are expected. Moreover, the singularity in the collision kernel brings severe restrictions. Existence results to the Cauchy problem are obtained for initial data small enough, and locally in time. The entropy of the solution is controlled.

Chapter 5

Main results

Contents

5.1 Recent mathematical results 49

5.2 Our results 50

5.3 Proof of Proposition 5.2.1 51

5.1 Recent mathematical results

We focus on the following Cauchy problem

$$\begin{cases} \dfrac{\partial F}{\partial t}(t,k) = Q(F)(t,k), \quad t \in [0,T],\ k \geq 0, \\ F(0,k) = F_0(k), \end{cases} \tag{5.1}$$

with

$$Q(F)(t,k) = \int_0^\infty b(k,k')[F'(k^2+F)e^{-k} - F(k'^2+F')e^{-k'}]\ dk'.$$

As recalled in 2.2.3, M. Escobedo and S. Mischler ([22]) proved the existence and uniqueness of a measure solution of the problem (5.1) for different types of the cross section b.

5.2 Our results

The cross-section b defined in (3.5) does not satisfy conditions (2.29)-(2.30). $b(k,k')$ is singular at $k = k' = 0$. Still, we have remarked that measure solutions are expected for the Cauchy problem. We need to give a sense to

$$\int_s^t \int_0^\infty \phi(t,k)\ Q(F)(\tau,k)\ dkd\tau,$$

for any continuous and bounded test function ϕ. The a priori estimates of Propositions 4.1.1-4.3.1 are not sufficient to obtain finite

$$\Big| \int_s^t \int_0^\infty \phi(t,k)\ Q(F)(\tau,k)\ dkd\tau \Big|,$$

for any test function ϕ. Denote by $M^1(I\!R_+)$ the space of bounded measures on $I\!R_+$, and by $m(k) := \dfrac{k^2}{e^k - 1}$. In order to deal with solutions F to (5.1) in $C([0,T], M^1(I\!R_+))$, the following bound on F is required.

Proposition 5.2.1
Let $F \in C([0,T], M^1(I\!R_+))$ be such that $F(\tau,.) \neq m + \alpha\delta_{k=0},\ \alpha \in I\!R_+$ for all τ in $[0,T]$. If for any continuous and bounded function ϕ with second order with respect to k in the neighborhood of 0 and for any interval $J \subset [0,T]$,

$$\Big| \int_J \int_0^\infty \phi(\tau,k)\ Q(F)(\tau,k)\ dk\ d\tau \Big| \ < \ +\infty,$$

then

$$\int_0^\infty \frac{F}{k}(\tau,k)\ dk \ < \ +\infty, \quad a.a.\ \tau \in [0,T].$$

Remark 5.2.1
The condition "$F(\tau,.) \neq m + \alpha\ \delta_{k=0},\ \alpha \in I\!R_+$ for all τ in $[0,T]$" is not restrictive in the frame of the existence (and not for the uniqueness) of a solution to the Cauchy problem. At a first possible time t_* such that $F(t_*,.) = m + \alpha\delta_{k=0}$, we extend the solution obtained on $[0,t_*]$ by

$$F(\tau,.) = F(t_*,.), \quad \tau \in [t_*,T].$$

Remark 5.2.2
This boundedness of $\dfrac{F}{k}$ is important to establish the local existence result developped in the following theorem.

Let $c_1,\ c_2,\ c_3$ be the constants independant of F_0 defined further on in Lemmas 6.1.1, 6.1.2, 6.1.3.

Theorem 5.2.1
Let $T > 0$ and the initial datum F_0 satisfy

$$U := \Big(\int_0^{\frac{c_1}{8\pi}} (1+k)\frac{F_0(k)}{k}dk + \int_{\frac{c_1}{8\pi}}^{\infty} F_0(k)dk \Big)\ \exp(T\max\{c_1, \frac{32\pi^{3/2}}{c_1} + 8\pi\frac{c_3}{c_2}\}) \leq \frac{c_1}{c_2}\frac{c_1}{c_1+8\pi}. \tag{5.2}$$

Then, there exists a nonnegative solution $F \in C([0,T], M^1(0,+\infty))$ to the problem (5.1), such that

$$\frac{F(t,k)}{k} \in L^\infty_+(0,T; M^1(0,+\infty))$$

and

$$\int_0^\infty kF(t,k)dk < d,\ a.a.\ t > 0,$$

for some constant $d > 0$.
Moreover, if the initial datum F_0 has a finite entropy, then F is an entropy solution in the sense that

$$H(F)(t) \geq \alpha, \quad a.a.\ t > 0, \tag{5.3}$$

for some constant α.

Remark 5.2.3 *The solution F to the problem (5.1) in theorem 5.2.1 is meant in a weak sense, for continuous and bounded test functions, with second order with respect to k in the neighborhood of* 0.

5.3 Proof of Proposition 5.2.1

Let

$$\mathcal{I}(\phi) = \int_J \int_0^\infty \phi(\tau,k)\ Q(F)(\tau,k)\ dkd\tau.$$

It can be written as

$$\begin{aligned}\mathcal{I}(\phi) &= \int_J \int_0^\infty \int_0^\infty \frac{\phi(\tau,k)}{kk'} h(k,k')[F'(k^2+F)e^{-k} - F(k'^2+F')e^{-k'}]\ dk'dkd\tau \\ &= \mathcal{I}_1(\phi) + \mathcal{I}_2(\phi) + \mathcal{I}_3(\phi) + \mathcal{I}_4(\phi),\end{aligned}$$

with

$$h(k,k') = \int_0^\pi \frac{(1+\cos^2\theta)\sin\theta}{|w|}\ \exp(-\frac{A^2c}{2|w|^2}+k')\ d\theta,$$

$$A = k'-k+\frac{|w|^2}{2c}, \quad |w|^2 = k^2+k'^2-2kk'\cos\theta,$$

and,

$$\mathcal{I}_1(\phi) = -\int_J\int_0^\infty\int_0^\infty \frac{\phi(\tau,k)}{k}\ h(k,k')\ F\ k'e^{-k'}\ dk'\ dk\ d\tau,$$

$$\mathcal{I}_2(\phi) = \int_J\int_0^\infty\int_0^\infty \frac{\phi(\tau,k)}{kk'}\ h(k,k')[FF'(1-e^{-k'})]\ dk'\ dk\ d\tau,$$

$$\mathcal{I}_3(\phi) = \int_J\int_0^\infty\int_0^\infty \frac{\phi(\tau,k)}{kk'}\ (h(k,k')-h(k,0))\ [F'((k^2+F)e^{-k}-F)]\ dk'\ dk\ d\tau,$$

$$\mathcal{I}_4(\phi) = \int_J\int_0^\infty \frac{\phi(\tau,k)}{k}\ h(k,0)\ [(k^2+F)e^{-k}-F]\Big(\int_0^\infty \frac{F'}{k'}\ dk'\Big)\ dk\ d\tau.$$

Lemma 5.3.1
Let $F \in C([0,T], M^1(\mathbb{R}_+))$ be such that the mass $M(F)(t)$ is uniformly bounded from above.
For any continuous and bounded function ϕ with second order with respect to k in the neighborhood of 0,

$$|\mathcal{I}_j(\phi)| < \infty, \quad 1 \le j \le 3.$$

Proof of lemma 5.3.1.

$|\mathcal{I}_1(\phi)|$ and $|\mathcal{I}_2(\phi)|$ are finite because the second order with respect k of ϕ in the neighborhood of 0 deals with the singularity of $h(k,k')$ in $k = k' = 0$.

$\mathcal{I}_3(\phi)$ can be written as

$$\mathcal{I}_3(\phi) = \int_J\int_0^\infty\int_0^\infty\int_0^1 F'[ke^{-k}+F\ \frac{e^{-k}-1}{k}]\phi(\tau,k)\ \frac{\partial h}{\partial k'}(k,\gamma k')\ d\gamma\ dk\ dk'\ d\tau.$$

Here again, the second order with respect to k of ϕ in the neighborhood of 0 deals with the singularity of $\dfrac{\partial h}{\partial k'}$.

Thus, $|\mathcal{I}_3(\phi)|$ is finite.

So, proving proposition 5.2.1 comes back to prove the following lemma

Lemma 5.3.2

For any continuous and bounded function ϕ vanishing in a neighborhood of 0 with respect to k,

$$|\mathcal{I}_4(\phi)| < \infty \Longrightarrow \int_0^\infty \frac{F}{k}(\tau, k)\ dk \ < \ +\infty, \quad a.a.\ \tau \in [0, T].$$

Proof.

Consider

$$\mathcal{I}_4(\phi) = \int_J \int_0^\infty \psi(\tau, k)\ (F(\tau, k) - m(k))\ \Big(\int_0^\infty \frac{F'}{k'}\ dk' \Big)\ dk\ d\tau,$$

where

$$\psi(\tau, k) = \frac{8}{3}\frac{\phi(\tau, k)}{k^2}\ \exp(-\frac{1}{2}(-1 + \frac{1}{2}k)^2)\ (e^{-k} - 1).$$

It is sufficient to prove that for all $t \in [0, T]$, there exists a neighborhood V_t of t such that for almost all $s \in V_t$,

$$\int_0^\infty \frac{F(s, k')}{k'}\ dk'$$

is finite. We prove it ad absurdum. Let

$$S := \Big\{ t \in [0, T]; \quad \int_0^\infty \frac{F(t, k')}{k'}\ dk' = +\infty \Big\},$$

and

$$F(t, .) = L(t, .) + H_c(t, .) + H_d(t, .)$$

the decomposition at all time t of the bounded measure $F(t, .)$. $L(t, .)$ is the continuous absolute Lebesgue part of $F(t, .)$. $H_c(t, .)$ and $H_d(t, .)$ are respectively the continuous singular part and the discrete singular part of $F(t, .)$. We arrange the Dirac mesaures in $H_d(t, .)$ such that

$$H_d(t, .) = \sum_{j \geq 1} a_j(t) \delta_{k_j},$$

with the decreasing sequence of positive coefficients $a_j(t)$. We assume that there exists $t \in [0,T]$ such that for all neigborhood V_t of t, $|V_t \cap S| > 0$. The three following cases are to be considered.

- Either $\int_0^\infty H_c(t,k)\ dk > 0$:
  then, $\int_0^\infty H_c(t,k)\ dk > 0$ for $\alpha > 0$. The support of H_c limited to $]\alpha, +\infty[$ is include in a denumerable union of open intervals with small arbitrarily measure. In particular, it is include in $\cup I_n$, with

$$\int_{\cup I_n} m\ dk < \frac{1}{2}\int_\alpha^\infty H_c(t,k)\ dk.$$

  If for all integer n,

$$\int_{I_n} H_c(t,k)\ dk < \int_{I_n} m(k)\ dk,$$

  then

$$\begin{aligned}\int_\alpha^\infty H_c(t,k)\ dk &< \sum_n \int_{I_n} H_c(t,k)\ dk \\ &\leq \int_{\cup I_n} m\ dk < \frac{1}{2}\int_\alpha^\infty H_c(t,k)\ dk.\end{aligned}$$

  Thus, there exists an interval $I \subset]\alpha, +\infty[$ such that

$$\int_I (H_c(t,k) + L - m)\ dk > 0.$$

  By continuity in time of F, this is also true for a neighborhood V_t of t. Restricting eventually V_t, there exists an integer n such that

$$\sum_{j>n} a_j(s) < \frac{1}{4}\int_I (H_c + L - m)(s,k)\ dk, \quad s \in V_t.$$

  We construct a continuous function ψ, which is equal to 1 on I, which vanishes quickly on the boundary of I and on some small neigborhoods of eventual k_i, $1 \leq i \leq n$, being in I. For this function ψ, $\mathcal{I}_4 = +\infty$.

- Or $H_c(t,.) = 0$ and $\int_0^\infty |L(t,k) - m(k)|\, dk > 0$:

  then, $\int_\alpha^{+\infty} \mid L(t,k) - m(k) \mid dk > 0$ for $\alpha > 0$. By continuity in time of F, we can restrict V_t in order to obtain

$$\int_0^\infty |L(s,k) - m(k)|\, dk > 0, \quad a.a.\ s \in V_t.$$

  For almost all $s \in V_t$, there exists a set I_s of positive measure in $[\alpha, \infty[$, such that

$$a(s,k) := L(s,k) - m(k) \neq 0, \quad k \in I_s.$$

  Let $n(t)$ be such that

$$\sum_{j>n(t)} a_j(t) < \frac{1}{4} \int \mid L(t,k) - m(k) \mid dk.$$

  Let $\mathcal{X}$ be the function defined by

$$\begin{aligned} \mathcal{X}(s,k) &= \mathrm{sgn}(a(s,k)), \quad s \in V_t,\ k \in I_s, \\ \mathcal{X}(s,k) &= 0 \quad otherwise. \end{aligned}$$

  Let $\bar{\mathcal{X}}(s,k)$ be the characteristic function of the complementary of the support of $H_c(t,.) + H_d(t,.)$. Let

$$G_n(s) = \min\Big\{ \int_0^\infty \frac{F(s,k')}{k'}\, dk', n \Big\}.$$

  Then $G_n = n$ on V_t. The function a belonging to $L^1((0,T) \times I\!R_+)$, let $\varepsilon > 0$ be such that

$$\int_\Omega |a| < \frac{1}{4} \int_{V_t \times I\!R_+} |a|, \quad |\Omega| < \varepsilon.$$

  Take ψ continuous such that $|\psi| \leq 1$, $\psi = \bar{\mathcal{X}}\mathcal{X}$ outside of a set Ω of measure smaller that ε, and which vanishes in k_1, ..., k_n, we obtain

$$\begin{aligned} \Big| \int_{(0,T)\times I\!R_+} & (\psi(F-m)G_n - \bar{\mathcal{X}}\mathcal{X}(F-m)G_n)\, d\tau dk \Big| \\ &\leq (2n+1) \int_\Omega |a|\, d\tau dk \\ &\leq \frac{2n+1}{4} \int_{V_t \times I\!R_+} |a|\, d\tau dk \\ &\leq \frac{2n+1}{4n} \int_{(0,T)\times I\!R_+} \bar{\mathcal{X}}\mathcal{X}(F-m)\, G_n\, d\tau dk. \end{aligned}$$

Thus,

$$\int_{(0,T)\times I\!R_+} \bar{\mathcal{X}}\mathcal{X}\ (F-m)\ G_n\ d\tau\ dk \leq \frac{4n}{2n-1} \int_{(0,T)\times I\!R_+} \psi\ (F-m)\ G_n\ d\tau\ dk.$$

Passing to the limit in the previous inegality when $n \to +\infty$ leads to $\mathcal{I}_4 = +\infty$.

- Or $H_c(t,.) = 0$, $\int_0^\infty |L(t,k) - m(k)|\ dk = 0$ and $H_d(t,.) \neq 0$.
  Let n be such that
  $$\sum_{j>n} a_j < \frac{1}{4}\ a_1.$$
  Let I be a neighborhood of k_1 such that $k_2, \ldots, k_n \notin I$, so that
  $$\int_I (H_d(t,.) - a_1\ \delta_{k_1}) < \frac{1}{4}\ a_1.$$
  Restricting I if we need, and by continuity in time of $F(t,.)$, there exists a neighborhood W_t of t such that
  $$\int_I (F(s,k) - m(k))\ dk > \frac{1}{2}\ a_1, \quad s \in W_t.$$
  We choose a continuous function ψ which approaches the characteristic function of I and which is equal to 0 outside I. Then,
  $$\int_{W_t} \Big(\int_0^\infty \psi(s,k)\ (F(s,k) - m(k))\ dk \Big) \Big(\int_0^\infty \frac{F(s,k')}{k'}\ dk' \Big)\ ds = +\infty.$$

□

Lemmas 5.3.1-5.3.2 lead to Proposition 5.2.1.

The proof of Theorem 5.2.1 is done in the next chapter.

Chapter 6

Proof of the existence theorem

Contents

6.1	**Technical bounds on the cross-section h . . . . . .**	**58**
6.2	**Existence of a solution to the Cauchy problem . .**	**60**
6.3	**Study of the entropy and boundedness of the energy.**	**67**
6.4	**Conclusion. . . . . .**	**71**

In this section, we prove theorem 5.2.1. Solutions $F \in C(0,T;M^1(I\!R_+))$ to (5.1), such that

$$\frac{F(t,k)}{k} \in L^\infty_+(0,T;M^1(I\!R_+))$$

are considered .

Compared to the existence results in [22], the main problem here is to reach the frame $\frac{F(t,k)}{k} \in L^\infty_+(0,T;M^1(I\!R_+))$. Hence, the function $G(t,k) = \frac{F(t,k)}{k}$ is introduced. The problem to be solved is

$$\begin{cases} \dfrac{\partial G}{\partial t} = 2c^3 r_0^2 \pi^2 \displaystyle\int_0^\infty h(k,k')[G'(1+\frac{G}{k})e^{-k} - \frac{G}{k}(k'+G')e^{-k'}]\ dk',\ t \in [0,T],\ k>0, \\ G(0,k) = \dfrac{F_0(k)}{k}, \end{cases} \tag{6.1}$$

with $G \in L^\infty_+(0,T;M^1(I\!R_+))$. Here,

$$h(k,k') = \int_0^\pi \frac{(1+\cos^2\theta)\sin\theta}{|w|}\ \exp(-\frac{A^2 c}{2|w|^2} + k')\ d\theta,$$

$$A = k' - k + \frac{|w|^2}{2c}, \quad |w|^2 = k^2 + k'^2 - 2kk'\cos\theta.$$

For the sake of simplicity, $2c^3 r_0^2 \pi^2$ is taken equal to 1. Using the properties of h derived in Lemmas 6.1.1, 6.1.2, 6.1.3, we will use the equation (6.1) written in the following special shape

$$\begin{cases} \dfrac{\partial G}{\partial t} = \displaystyle\int_0^\infty h(k,k')G'e^{-k}\,dk' + \frac{G}{k}\Big[\int_0^\infty h(k,k')G'(e^{-k}-e^{-k'})\,dk' \\ \qquad\qquad - \displaystyle\int_0^\infty h(k,k')k'e^{-k'}\,dk'\Big], \\ G(0,k) = \dfrac{F_0(k)}{k}. \end{cases} \tag{6.2}$$

The proof of the theorem splits into three parts. In part 6.1, we obtain bounds on h, that will be useful in dealing with its singularity. Part 6.2 proves the existence of a nonnegative solution $F \in C([0,T], M^1(0,\infty))$ to (5.1), such that $\dfrac{F(t,k)}{k} \in L^\infty_+(0,T; M^1(I\!R_+))$. Part 6.3 states the entropy feature of F.

6.1 Technical bounds on the cross-section h

Lemma 6.1.1
There exists a constant $c_1 > 0$ such that,

$$4c_1 < \int_0^\infty h(k,k')k'e^{-k'}dk', \quad 0 < k < c_1,\ k' \geq 0.$$

Proof.

Let l be the positive limit of $\displaystyle\int_0^\infty h(k,k')k'e^{-k'}dk'$ when $k \to 0$. Then,

$$\int_0^\infty h(k,k')k'e^{-k'}dk' > \frac{l}{2}, \quad k < \eta, \text{ for some } \eta > 0.$$

Choose $c_1 = \min\{\dfrac{l}{8}, \eta\}$. □

Lemma 6.1.2
There exists a constant $c_2 > 0$ such that

$$h(k,k')(e^{-k} - e^{-k'}) \leq c_2, \quad 0 < k < c_1,\ k' \geq 0.$$

Proof.

For $0 < k' < 2c_1$,

$$h(k,k')|e^{-k} - e^{-k'}| \leq d\,\frac{|e^{-k} - e^{-k'}|}{|k'-k|} \leq d, \quad d > 0.$$

For $k' > 2c_1$,

$$\begin{aligned} h(k,k')(e^{-k} - e^{-k'}) &\leq \int_0^\pi \frac{(1+\cos^2\theta)\sin\theta}{|w|}\; e^{-\frac{A^2c}{2|w|^2}+k'-k}\; d\theta \\ &\leq \frac{d}{|k'-k|}, \quad d > 0, \end{aligned}$$

since $-\dfrac{A^2c}{2|w|^2} + k' - k \leq 0$. □

Lemma 6.1.3
There exists a constant $c_3 > 0$ such that

$$h(k,k')e^{-k} \leq c_3, \quad k' \geq 0, \quad k > c_1.$$

Proof.

First, $-\dfrac{A^2c}{2|w|^2} + k' - k \leq 0$, so that $\exp(-\dfrac{A^2c}{2|w|^2} + k' - k) \leq 1$. Then,

$$h(k,k')e^{-k} \leq \frac{2\pi}{|k-k'|}, \quad k > c_1, \quad k' \leq \frac{c_1}{2}.$$

Moreover,

$$h(k,k')e^{-k} \leq \frac{2\pi}{\sqrt{k}\sqrt{k'}}, \quad k > c_1, \quad k' \geq \frac{c_1}{2}.$$

Choose $c_3 = \dfrac{4\pi}{c_1}$. □

Truncated cross-section h_n will be used in the existence proof in order to avoid the singularity of h at $k = k' = 0$ in the approximation procedure.
Let $(h_n)_{n\in I\!N^*}$ be defined such that

$$h_n(k,k') = h(k,k')\ 1\!\!1_{\{k\in[\frac{1}{n},n]\}}.$$

Remark 6.1.1 *The constants c_1, c_2 and c_3 are linked to the function $h(k,k')$.*

6.2 Existence of a solution to the Cauchy problem

Throughout the proof, fixed point arguments will be used in the closed convex set K of nonnegative measures G, such that

$$\int_0^\infty G(t,k)dk \leq \frac{c_1}{c_2}, \quad a.a.\ t \in [0,T].$$

One solution is obtained as a limit of an approximated sequence.

The proof splits into three parts. The first proves the existence and uniqness of a solution to the approximated problem (6.3). The second proves the existence of a nonnegative solution $F \in C([0,T], M^1(\mathbb{R}_+))$ to (6.7) such that $\frac{F(t,k)}{k} \in L^\infty_+(0,T; M^1(\mathbb{R}_+))$. The third part states the passage to the limit when $n \to \infty$ in the weak formulation.

First step : proof of the existence and unicity of the truncated equation (6.3).

Let $g(t,k) : [0,T] \times [0,\infty[\to I\!R^+$ such that $\int_0^\infty g(t,k)dk \leq \frac{c_1}{c_2}$ and $n > \frac{c_1}{8\pi}$ be given. In this first step, the problem

$$\begin{cases} \dfrac{\partial G_n}{\partial t} = e^{-k}\displaystyle\int_0^\infty h_n(k,k')\ G_n'\ dk' + \frac{G_n}{k}\int_0^\infty h_n(k,k')\ (e^{-k} - e^{-k'})\ g'\ dk' \\ \qquad\qquad - \dfrac{G_n}{k}\displaystyle\int_0^\infty h_n(k,k')\ k'\ e^{-k'}\ dk', \\ G_n(0,k) = \dfrac{F_0(k)}{k}, \quad k \geq 0, \end{cases} \tag{6.3}$$

with unknown G_n will be solved in K with a Banach fixed point theorem.
For $u \in L^\infty_+(0,T; L^1(I\!R^+))$, define $\mathcal{F}(u) = U$ as the solution to

$$\begin{cases} \dfrac{\partial U}{\partial t} = e^{-k}\displaystyle\int_0^\infty h_n(k,k')\ u(t,k')\ dk' + \frac{U}{k}\int_0^\infty h_n(k,k')\ (e^{-k} - e^{-k'})\ g(t,k')\ dk' \\ \qquad\qquad - \dfrac{U}{k}\displaystyle\int_0^\infty h_n(k,k')\ k'\ e^{-k'}\ dk', \\ U(0,k) = \dfrac{F_0(k)}{k}, \quad k \geq 0. \end{cases} \tag{6.4}$$

It follows from the exponential form of U, that

$$U(t,k) \geq 0 \quad a.a.\ t \geq 0,\ k \geq 0.$$

Integrating (6.4) with respect to the variable k implies that

$$\frac{\partial}{\partial t}\int_0^\infty U(t,k)dk \leq \lambda_n \ \|u\|_{L^\infty_+(0,T;L^1(R_+))} + \tilde{\lambda}_n \ c_1 \int_0^\infty U(t,k)\ dk.$$

The constants λ_n and $\tilde{\lambda}_n$ take into account the compact support $[\frac{1}{n}, n]$ with respect to k of h_n. And so, using Gronwall's argument, the function U belongs to $L^\infty_+(0,T;L^1(I\!R_+))$.

Analogously, for any $u,\ \tilde{u} \in L^1_k(0,+\infty)$, the corresponding solutions $U,\ \tilde{U}$ to (6.4) satisfy

$$\frac{\partial}{\partial t}|U-\tilde{U}| \leq c_3 \int_0^\infty |u-\tilde{u}|\ dk - 4\pi\ |U-\tilde{U}|.$$

Hence,

$$\int_0^\infty |U-\tilde{U}|(t,k)\ dk \leq \frac{c_3}{4\pi}(1-e^{-4\pi t})\int_0^\infty |u-\tilde{u}|(t,k)\ dk, \quad a.a.\ t \in [0,\tilde{T}].$$

This implies that for $\tilde{T}$ small enough only depending on n, the map $\mathcal{F}: u \to U$ is a contraction from $L^\infty_+(0,\tilde{T};L^1(I\!R^+))$ into itself. Then, $\mathcal{F}$ admits a unique fixed point on $L^\infty_+(0,\tilde{T};L^1(I\!R^+))$, denoted by U.
The argument can be iterated to obtain a unique solution $U = G_n$ in $L^\infty_+(0,T;L^1(I\!R^+))$ to (6.3). □

Furthermore, G_n belongs to the convex set K. Indeed, it follows from (6.3) and Lemma 6.1.1, that, for $0 < k < \frac{c_1}{8\pi}$,

$$\begin{aligned}
\frac{\partial}{\partial t}\int_0^{\frac{c_1}{8\pi}} G_n(t,k)\ dk \ &\leq \ \int_0^{\frac{c_1}{8\pi}} e^{-k}\int_0^\infty h(k,k')\ G_n'\ dk'\ dk \\
&+ \ \int_0^{\frac{c_1}{8\pi}} \frac{G_n}{k}\int_0^\infty h_n\ (e^{-k}-e^{-k'})\ g'\ dk'dk \\
&- \ 2c_1\int_0^{\frac{c_1}{8\pi}} \frac{G_n}{k}\ dk.
\end{aligned}$$

Then, by Lemma 6.1.2,

$$\begin{aligned}
\frac{\partial}{\partial t}\int_0^{\frac{c_1}{8\pi}} G_n(t,k)\ dk &\leq \int_0^{\frac{c_1}{8\pi}} e^{-k}\int_0^{\infty} h(k,k')\ G_n'\ dk'\ dk\ -\ c_1\int_0^{\frac{c_1}{8\pi}}\frac{G_n}{k}\ dk \\
&+\ c_2\int_0^{\frac{c_1}{8\pi}}\frac{G_n}{k}\left(\int_0^{\infty} g'\ dk' - \frac{c_1}{c_2}\right) dk \\
&\leq \int_0^{\frac{c_1}{8\pi}} e^{-k}\int_0^{\infty} h(k,k')\ G_n'\ dk'\ dk\ -\ c_1\int_0^{\frac{c_1}{8\pi}}\frac{G_n}{k}\ dk,
\end{aligned}$$

since $g \in K$.
And so,

$$\begin{aligned}
\frac{\partial}{\partial t}\int_0^{\frac{c_1}{8\pi}} G_n(t,k)\ dk &\leq 4\pi\int_0^{\frac{c_1}{8\pi}}\frac{1}{\sqrt{k}}\ dk\int_0^{\infty}\frac{G_n'}{\sqrt{k'}}\ dk' - c_1\int_0^{\frac{c_1}{8\pi}}\frac{G_n}{k}\ dk \\
&\leq \sqrt{2c_1\pi}\int_0^{\infty}\frac{G_n}{\sqrt{k}}\ dk - c_1\int_0^{\frac{c_1}{8\pi}}\frac{G_n}{k}\ dk \\
&\leq \int_0^{\frac{c_1}{8\pi}}\frac{G_n}{\sqrt{k}}\ (\sqrt{2c_1\pi} - \frac{c_1}{\sqrt{k}})\ dk + \sqrt{2c_1\pi}\int_{\frac{c_1}{8\pi}}^{\infty}\frac{G_n}{\sqrt{k}}\ dk \\
&\leq \sqrt{2c_1\pi}\int_{\frac{c_1}{8\pi}}^{\infty}\frac{G_n}{\sqrt{k}}\ dk.
\end{aligned}$$

Hence,

$$\frac{\partial}{\partial t}\int_0^{\frac{c_1}{8\pi}} G_n(t,k)\ dk \leq \frac{32\pi^{3/2}}{c_1}\int_{\frac{c_1}{8\pi}}^{\infty} k\ G_n\ dk. \tag{6.5}$$

Using (6.3) and Lemmas 6.1.2 and 6.1.3 implie that

$$\begin{aligned}
\frac{\partial}{\partial t}\int_0^\infty k\ G_n(t,k)\ dk &= \int_0^\infty G_n \int_0^\infty h_n(k,k')\ (e^{-k}-e^{-k'})\ g'\ dk'\ dk \\
&= \int_0^{\frac{c_1}{8\pi}} G_n \int_0^\infty h_n(k,k')\ (e^{-k}-e^{-k'})\ g'\ dk'\ dk \\
&+ \int_{\frac{c_1}{8\pi}}^\infty G_n \int_0^\infty h_n(k,k')\ (e^{-k}-e^{-k'})\ g'\ dk'\ dk \\
&\le c_2 \int_0^{\frac{c_1}{8\pi}} G_n \int_0^\infty g'\ dk'\ dk \\
&+ \int_{\frac{c_1}{8\pi}}^\infty G_n \int_0^\infty h_n(k,k')\ e^{-k}\ g'\ dk'\ dk \\
&\le c_1 \int_0^{\frac{c_1}{8\pi}} G_n\ dk + c_3\ \frac{c_1}{c_2} \int_{\frac{c_1}{8\pi}}^\infty G_n\ dk.
\end{aligned}$$

Therefore,

$$\frac{\partial}{\partial t}\int_0^\infty k\ G_n(t,k)\ dk \le c_1\ \Big(\int_0^{\frac{c_1}{8\pi}} G_n\ dk + \frac{8\pi c_3}{c_1\ c_2}\int_{\frac{c_1}{8\pi}}^\infty k\ G_n\ dk\Big). \tag{6.6}$$

It follows from (6.5) and (6.6) that

$$\begin{aligned}
\frac{\partial}{\partial t}\Big(\int_0^{\frac{c_1}{8\pi}}(1+k)G_n\ dk + \int_{\frac{c_1}{8\pi}}^\infty kG_n dk\Big) &\le c_1\int_0^{\frac{c_1}{8\pi}} G_n dk + \Big(\frac{32\pi^{3/2}}{c_1} + 8\pi\frac{c_3}{c_2}\Big)\int_{\frac{c_1}{8\pi}}^\infty kG_n dk \\
&\le \max\{c_1, \frac{32\pi^{3/2}}{c_1} + 8\pi\frac{c_3}{c_2}\}\Big(\int_0^{\frac{c_1}{8\pi}}(1+k)G_n dk + \int_{\frac{c_1}{8\pi}}^\infty kG_n dk\Big).
\end{aligned}$$

And so, by Gronwall's argument,

$$\begin{aligned}
&\int_0^{\frac{c_1}{8\pi}}(1+k)\ G_n(t,k)\ dk + \int_{\frac{c_1}{8\pi}}^\infty k\ G_n\ dk \\
&\quad\le \Big(\int_0^{\frac{c_1}{8\pi}}(1+k)G(0,k)dk + \int_{\frac{c_1}{8\pi}}^\infty kG(0,k)dk\Big)\ \exp(T\max\{c_1, \frac{32\pi^{3/2}}{c_1} + 8\pi\frac{c_3}{c_2}\}).
\end{aligned}$$

Hence,

$$\begin{aligned}
\int_0^\infty G_n(t,k)\ dk &\le \int_0^{\frac{c_1}{8\pi}}(1+k)\ G_n\ dk + \int_{\frac{c_1}{8\pi}}^\infty G_n\ dk \\
&\le \int_0^{\frac{c_1}{8\pi}}(1+k)\ G_n\ dk + \frac{8\pi}{c_1}\int_{\frac{c_1}{8\pi}}^\infty k\ G_n\ dk.
\end{aligned}$$

Then,

$$\begin{aligned}\int_0^\infty & G_n(t,k)\ dk \\ & \leq (1+\frac{8\pi}{c_1})\Big(\int_0^{\frac{c_1}{8\pi}}(1+k)\ G(0,k)\ dk+\int_{\frac{c_1}{8\pi}}^\infty k\ G(0,k)\ dk\Big)e^{T\max\{c_1,\frac{32\pi^{3/2}}{c_1}+8\pi\frac{c_3}{c_2}\}} \\ & := (1+\frac{8\pi}{c_1})\ U,\end{aligned}$$

which implies that $G_n \in K$ by assumption (5.2) of Theorem 5.2.1. □

Second step : proof of the existence of a solution G_n to (6.7).

In this second step, a Schauder fixed point theorem is used to prove the existence of a solution $G_n \in K$ to

$$\left\{\begin{array}{l}\dfrac{\partial G_n}{\partial t} = e^{-k}\displaystyle\int_0^\infty h_n(k,k')\ G_n'\ dk' + \frac{G_n}{k}\int_0^\infty h_n(k,k')\ (e^{-k}-e^{-k'})\ G_n'\ dk' \\ \qquad\qquad - \dfrac{G_n}{k}\displaystyle\int_0^\infty h_n(k,k')\ k'\ e^{-k'}\ dk', \\ G_n(0,k) = \dfrac{F_0(k)}{k}, \quad k \geq 0,\end{array}\right. \tag{6.7}$$

such that $\displaystyle\int_0^\infty G_n(t,k)\ dk \leq \frac{c_1}{c_2}, \quad a.a\ t \in (0,T)$.

Let $\mathcal{H}$ be the map defined on K by $\mathcal{H}(g) = G_n$ where $G_n \in K$ is the solution of (6.3).
The map $\mathcal{H}$, taking its values in the convex set K, is compact for the weak * topology of $L^\infty_+(0,T;M^1(I\!R_+))$. It is moreover continuous. Indeed, let $g_j \rightharpoonup g$ for the weak * topology of $L^\infty_+(0,T;M^1(I\!R^+))$. Denote by $(G_j) = (\mathcal{H}(g_j))_{j\in I\!N}$. By the compactness of $\mathcal{H}$, there is a subsequence (G_{jl}) of (G_j) and a function G in K such that $G_{jl} \rightharpoonup G$. Moreover G is the unique solution to (6.3). Hence, the whole sequence (G_j) converges to G for the weak * topology of $L^\infty_+(0,T;M^1(I\!R_+))$. By the Schauder fixed point theorem, $\mathcal{H}$ admits a fixed point, denoted by G_n, solution in K to (6.7).
The nonnegative function $F_n = kG_n$ is such that

$$\int_0^\infty F_n(t,k)\ dk \leq \int_0^\infty F(0,k)\ dk, \qquad \int_0^\infty \frac{F_n}{k}(t,k)\ dk \leq \frac{c_1}{c_2}, \quad a.a.\ t \in (0,T), \tag{6.8}$$

and is solution to

$$\left\{\begin{array}{l} \dfrac{\partial F_n}{\partial t} = ke^{-k}\displaystyle\int_0^\infty h_n(k,k')\ \frac{F_n'}{k'}\ dk' + \frac{F_n}{k}\int_0^\infty h_n(k,k')\ (e^{-k}-e^{-k'})\ \frac{F_n'}{k'}\ dk' \\ \qquad\qquad - \dfrac{F_n}{k}\displaystyle\int_0^\infty h_n(k,k')\ k'\ e^{-k'}\ dk', \\ \qquad\qquad F_n(0,k) = F_0(k). \end{array}\right. \tag{6.9}$$

Third step : passage to the limit in (6.9) when n tends to infinity.

In this third step, the passage to the limit when $n \to +\infty$ in (6.9) is performed, which leads to a solution F to the genuine problem (5.1).
By (6.9), there is a measure $G \in L^\infty_+(0,T;M^1(I\!R_+))$ such that $F_n \rightharpoonup kG$ and $\dfrac{F_n}{k} \rightharpoonup G$ in $L^\infty_+(0,T;M^1(I\!R_+))$ for the weak $*$ topology.
As it is writen in 5.2.1, we consider continuous and bounded test functions ϕ with second order with respect to k in the neigborhood of 0.
Multiplying (6.9) by ϕ and integrating on $[0,t]\times\mathbb{R}_+$ leads to

$$\int_0^\infty F(t,k)\ \phi(t,k)\ dk - \int_0^\infty F_0(k)\ \phi(0,k)\ dk - \int_0^\infty\int_0^t F(s,k)\frac{\partial\phi}{\partial s}(s,k)\ ds\ dk$$

$$= A_n + B_n + C_n,$$

with

$$\begin{aligned} A_n &= \int_0^t\int_0^\infty \frac{F_n}{k}\ \phi(s,k)\int_0^\infty h_n(k,k')\ (e^{-k}-e^{-k'})\ \frac{F_n'}{k'}\ dk'\ dk\ ds, \\ B_n &= \int_0^t\int_0^\infty k\ e^{-k}\ \phi(s,k)\int_0^\infty h_n(k,k')\ \frac{F_n'}{k'}\ dk'\ dk\ ds, \\ C_n &= -\int_0^t\int_0^\infty \frac{F_n}{k}\ \phi(s,k)\int_0^\infty h_n(k,k')\ k'\ e^{-k'}\ dk'\ dk\ ds. \end{aligned}$$

Let $U(k,k') = h(k,k')\ (e^{-k}-e^{-k'})$. For all $K>0$, A_n can be written as

$$A_n = X_{n,K} + \bar{X}_n + A_{n,K} + \bar{A}_{n,K},$$

where

$$\begin{aligned}
X_{n,K} &= \int_0^t \int_0^K \frac{F_n}{k}\,\phi(s,k) \int_0^K U(k,k')\,\frac{F_n'}{k'}\,dk'\,dk\,ds \\
\bar{X}_n &= -\int_0^t \int_0^{\frac{1}{n}} \frac{F_n}{k}\,\phi(s,k) \int_0^\infty U(k,k')\,\frac{F_n'}{k'}\,dk'\,dk\,ds \\
A_{n,K} &= \int_0^t \int_0^K \frac{F_n}{k}\,\phi(s,k) \int_K^\infty U(k,k')\,\frac{F_n'}{k'}\,dk'\,dk\,ds \\
\bar{A}_{n,K} &= \int_0^t \int_K^n \frac{F_n}{k}\,\phi(s,k) \int_0^\infty U(k,k')\,\frac{F_n'}{k'}\,dk'\,dk\,ds.
\end{aligned}$$

First, $\bar{X}_n \underset{n\to\infty}{\longrightarrow} 0$ thanks to the second order with respect to k of ϕ in the neighborhood of 0.
Then, $A_{n,K}$ and $\bar{A}_{n,K}$ tend to 0 when $K \to \infty$, uniformly with respect to n.
Finally, by the Stone-Weierstrass theorem, for $K > 0$ large enough and every $\varepsilon \in \mathbb{R}_+^*$, there exist $J \in \mathbb{N}^*$ and continuous functions

$$\beta_1, \cdots, \beta_J, \gamma_1, \cdots, \gamma_J : \mathbb{R}_+ \to \mathbb{R},$$

such that

$$\text{for all } \ 0 < k < K,\ 0 < k' < K, \quad \left| U(k,k') - \sum_{j=1}^J \beta_j(k)\gamma_j(k') \right| \le \varepsilon.$$

Let

$$U_J(k,k') = \sum_{j=1}^J \beta_j(k)\gamma_j(k').$$

Then,

$$|X_{n,K} - X| \le \left| \left\langle \frac{F_n}{k} \otimes \frac{F_n'}{k'} - \frac{F}{k} \otimes \frac{F'}{k'}, \phi\,(U - U_J) \right\rangle \right| + \left| \left\langle \frac{F_n}{k} \otimes \frac{F_n'}{k'} - \frac{F}{k} \otimes \frac{F'}{k'}, \phi\, U_J \right\rangle \right|.$$

The first term tends to 0 when $J \to \infty$ uniformly with respect to n because

$$\left| \left\langle \frac{F_n}{k} \otimes \frac{F_n'}{k'} - \frac{F}{k} \otimes \frac{F'}{k'}, \phi\,(U - U_J) \right\rangle \right| \ \le \ 2|\phi|_\infty \Big(\int \frac{F_n}{k} dk \Big)^2 \sup_{k,k'} |(U - U_J)(k,k')|.$$

The second term tends to 0 when $n \to \infty$ for all J.

Therefore,

$$\int_0^t \int_0^\infty \frac{F_n}{k}\ \phi(s,k) \int_0^\infty h_n(k,k')\ (e^{-k} - e^{-k'})\ \frac{F_n'}{k'}\ dk'\ dk\ ds$$

tends to

$$\int_0^t \int_0^\infty \frac{F}{k}\ \phi(s,k) \int_0^\infty h(k,k')\ (e^{-k} - e^{-k'})\ \frac{F'}{k'}\ dk'\ dk\ ds,$$

when n tends to infinity.
The passage to the limit in B_n and C_n when $n \to \infty$ can be done analogously. So, performing the passage to the limit when $n \to +\infty$ in (6.9) implies that F is a solution to

$$\begin{cases} \dfrac{\partial F}{\partial t} = k\ e^{-k} \displaystyle\int_0^\infty h(k,k')\ \frac{F'}{k'}\ dk' + \frac{F}{k} \int_0^\infty h(k,k')\ (e^{-k} - e^{-k'})\ \frac{F'}{k'}\ dk' \\ \qquad\qquad\qquad\qquad - \dfrac{F}{k} \displaystyle\int_0^\infty h(k,k')\ k'\ e^{-k'}\ dk', \\ \qquad\qquad\qquad\qquad F(0,k) = F_0(k), \end{cases}$$

which also means that F is a solution of the problem (5.1). The continuity of F with respect to time follows from the boundedness of $Q(F)$ in $L^\infty_+((0,T); M^1(I\!R_+))$.

6.3 Study of the entropy and boundedness of the energy.

In order to prove the entropy feature of F stated in Theorem 5.2.1, the following Lemma is established.

Lemma 6.3.1
If $F_n(t,\cdot) \rightharpoonup F(t,\cdot) = \bar{F}(t,\cdot)dk + \mu_s$, then

$$\liminf_{n\to\infty} -H(F_n)(t) \geq -H(F)(t) - < \mu_s, k >, \tag{6.10}$$

$\bar{F}(t,\cdot)$ and μ_s being respectively the absolute Lebesgue part and the singular part of $F(t,\cdot)$.

Proof of lemma 6.3.1.

Recall that

$$H(\bar{F})(t) = \int_0^\infty [(k^2+\bar{F}(t,k))\ln(k^2+\bar{F}(t,k)) - \bar{F}(t,k)\ln\bar{F}(t,k) - k^2\ln k^2 - k\bar{F}(t,k)]\,dk.$$

Let

$$h(y,k) = -(k^2+y)\ln(k^2+y) + y\ln y + k^2\ln k^2 + ky. \tag{6.11}$$

It is a convex function with respect to the variable y.
Prove that

$$\int_\gamma^\delta h(k,\bar{F}(t,k))\,dk \le \liminf_{n\to\infty}\int_\gamma^\delta h(k,F_n(t,k))\,dk, \quad \delta \ge \gamma \ge 0. \tag{6.12}$$

Let $j \in I\!N^*$ and O be an open neighborhood of support μ_s such that $|O| < (\frac{\delta-\gamma}{j})^2$.
O is the denumerable union of open intervals. Denote by O_1 one of the intervals where μ_s has its bigger mass, ..., O_{l+1} one of the intervals where μ_s has its bigger mass after O_l, $l \ge 1$. μ_s being of finite mass, for any $\alpha > 0$, there is an integer l_α such that

$$\mu_s(\bigcup_{l\ge l_\alpha} O^l) < \alpha,$$

and for l_α large enough,

$$\int_{\bigcup\limits_{l\ge l_\alpha} O^l} F(t,k)\,dk < \alpha.$$

Hence,

$$\lim_{n\to\infty}\int_{\bigcup\limits_{l\ge l_\alpha} O^l} F_n(t,k)\,dk \quad < \quad 2\alpha. \tag{6.13}$$

Let α be such that $\alpha << \dfrac{\delta-\gamma}{j}$ and $\tilde{I}_i = I_i \setminus (O \cap I_i)$, with

$$I_i =]\gamma + i(\frac{\delta-\gamma}{j}), \gamma + (i+1)(\frac{\delta-\gamma}{j})[.$$

Then,

$$\int_{\tilde{I}_i} F_n(t,k)\,dk = \int_{I_i\setminus\bigcup\limits_{l=1}^{l_\alpha-1} O^l} F_n\,dk - \int_{\bigcup\limits_{l\ge l_\alpha} O^l} F_n\,dk \underset{n\to\infty}{\to} \int_{I_i\setminus\bigcup\limits_{l=1}^{l_\alpha-1} O^l} (\bar{F}dk + d\mu_S) - A' := U,$$

where $A' < 2\alpha$ by (6.13).
Thus,

$$U = \int_{\tilde{I}_i} \bar{F}\ dk + B,$$

with

$$B := \int_{\bigcup\limits_{l \geq l_\alpha} O^l} \bar{F}\ dk + \int_{I_i \setminus \bigcup\limits_{l=1}^{l_\alpha - 1} O^l} d\mu_s - A' < 4\alpha.$$

Hence,

$$\liminf_{n\to\infty}\ h(\gamma + i(\frac{\delta-\gamma}{j}), \frac{1}{|\tilde{I}_i|}\int_{\tilde{I}_i} F_n\ dk) = h(\gamma + i(\frac{\delta-\gamma}{j}), \frac{1}{|\tilde{I}_i|}\int_{\tilde{I}_i} \bar{F}\ dk + \frac{B}{|\tilde{I}_i|}). \tag{6.14}$$

Let $\varepsilon > 0$ be given. First, it holds that for some $\lambda_\varepsilon > 0$,

$$h(k,\lambda) < \varepsilon, \quad \lambda > \lambda_\varepsilon, \quad k \in [\gamma, \delta].$$

Then, by the uniform continuity of $h(k,\lambda)$ on $[\gamma,\delta] \times [0, \lambda_\varepsilon]$, it holds that

$$\int_\gamma^\delta h(k, F_n)\ dk = \lim_{j\to\infty} \sum_{i=0}^{j-1} \int_{\tilde{I}_i} h(\gamma + i(\frac{\delta-\gamma}{j}), F_n)\ dk.$$

Thanks to Jensen's inequality,

$$\frac{1}{|\tilde{I}_i|}\int_{\tilde{I}_i} h(\gamma + i(\frac{\delta-\gamma}{j}), F_n(t,k))\ dk \geq h(\gamma + i(\frac{\delta-\gamma}{j}), \frac{1}{|\tilde{I}_i|}\int_{\tilde{I}_i} F_n(t,k)\ dk).$$

It follows from the constant sign of $h(k, F_n) - kF_n$ that

$$\begin{aligned}
\liminf_{n\to\infty} \int_\gamma^\delta h(k, F_n)\ dk &\geq \liminf_{n\to\infty}\ \lim_{j\to\infty} \sum_{i=0}^{j-1} |\tilde{I}_i|\ h(\gamma + i(\frac{\delta-\gamma}{j}), \frac{1}{|\tilde{I}_i|}\int_{\tilde{I}_i} F_n\ dk) \\
&= \lim_{j\to\infty}\ \liminf_{n\to\infty} \sum_{i=0}^{j-1} |\tilde{I}_i|\ h(\gamma + i(\frac{\delta-\gamma}{j}), \frac{1}{|\tilde{I}_i|}\int_{\tilde{I}_i} F_n\ dk).
\end{aligned}$$

And so, by (6.14),

$$\liminf_{n\to\infty} \int_\gamma^\delta h(k, F_n)\ dk \geq \lim_{j\to\infty} \sum_{i=0}^{j-1} |\tilde{I}_i|\ h(\gamma + i(\frac{\delta-\gamma}{j}), \frac{1}{|\tilde{I}_i|}\int_{\tilde{I}_i} \bar{F}\ dk + \frac{B}{|\tilde{I}_i|}).$$

Hence, for $j \to \infty$ and $\alpha \to 0$,

$$\liminf_{n\to\infty} \int_\gamma^\delta h(k, F_n)\ dk \geq \int_\gamma^\delta h(k, \bar{F})\ dk.$$

For $\delta \to \infty$ and $\gamma \to 0$,

$$\liminf_{n\to\infty} \int_0^\infty h(k, F_n)(t,k)\ dk \geq \int_0^\infty h(k, \bar{F})(t,k)\ dk,$$

$$\text{i.e} \quad \liminf_{n\to\infty} -H(F_n)(t) \geq -H(\bar{F})(t), \quad a.a.\ t > 0.$$

By definition ([17]), $H(F) = H(\bar{F}) - M(k\mu_s)$, so that,

$$\liminf_{n\to\infty} -H(F_n)(t) \geq -H(F)(t) - < \mu_s, k >, \quad a.a.\ t > 0.$$

□

Proof of (5.3).

The proof of Proposition 4.2.1 implies that

$$\frac{d}{dt}H(F_n) = \frac{1}{2}\int_0^\infty \int_0^\infty b(k,k')\ j(F_n(k'^2 + F_n')e^{-k'}, F_n'(k^2 + F_n)e^{-k})\ dk'\ dk, \tag{6.15}$$

with j defined in the proof of Proposition 4.2.1. This implies that

$$H(F_n)(t) \geq H(F_n(0)) = H(F_0) \quad a.a.\ t > 0, \tag{6.16}$$

so that

$$H(F)(t) \geq H(F_0) - < \mu_s, k > .$$

The control of the entropy H enables to bound the energy.
$< \mu_s, k >$ is bounded from above. Indeed, by (4.2), (6.8) and (6.16),

$$\int_0^\infty kF_n(t,k)\ dk < c,$$

uniformly with respect to n. □

Remark 6.3.1
F. Demengel studied the passage to the limit of functionals of bounded measures ([17] and [16]) in the following frame

Let Y an euclidien space with finite dimension and Ψ a proper convex l.s.c function from Y into $\bar{\mathbb{R}}$. It is assumed that

$$\Psi(0) = 0, \quad \Psi \geq 0,$$

and that there exist any constants c_0, $c_1 > 0$, such that

$$c_0(|\zeta| - 1) \leq \Psi(\zeta) \leq c_1(|\zeta| + 1), \quad \zeta \in Y.$$

The asymptotic function $\Psi_\infty(\zeta)$ of Ψ is defined by

$$\Psi_\infty(\zeta) = \lim_{t \to \infty} \frac{\Psi(t\zeta)}{t}.$$

For any bounded open set Ω of $\mathbb{R}^n$ and any bounded measure $\mu \in M(\Omega, Y)$, $\Psi(\mu)$ is defined by

$$\Psi(\mu) = \Psi \circ g \; dx + \Psi_\infty(\mu^s), \tag{6.17}$$

where $\mu = g \; dx + \mu^s$ is the Lebesgue decomposition of μ. If $\mu \geq 0$,

$$\Psi_\infty(\mu^s) = (\Psi_\infty \circ h^s) \; |\mu^s|.$$

Lemma 6.3.2
If $< \mu_n, \varphi > \; \to \; < \mu, \varphi >$, $\varphi \in C_c(\Omega, Y)$, then $\Psi(\mu) \leq \liminf_{n \to \infty} \Psi(\mu_n)$.

The function h defined in (6.11) does not satisfy the assumptions of Demengel's Lemma, because h not only depends on F but also on k.

6.4 Conclusion.

In this first part of this thesis, we have proven the existence of a solution to a homogeneous quantum kinetic evolutionary problem describing the Compton effect. Due to a strong singularity in the collision operator, the mathematical framework is the set of photon distribution functions F such that F and $\dfrac{F(t,k)}{k}$ are bounded measures. A local in time existence theorem is proven for small initial data. The mathematical entropy of the solutions is bounded from below. As in many nonlinear problems, obtaining a solution as the limit of an approximated sequence does not provide its uniqueness.

An interesting topic to study, after having proven the existence of a solution to the equation (3.1), is the formation of Bose-Einstein condensates.

By isolating in the measure solution F of equation (5.1) its possible singular part at energy zero, i.e. by splitting $F = \alpha(t)\ \delta_{\{k=0\}} + G$, we obtain equations describing the evolution of α and G. The Bose-Einstein condensates are described by $\alpha(t)\ \delta_{\{k=0\}}$. So, the knowledge of α provides the evolution of possible Bose condensates.

So far, Bose-Einstein condensation has been obtained asymptotically in time from a quantum Boltzmann equation with a simplified collision kernel. In order to study Bose-Einstein condensation, the Gross-Pitaevskii equation may be needed.
W. Bao, L. Pareschi and P.A. Markowich in [3] have studied Bose-Einstein condensation in a dilute gas at a numerical level.

Part II

Modelling and 3D simulation of the satellite charge in plasmic environment

Chapter 7

The spatial plasma environment

Contents

7.1 The plasmas 75

7.1.1 Fundamental quantities in plasma physics 76

7.1.2 Sheath and presheath 77

7.2 The earth magnetosphere 77

7.3 Plasma engines 80

7.1 The plasmas

A plasma is a gas electrically charged. Its temperature is over 25000 degrees. It is made of ions and free electrons. In the earth magnetosphere, the ions are mainly H^+, He^+ and O^+. As the ion mass is larger than the electron mass, ions can be considered to be motionless with respect to the electrons. The interactions between charged particles constrain the electrons to surround the ions.

We focus on the simulation a satellite charge in a spatial plasma environment. We refer to the modelling introduced by O. Chanrion during his thesis ([13]) in a two-dimensional axisymmetric frame. Satellites in geostationary orbit using an electric engine with Hall effect ($SPT-100$ type) are considered here.

7.1.1 Fundamental quantities in plasma physics

The Debye length

Consider a collection of charged particles. If one of them, called the test charge is placed at a given position, the other will react. The nearby particles of the opposite sign to the test charge move slightly away. The net effect is to screen the test charge. The distance beyond which the test charge is effectively screened, is called the Debye length.
It is proportional to the square of the ratio of the temperature over the plasma density. It is given by

$$\lambda_d = \sqrt{\frac{\epsilon_0 k T_e}{n_0 e^2}},$$

where
- ϵ_0 is the electric permittivity of vacuum,
- e is the elementary charge,
- T_e is the temperature of electrons,
- k is the Boltzmann constant,
- n_0 is the plasma density.

In spatial plasma environment with high temperature and low density, the Debye length is about thousand metres.

We introduce the Debye number which enable us to compare the Debye length to the caracteristic length of the satellite (D),

$$N_D = \frac{\lambda_d}{D}.$$

The individual interaction between two particles for which the distance is larger than the Debye length is negligible. So, the far-away plasma parts interact via collective interactions.
The collective interactions take place via electric and magnetic forces. These interactions are due to the repartition of the charge density and of the electric current in the plasma.

The Larmor radius

The characteristic dimension of a plasma which measures the effect of an exterior magnetic field (of the plasma) is given by the Larmor radius. This length

is defined by the curve radius of the particles trajectories in the presence of the magnetic field. The Larmor radius writes as

$$\rho_L = m \frac{v_\perp}{eB},$$

where
• B is the magnetic field,
• $v_\perp$ is the velocity perpendicular to the particle velocity.
Let

$$N_L = \frac{\rho_L}{D},$$

be the number Larmor. It is sufficiently large near the satellite to neglect all magnetic phenomena.

The typical characteristics of the magnetospheric plasma are

$n(m^{-3})$	1×10^6
$kT_e(eV)$	1.2×10^4
$\lambda_d(m)$	8.14×10^2

n denotes the plasma density, T_e is the electron temperature, k is the Boltzmann constant and λ_d is the Debye length.

7.1.2 Sheath and presheath

When a plasma is limited by a boundary (for example a metallic wall), a sheath is formed around this boundary. The properties of the plasma in the sheath are particular. In the sheath, the ion and electron densities are unequal and the potential can vary. Its characteristic spatial scale is the Debye length.
In the presheath, the plasma is quasineutral.

7.2 The earth magnetosphere

The earth magnetic field originates in its liquid core, where electric currents are excited by fluid flows. The field intensity is about 6×10^{-5} tesla at the

magnetic poles, located about 10 degrees off the geographic poles. At the surface, the field resembles a dipole with added irregular components, and the field is dipole-like up to distances of 5 r to 8 r, where r is the earth radii.
The distant field of earth is greatly modified by the solar wind, a hot outflow from the sun, consisting of solar ions (mainly hydrogen) moving at about 400 km/s with typical density at earth's orbit of 6 ions/cm^3. The earth field forms an obstacle to the solar wind, that confines the field lines and plasmas into an elongated cavity, known as the earth magnetosphere. The boundary between the two is called the magnetopause. It roughly behaves like a droplet of liquid exposed to a supersonic flow.
Outside the magnetopause is the bow shock, where the velocity of the solar wind abruptly drops as it approaches the magnetosphere. On the sun side of the earth, the magnetopause distance is approximately 10 earth radii. On the night side, it extends into a long cylindrical magnetotail at least several hundred radii long, gradually turning into a wake.
The region between the bow shock and the magnetopause is called the magnetosheath. The particles in this region originate from the solar wind. The plasma density typically decreases from the bow shock to the magnetopause; however, it is always higher than the magnetospheric plasma density.
The magnetosphere contains magnetically trapped plasma (gas of free ions and electrons) and is composed of several regions that create the field topology. The magnetotail is formed by tail lobes and the plasma sheet (an open polar cap and closed nightside auroral field lines, respectively). In the inner magnetosphere there is plasmasphere from mid to low latitudes. Both overlapping the plasmasphere and the inner plasmasheet, are radiation belts and ring current; The geostationary orbit is also around. Closest regions to the magnetopause are called boundary layers. Their cusps are shown on the picture 7.1. The particles coming from the solar wind during a solar eruption come into the magnetosphere via the cusps.

Picture 7.1 illustrates formally the mentioned regions.

Picture 7.2 shows a solar eruption.

The earth magnetosphere is a hot collisionless plasma (when solar eruption occurs). Each volume which dimension is about the Debye length contains a large number of particles.

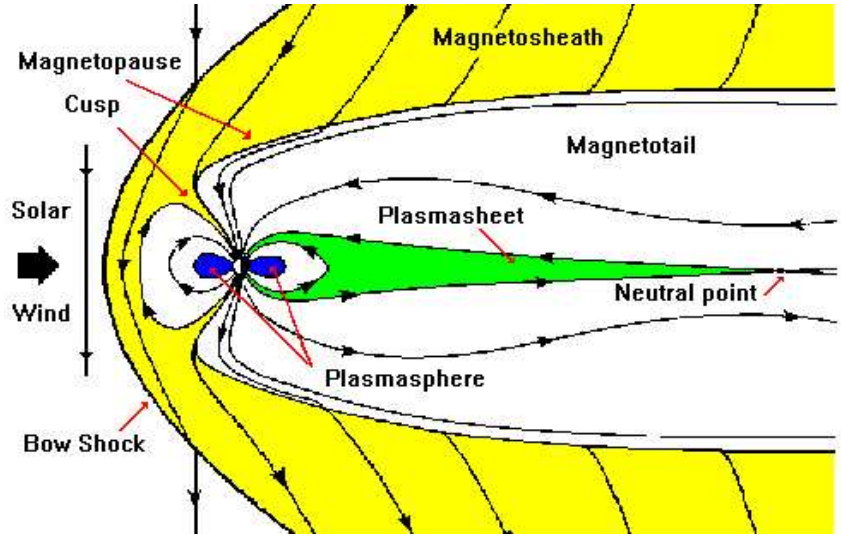

Figure 7.1: Earth's magnetosphere

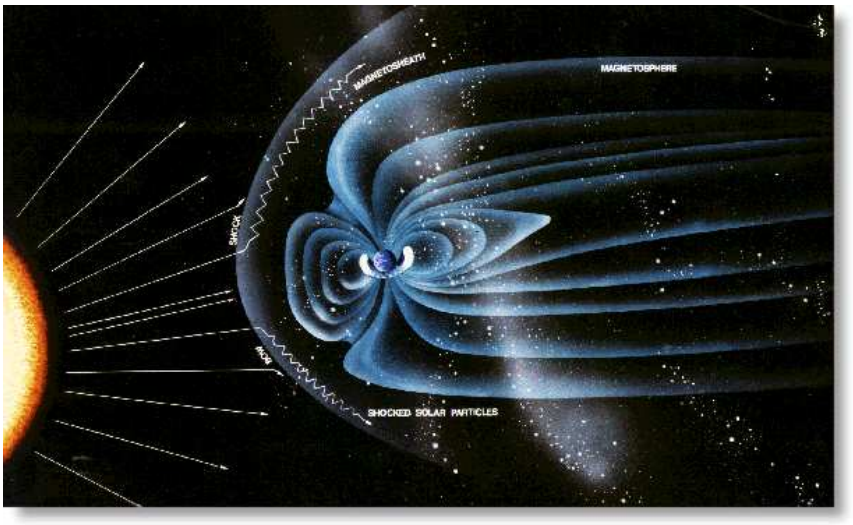

Figure 7.2: Solar eruption

7.3 Plasma engines

Plasma engines used by space vehicles are powered by xenon, a gas which is electrically charged.
The experiments have shown that the plasma engines are more efficient than traditional fuel-powered ones, because elastic propulsion systems weigh a few hundred kilogrammes, as opposed to the tonnes of liquid fuels. It results that the rockets are more efficient and can carry more materials into space.
The only trouble is that the plasma liberated by the engine is so hot that no materials resist its heat.
Indeed, the fast particles of xenon are ejected to infinity and do not come back, whereas the slow particles tend to come back to the satellite.
Since the plasma ejected by the engine is hot, the satellite is usually recovered by ceramics materials.

To sum up, satellites in geostationary orbit are in a mixture of charged particles. These particles come first from the solar wind. The slow particles ejected by the sun during its eruptions accumulate electricity on the external surface of the satellite. Whereas the fast particles come into the satellite and charge the electronic system.
These particles secondly come from the plasma ejected by the engines. The fast xenon particles are ejected at infinity, but the slow particles come back to the surface of the satellite.

For more details, we can refer to [34].

Chapter 8

Interactions on the surface of a satellite. A first model.

Contents

8.1 Physical context and notations 81

8.2 Electrostatic interactions 84

8.3 Reemissions at the surface of the satellite 87

8.3.1 Secondary electron emission 87

8.3.2 Secondary emission for ions 88

8.3.3 Photoemission 88

8.4 Mathematical model of Vlasov-Poisson 88

8.4.1 The system of Vlasov-Poisson 88

8.4.2 Existence and uniqueness results for the Vlasov-Poisson system 90

8.4.3 Dimensionless Vlasov and Poisson equations 90

In this chapter, we recall the problem introduced and studied in the one-dimensional and in the two-dimensional axisymmetric frames by O. Chanrion in [13].

8.1 Physical context and notations

The picture 8.1 represents a telecommunication satellite. The satellite has a metallic structure, solar panels and antennas. The different components of the

satellite are covered by different dielectric materials.
The characteristic lengths of a satellite and a dielectric are respectively about ten meters and a hundred microns.

Figure 8.1: A telecommunication satellite

The satellite is a perfect conductor covered by a layer of dielectrics. The particles (ions, electrons) coming from the spatial plasma interact with the surface of the satellite. Some of them are attracted by the surface of the satellite, some are reemitted, and others are driven towards the perfect conductor via conductivity.

The conductor is represented by an open set Ω_0 covered by a finite number d_k of dielectrics, with thickness d_k. The dielectrics are represented by open sets $(\Omega_k)_{k=1..N_d}$. The open set representing the satellite is denoted by Ω and is equal to $\overset{\circ}{\bigcup_{k=0}^{N_d}} \Omega_k$. Let Ω^c be its complementary in $\mathbb{R}^3$. For each dielectric, ϵ_k and σ_k are respectively the permittivity and the electrical conductivity.

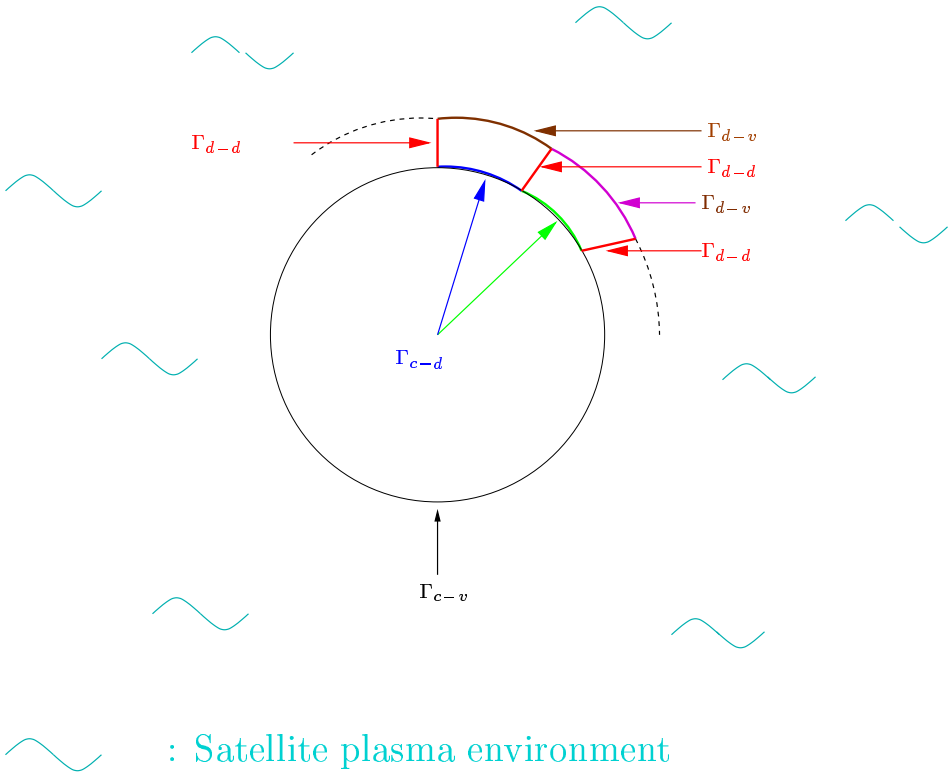

Figure 8.2: The satellite boundaries

Moreover, let

$\Gamma = \bigcup_{k=0}^{N_d} \partial\Omega_k$ the boundary between the subsets,

$\Gamma_{c-v} = \partial\Omega_0 \setminus \left(\partial\Omega_0 \bigcap \left(\bigcup_{k=1}^{N_d} \partial\Omega_k\right)\right)$ the boundary between the conductor and the vacuum,

$\Gamma_{c-d} = \partial\Omega_0 \setminus \Gamma_{c-v}$ the boundary between the conductor and the dielectric,

$\Gamma_{d-v} = \partial\Omega \setminus \Gamma_{c-v}$ the boundary between the dielectric and the vacuum,

$\Gamma_{d-d} = \Gamma \setminus (\partial\Omega_0 \cup \partial\Omega)$ the boundary between 2 neighbouring dielectrics.

Picture 8.2 explains the notations given before. For the sake of simplicity, the satellite is assumed to be a sphere recovered by a single layer of dielectrics. Let Φ_c be the potential of the perfect conductor.

8.2 Electrostatic interactions

Maxwell equations drive the evolution of the charge and the conductivity.

$$\begin{array}{rcl} -\dfrac{\partial D}{\partial t} & + & \mathrm{rot}H = J, \\ \mathrm{div}D & = & \rho, \\ \dfrac{\partial B}{\partial t} & + & \mathrm{rot}E = 0, \\ \mathrm{div}B & = & 0, \\ D = \epsilon E & , & B = \mu H. \end{array}$$

E and H are the electric and magnetic fields, D and B are the electric and magnetic displacements. J and ρ are the volumic densities of current and of the electric charge. ϵ and μ are respectively the electric permittivity and the magnetic permeability. They are constant for each dielectric. The induction phenomena is neglected, i.e. $\dfrac{\partial B}{\partial t} = 0$. Hence, $E = -\nabla\Phi$. By taking the divergence of the first equation, Maxwell equations imply that,

$$\begin{array}{l} -\dfrac{\partial}{\partial t}\mathrm{div}D = \mathrm{div}J, \\ \mathrm{div}D = \rho, \\ E = -\nabla\Phi, \\ B(t=0) = B_0,\ \mathrm{div}B_0 = 0, \\ \dfrac{\partial B}{\partial t} = 0, \\ D = \epsilon E,\ B_0 = \mu H_0, \end{array}$$

where H_0 is the constant magnetic field corresponding to the constant displacement B_0 satisfying $\mathrm{div}B_0 = 0$. Recalling that $E = -\nabla\Phi$, we only keep the two first equations written as

$$-\frac{\partial}{\partial t}\rho = \mathrm{div}J, \tag{8.1}$$

$$-\mathrm{div}(\epsilon\nabla\Phi) = \rho. \tag{8.2}$$

Let J_{ext} the current density outside of the satellite, which is regular in Ω^c and in each Ω_k and is equal to 0 in Ω_0. Normal vectors are directed to the inside

of the satellite and the conductor.

Moreover, the energy of particles is trapped on the surface of the dielectrics. So, a leakage current exists via conductivity to the perfect conductor. It writes as $J_k = \sigma_k E_k$. Furthermore, the conductivity between two dielectrics is neglected. By nature of the conductors, the field E is equal to 0 inside of the conductor. On the surface of the conductor there is a current J_Γ, which is equal to 0 outside of $\partial\Omega$.
By writing $divD$ in the sense of distributions, we obtain

$$\begin{aligned}
\int_{\mathbb{R}^3} \Psi\ divD dx &= -\int_{\mathbb{R}^3} D.\nabla\Psi dx, \quad \Psi \in \mathcal{D}(\mathbb{R}^3), \\
&= -\int_{\Omega^c} D.\nabla\Psi dx - \sum_k \int_{\Omega_k} D.\nabla\Psi dx, \\
&= \int_{\Omega^c} \Psi\ divD dx + \sum_k \int_{\Omega_k} \Psi\ divD dx - \int_\Gamma [D.n]\Psi d\gamma,
\end{aligned}$$

where $[\bullet]$ is the jump of the quantity $\bullet$ through the considered surfaces. There is no charge inside the dielectrics because they are too thin. So,

$$\begin{aligned}
divD &= 0 \text{ in each } \Omega_k, \\
divD &= \left[\epsilon_k \frac{\partial\Phi}{\partial n}\right] \text{ on } \Gamma.
\end{aligned}$$

By writing $div\ J$ in the sense of distributions with $J = J_{ext} + J_\Gamma \delta_\Gamma$,

$$\begin{aligned}
&\int_{\mathbb{R}^3} \Psi\ divJ dx = -\int_{\mathbb{R}^3} J.\nabla\Psi d\gamma, \\
&= -\int_{\mathbb{R}^3} J_{ext}.\nabla\Psi dx - \int_{\partial\Omega_0} J_\Gamma.\nabla\Psi d\gamma, \\
&= -\int_{\Omega^c} J_{ext}.\nabla\Psi dx - \sum_k \int_{\Omega_k} J.\nabla\Psi dx - \int_{\partial\Omega_0} J_\Gamma.\nabla\Psi d\gamma, \\
&= \int_{\Omega^c} \Psi\ div J_{ext} dx + \sum_k \int_{\Omega_k} \Psi\ divJ dx + \int_\Gamma \Psi [J_{ext}.n] d\gamma + \int_{\partial\Omega_0} \Psi\ div_\Gamma J_\Gamma d\gamma,
\end{aligned}$$

where $div_\Gamma J_\Gamma$ is the surfacic divergence of the current density J_Γ. Moreover, J_Γ satisfies

$$\int_{\partial\Gamma_0} divJ_\Gamma = 0, \quad \text{where} \quad \Gamma_0 = \Gamma_{c-v} \bigcup \Gamma_{c-d}.$$

Equation (8.1) becomes

$$\frac{\partial}{\partial t}\Big(\epsilon_k \frac{\partial \Phi^{diel}}{\partial n} - \epsilon_0 \frac{\partial \Phi}{\partial n}\Big) + \sigma_k \frac{\partial \Phi^{diel}}{\partial n} - J_{ext}.n = 0 \text{ on } \Gamma_{d-v}, \tag{8.3}$$

$$\frac{\partial}{\partial t}\Big(- \epsilon_0 \frac{\partial \Phi}{\partial n}\Big) + div J_\Gamma - J_{ext}.n = 0 \text{ on } \Gamma_{c-v}, \tag{8.4}$$

$$div J_\Gamma + \frac{\partial}{\partial t}\Big(- \epsilon_k \frac{\partial \Phi^{diel}}{\partial n}\Big) - \sigma_k \frac{\partial \Phi^{diel}}{\partial n} = 0 \text{ on } \Gamma_{c-d}, \tag{8.5}$$

with

$$\frac{\partial \Phi^{diel}}{\partial n} = \frac{\Phi_c(t) - \Phi(t,x)}{d_k}.$$

$\Phi(t,x)$ denotes the potential at point (t,x), where t is the time variable and x the space variable.
Equations (8.3), (8.4) and (8.5) describe the charge phenomenon of the satellite.
The charges on Γ_{d-d} are neglected because the surfaces of the dielectrics are thin and the particles are not enough energetic to go inside the dielectrics.
By integrating equations (8.4) and (8.5), and by using that

$$\int_{\partial\Omega_0} div_\Gamma J_\Gamma = 0,$$

we obtain

$$\int_{\Gamma_{c-v}} \Big[\frac{\partial}{\partial t}\Big(- \epsilon_0 \frac{\partial \Phi}{\partial n}\Big) - J_{ext}.n\Big]\, d\gamma + \int_{\Gamma_{c-d}} \Big[\frac{\partial}{\partial t}\Big(- \epsilon_k \frac{\partial \Phi^{diel}}{\partial n}\Big) - \sigma_k \frac{\partial \Phi^{diel}}{\partial n}\Big]\, d\gamma = 0. \tag{8.6}$$

Furthermore, we suppose that there is no charge inside the dielectrics, and that

$$\int_{\Gamma_{d-v}} \frac{\partial \Phi}{\partial n}\, d\gamma = \int_{\Gamma_{c-d}} \frac{\partial \Phi}{\partial n}\, d\gamma. \tag{8.7}$$

The equations to be solved by the potentials $\Phi(t,x)$ and $\Phi_c(t)$ are

$$\Delta \Phi(t,x) = \rho \text{ in } \Omega^c,$$

$$\frac{\partial}{\partial t}\Big(\epsilon_k \frac{\partial \Phi^{diel}}{\partial n} - \epsilon_0 \frac{\partial \Phi}{\partial n}\Big) + \sigma_k \frac{\partial \Phi^{diel}}{\partial n} - J_{ext}.n = 0 \text{ on } \Gamma_{d-v},$$

$$\int_{\Gamma_{c-v}} \Big[\frac{\partial}{\partial t}\Big(- \epsilon_0 \frac{\partial \Phi}{\partial n}\Big) - J_{ext}.n\Big]\, d\gamma + \int_{\Gamma_{c-d}} \Big[\frac{\partial}{\partial t}\Big(- \epsilon_k \frac{\partial \Phi^{diel}}{\partial n}\Big) - \sigma_k \frac{\partial \Phi^{diel}}{\partial n}\Big]\, d\gamma = 0,$$

$$\Phi(x) = \Phi_c(t) \ \text{ on } \ \Gamma_{c-v},$$

$$\Phi \to 0 \text{ at infinity },$$

with some initial conditions at $t = 0$ for Φ and Φ_c on Γ_{c-v}.

ρ is the charge density. We will give its expression below.

Hence, the problem considered by O. Chanrion in [13] is a coupled system for the variables Φ and Φ_c. It is also closed. Indeed, equation (8.9) is a scalar closure equation for the determination of Φ_c. The problem considered by O. Chanrion is the following,

$$\Delta\Phi(t,x) = \rho \text{ in } \Omega^c,$$

$$\frac{\partial}{\partial t}\Big(\epsilon_k \frac{\Phi_c - \Phi}{d_k} - \epsilon_0 \frac{\partial \Phi}{\partial n}\Big) + \sigma_k \frac{\Phi_c - \Phi}{d_k} - J_{ext}.n = 0 \ \ \forall x \in \Gamma_{d-v}, \tag{8.8}$$

$$\int_{\Gamma_{c-v}} \Big[\frac{\partial}{\partial t}\Big(-\epsilon_0 \frac{\partial \Phi}{\partial n}\Big) - J_{ext}.n\Big]\, d\gamma + \int_{\Gamma_{c-d}} \Big[\frac{\partial}{\partial t}\Big(-\epsilon_k \ \frac{\Phi_c - \Phi}{d_k}\Big) - \sigma_k \ \frac{\Phi_c - \Phi}{d_k}\Big]\, d\gamma = 0, \tag{8.9}$$

$$\Phi(x) = \Phi_c(t) \ \text{ on } \Gamma_{c-v}, \tag{8.10}$$

$$\Phi \to 0, \quad \|x\| \to \infty, \tag{8.11}$$

with some initial conditions at $t = 0$ for Φ and Φ_c on Γ_{c-v}.

8.3 Reemissions at the surface of the satellite

8.3.1 Secondary electron emission

When incident electrons interact with the surfaces of the satellite, there exist some secondary electrons reemitted by the surfaces. There are two types of reemissions.
In the first case, the electrons are diffused in an elastic way ("backscattering") and their energy is close to the energy of incident electrons. So, these electrons are backscattered.

In the second case, the secondary electrons are really reemitted by the surfaces. These electrons are at low energy and correspond to the electrons which are extracted from the surface of the satellite.

8.3.2 Secondary emission for ions

Ions do not enter materials the same way as electrons do, because they have not the same mass. Their trajectories differ. However, the secondary emissions are similar.

8.3.3 Photoemission

The surfaces which are exposed to the solar radiation emit electrons (called photoelectrons) at low energy. This reemission is responsible of a secondary current that has to be considered. Indeed, it is important in the charge mechanism.
In order to simplify the problem, all phenomena of reemissions are neglected. We refer to O. Chanrion thesis ([13]) for the consideration of reemission effects in the resolution of the Vlasov-Poisson system in a two-dimensional axisymmetric frame.

8.4 Mathematical model of Vlasov-Poisson

8.4.1 The system of Vlasov-Poisson

When it is possible to neglect the binary collisions between the particles in the case of tenuous plasma, these particles only interact via the electric field.
The Vlasov equation writes as

$$\frac{\partial f_{i/e}}{\partial t}(t,x,v)+v.\nabla_x f_{i/e}(t,x,v)-\frac{q_{i/e}}{m_{i/e}}\,E.\nabla_v f_{i/e}(t,x,v)=0,\ x\in\Omega^c,\ v\in\mathbb{R}^3,\ t\geq 0. \tag{8.12}$$

It describes the conservation of the ion distribution function f_i (resp. the electron distribution function f_e) along the ion trajectories (resp. electron) with an electric field $E(t,x)=-\nabla\Phi(t,x)$.
Here, v denotes the velocity of the particles, x the space variable and t the time variable. $q_{i/e}$ are respectively the ion and the electron charges.
In the geostationary frame, $f_{i/e}$ are given at infinity,

$$\lim_{\|x\|\to+\infty} f_{i/e}(t,x,v)=g_{i/e}(v),$$

where $g_{i/e}$ is a Maxwellian defined by

$$g_{i/e}(v) = n_0 \left(\frac{m_{i/e}}{2\pi k T_{i/e}}\right)^{\frac{3}{2}} exp\Big(- \frac{\frac{1}{2} m_{i/e}\ v^2}{k T_{i/e}}\Big).$$

By neglecting the reemissions effects, the boundary condition on the surface of the satellite is given by

$$f_{i/e}(t,x,v) = 0, \quad x \in \partial\Omega,\ v \in \mathbb{R}^3;\ v.\gamma_\Omega < 0$$

where γ_Ω is the inward normal vector to the satellite.

Equation (8.12), coupled with Maxwell equations which describe the evolution of the field E in presence of the charge density ρ and of the current J, constitutes the fundamental equation of the hot plasma physics.

Recall the Poisson equation,

$$\Delta\Phi(t,x) = \rho(t,x), \quad x \in \Omega^c, \tag{8.13}$$

where

$$\rho(t,x) = \frac{e}{\epsilon_0}(n_e(t,x) - n_i(t,x)).$$

n_e and n_i are respectively the densities of electrons and ions. They write as

$$n_{i/e}(t,x) = \int_{v\in\mathbb{R}^3} f_{i/e}(t,x,v)\ dv.$$

The four boundary conditions for the Poisson equation (8.13) are

$$\frac{\partial}{\partial t}\Big(\epsilon_k \frac{\Phi_c - \Phi}{d_k} - \epsilon_0 \frac{\partial\Phi}{\partial n}\Big) + \sigma_k \frac{\Phi_c - \Phi}{d_k} - J_{ext}.n = 0, \quad x \in \Gamma_{d-v}, \quad t \geq 0, \tag{8.14}$$

$$\int_{\Gamma_{c-v}} \Big[\frac{\partial}{\partial t}\Big(-\epsilon_0 \frac{\partial\Phi}{\partial n}\Big) - J_{ext}.n\Big] d\gamma + \int_{\Gamma_{c-d}} \Big[\frac{\partial}{\partial t}\Big(-\epsilon_k\ \frac{\Phi_c - \Phi}{d_k}\Big) - \sigma_k\ \frac{\Phi_c - \Phi}{d_k}\Big] d\gamma = 0, \tag{8.15}$$

$$\Phi(x) = \Phi_c(t) \ \text{ on } \Gamma_{c-v}, \tag{8.16}$$

$$\Phi \to 0, \quad \|x\| \to \infty, \quad t \geq 0, \tag{8.17}$$

where d_k is the thickness of the dielectric.

O. Chanrion proved in [13] the well-posedness of the system (8.13)-(8.17) in a one space dimensional frame.

8.4.2 Existence and uniqueness results for the Vlasov-Poisson system

Let us recall some of the former results on the Vlasov-Poisson system.

In [35], K. Pfaffelmoser showed the existence of global classical solutions in three dimensions for any initial datas.

In [4], C. Bardos and P. Degond studied the Vlasov Poisson equation in three space variables in the whole space. They showed the existence of a smooth solution for all times with initial data localised and small enough by using a dispersion property.

J. Batt, H. Berestycki, P. Degond and B. Perthame, in [5], studied the solutions of the Vlasov-Poisson system for locally isotropic stellar dynamic models.

R. Diperna and P.L. Lions, in [18], studied the Vlasov equations in any dimension. They established strong and weak stability solutions for the Vlasov-Poisson system as well as existence results for global solutions.

F. Poupaud showed in [36] the existence of solutions to the stationary Vlasov-Poisson system. He used oversolutions, which helped to control the concentration of the particles in the case of repulsives forces.

P.L Lions and B. Perthame in [30] studied the Vlasov-Poisson system in three dimensions. They showed that bounds on moments of order higher than three are preserved for solution of Vlasov-Poisson system.

8.4.3 Dimensionless Vlasov and Poisson equations

In this section, we recall the dimensionless variables and unknowns introduced by O. Chanrion in [13].

Dimensionless quantities

Let d, ϵ_0 and σ the characteristic thickness, the permittivity and conductivity of a dielectric.
Dimensionless variables and unknowns are introduced,

$$\tilde{t} = \frac{t}{T},\ \tilde{x} = \frac{x}{D},\ \tilde{v} = \frac{v}{V_e^{th}},$$

$$\tilde{f}_{i/e}(\tilde{t},\tilde{x},\tilde{v}) = \frac{f_{i/e}(t,x,v)}{f_0},\ \tilde{g}_{i/e}(\tilde{v}) = \frac{g_{i/e}(v)}{f_0},$$
$$\tilde{n}_{i/e}(\tilde{t},\tilde{x}) = \frac{n_{i/e}(t,x)}{n_0},\ \tilde{\Phi}(\tilde{t},\tilde{x}) = \frac{e\Phi(t,x)}{kT_e},$$
$$\tilde{d}_k = \frac{d_k}{d},\ \tilde{\epsilon}_k = \frac{\epsilon_k}{\epsilon_0},\ \tilde{\sigma}_k = \frac{\sigma_k}{\sigma},$$

and the dimensionless constants

$$\mu = \frac{m_e}{m_i},\ \eta = \frac{\lambda_d}{D},\ \nu = \frac{D}{d},\ \tau = \frac{\sigma T}{\epsilon_0},$$

with

$$\lambda_d = \sqrt{\frac{\epsilon_0\ kT_e}{n_0 e^2}},\ T = \eta^2\ \frac{D}{V_e^{th}},\ V_e^{th} = \sqrt{\frac{kT_e}{m_e}}.$$

The following equations are obtained,

$$\frac{1}{\eta^2}\ \frac{\partial \tilde{f}_i}{\partial \tilde{t}}(\tilde{t},\tilde{x},\tilde{v}) + \tilde{v}.\nabla_{\tilde{x}}\tilde{f}_i(\tilde{t},\tilde{x},\tilde{v}) - \mu\ \nabla_{\tilde{x}}\tilde{\Phi}(\tilde{t},\tilde{v}).\nabla_{\tilde{v}}\tilde{f}_i(\tilde{t},\tilde{x},\tilde{v}) = 0,\ \tilde{x}\in\tilde{\Omega}^c,\ \tilde{v}\in\mathbb{R}^3,\ \tilde{t}\geq 0,$$

$$\lim_{\|\tilde{x}\|\to\infty} \tilde{f}_i(\tilde{t},\tilde{x},\tilde{v}) = \tilde{g}_i(\tilde{v}),$$
$$\tilde{f}_i(\tilde{t},\tilde{x},\tilde{v}) = 0,\ \tilde{x}\in\partial\tilde{\Omega},\ \tilde{v}\in\mathbb{R}^3,\ \tilde{v}.\gamma_\Omega < 0,\ \tilde{t}\geq 0,$$

$$\frac{1}{\eta^2}\ \frac{\partial \tilde{f}_e}{\partial \tilde{t}}(\tilde{t},\tilde{x},\tilde{v}) + \tilde{v}.\nabla_{\tilde{x}}\tilde{f}_e(\tilde{t},\tilde{x},\tilde{v}) + \nabla_{\tilde{x}}\tilde{\Phi}(\tilde{t},\tilde{v}).\nabla_{\tilde{v}}\tilde{f}_e(\tilde{t},\tilde{x},\tilde{v}) = 0,\ \tilde{x}\in\tilde{\Omega}^c,\ \tilde{v}\in\mathbb{R}^3,\ \tilde{t}\geq 0,$$

$$\lim_{\|\tilde{x}\|\to\infty} \tilde{f}_e(\tilde{t},\tilde{x},\tilde{v}) = \tilde{g}_e(\tilde{v}),$$
$$\tilde{f}_e(\tilde{t},\tilde{x},\tilde{v}) = 0,\ \tilde{x}\in\partial\tilde{\Omega},\ \tilde{v}\in\mathbb{R}^3,\ \tilde{v}.\gamma_\Omega < 0,\ \tilde{t}\geq 0,$$

$$\Delta_{\tilde{x}}\tilde{\Phi}(\tilde{t},\tilde{x}) = \frac{1}{\eta^2}(\tilde{n}_e(\tilde{t},\tilde{x}) - \tilde{n}_i(\tilde{t},\tilde{x})),\ \tilde{x}\in\tilde{\Omega}^c,\ \tilde{t}\geq 0,$$
$$\frac{\partial}{\partial\tilde{t}}\Big(\nu\tilde{\epsilon}_k\frac{\tilde{\Phi}_c-\tilde{\Phi}}{\tilde{d}_k} - \frac{\partial\tilde{\Phi}}{\partial n}\Big) + \nu\tau\tilde{\sigma}_k\frac{\tilde{\Phi}_c-\tilde{\Phi}}{\tilde{d}_k} - \tilde{J}_{ext}.n = 0 \ \text{ on } \Gamma_{d-v},$$
$$\int_{\Gamma_{c-v}}\Big[\frac{\partial}{\partial\tilde{t}}\Big(-\frac{\partial\tilde{\Phi}}{\partial n}\Big) - \tilde{J}_{ext}.n\Big]d\gamma + \int_{\Gamma_{c-d}}\Big[\frac{\partial}{\partial\tilde{t}}\Big(-\nu\tilde{\epsilon}_k\frac{\tilde{\Phi}_c-\tilde{\Phi}}{\tilde{d}_k}\Big) - \nu\tau\tilde{\sigma}_k\frac{\tilde{\Phi}_c-\tilde{\Phi}}{\tilde{d}_k}\Big]d\gamma = 0,$$
$$\tilde{\Phi}(\tilde{t},\tilde{x}) = \tilde{\Phi}_c(\tilde{t}) \ \text{ on } \Gamma_{c-v},$$
$$\tilde{\Phi}\to 0,\quad \|\tilde{x}\|\to\infty,\quad \tilde{t}\geq 0.$$

Passage to the limit in a formal way

In a magnetospheric plasma in geostationary orbit, the Debye length is quite larger than the dimensions of the satellite. Hence, the parameter η is large. In order to simplify the equations, O. Chanrion performed the passage to the limit when $\eta^2 \to +\infty$ ([13]).

He obtained a stationary Vlasov equation (for the plasma) for ions and electrons and a negligible space charge $\tilde{\rho}$.

$$\tilde{v}.\nabla_{\tilde{x}}\tilde{f}_i(\tilde{t},\tilde{x},\tilde{v}) - \mu\ \nabla_{\tilde{x}}\tilde{\Phi}(\tilde{t},\tilde{v}).\nabla_{\tilde{v}}\tilde{f}_i(\tilde{t},\tilde{x},\tilde{v}) = 0,\ \tilde{x}\in\tilde{\Omega}^c,\ \tilde{v}\in\mathbb{R}^3,\ \tilde{t}\geq 0,$$

$$\lim_{\|\tilde{x}\|\to\infty}\tilde{f}_i(\tilde{t},\tilde{x},\tilde{v}) = \tilde{g}_i(\tilde{v}),$$

$$\tilde{f}_i(\tilde{t},\tilde{x},\tilde{v}) = 0,\ \tilde{x}\in\partial\bar{\Omega},\ \tilde{v}\in\mathbb{R}^3,\ \tilde{v}.\gamma_\Omega < 0,\ \tilde{t}\geq 0,$$

$$\tilde{v}.\nabla_{\tilde{x}}\tilde{f}_e(\tilde{t},\tilde{x},\tilde{v}) + \nabla_{\tilde{x}}\tilde{\Phi}(\tilde{t},\tilde{v}).\nabla_{\tilde{v}}\tilde{f}_e(\tilde{t},\tilde{x},\tilde{v}) = 0,\ \tilde{x}\in\tilde{\Omega}^c,\ \tilde{v}\in\mathbb{R}^3,\ \tilde{t}\geq 0,$$

$$\lim_{\|\tilde{x}\|\to\infty}\tilde{f}_e(\tilde{t},\tilde{x},\tilde{v}) = \tilde{g}_e(\tilde{v}),$$

$$\tilde{f}_e(\tilde{t},\tilde{x},\tilde{v}) = 0,\ \tilde{x}\in\partial\bar{\Omega},\ \tilde{v}\in\mathbb{R}^3,\ \tilde{v}.\gamma_\Omega < 0,\ \tilde{t}\geq 0,$$

$$\Delta_{\tilde{x}}\tilde{\Phi}(\tilde{t},\tilde{x}) = 0,\ \tilde{x}\in\tilde{\Omega}^c,\ \tilde{t}\geq 0,$$

$$\frac{\partial}{\partial\tilde{t}}\Big(\nu\tilde{\epsilon}_k\frac{\tilde{\Phi}_c-\tilde{\Phi}}{\tilde{d}_k} - \frac{\partial\tilde{\Phi}}{\partial n}\Big) + \nu\tau\tilde{\sigma}_k\frac{\tilde{\Phi}_c-\tilde{\Phi}}{\tilde{d}_k} - \tilde{J}_{ext}.n = 0,$$

$$\int_{\Gamma_{c-v}}\Big[\frac{\partial}{\partial\tilde{t}}\Big(-\frac{\partial\tilde{\Phi}}{\partial n}\Big) - \tilde{J}_{ext}.n\Big]d\gamma + \int_{\Gamma_{c-d}}\Big[\frac{\partial}{\partial\tilde{t}}\Big(-\nu\tilde{\epsilon}_k\frac{\tilde{\Phi}_c-\tilde{\Phi}}{\tilde{d}_k}\Big) - \nu\tau\tilde{\sigma}_k\frac{\tilde{\Phi}_c-\tilde{\Phi}}{\tilde{d}_k}\Big]d\gamma = 0,$$

$$\tilde{\Phi}(\tilde{x}) = \tilde{\Phi}_c(\tilde{t}) \quad \text{on } \Gamma_{c-v},$$

$$\tilde{\Phi}\to 0,\quad \|\tilde{x}\|\to\infty,\quad \tilde{t}\geq 0.$$

Remark 8.4.1 *These dimensionless equations are valid only when* $\|x\| < \lambda_d$.

Remark 8.4.2 *The variable* $\tilde{t}$ *is linked to the conductor and the dielectrics because the satellite is charging.*

From Chapter 9 on, the results of this thesis are presented. Contrary to O. Chanrion's frame, no dielectric will be considered and the satellite is a perfect conductor. The satellite potential Φ_c is a given constant.

Since the Debye length is larger than the dimension of the satellite in a manetospheric plasma, we usually neglect the space charge ρ (from above). In the next chapter, we start to solve the Laplace equation in the whole space.

Chapter 9

An infinite element method for the resolution of the Laplace equation in an infinite domain

Contents

9.1 Introduction 95

9.1.1 Variational formulation 96

9.2 Different methods used in problems with infinite domains 97

9.3 A new approach of infinite element 99

9.3.1 Computation of the terms in the elementary stiffness matrix 102

9.4 Numerical results 103

9.4.1 Case of a sphere 104

9.4.2 Case of two sources 107

9.1 Introduction

Here and in the following chapters, the satellite is assumed to be a perfect conductor without dielectrics. Moreover, the temperature T_e of electrons is supposed to be equal to the temperature T_i of ions and is denoted by T. Furthermore, the reemission phenomenon is neglected. Finally, the potential Φ_c

is a given constant.

The problem to be solved is

$$\begin{cases} \Delta_x \Phi(x) = 0, \quad \text{in } \Omega^c, \\ \Phi(x) = \Phi_c (:= \Phi(R)) \quad \text{on } \Gamma_{c-v}, \\ \Phi \to 0, \quad \|x\| \to \infty. \end{cases} \tag{9.1}$$

9.1.1 Variational formulation

Let

$$C = \{u \in H^1(\bar{\Omega}^c);\ \frac{u(x)}{(1+\|x\|^2)^{\frac{1}{2}}} \in L^2(\bar{\Omega}^c);\ u = 0 \text{ on } \Gamma_{c-v}\},$$

with

$$\|u\|_C^2 = \int_{\bar{\Omega}^c} u(x)^2\ dx + \int_{\bar{\Omega}^c} (\nabla u(x))^2\ dx.$$

Let

$$\bar{\Phi}(x) = \Phi(x) - \tilde{\Phi}_c,\ x \in \bar{\Omega}^c,$$

where $\tilde{\Phi}_c$ is such that $\gamma(\tilde{\Phi}_c) = \Phi_c$ on Γ_{c-v}, γ is the trace mapping.
We multiply equation (9.1) by a test function $\Psi \in C$ and we integrate on $\bar{\Omega}^c$.
We obtain the following formulation,

$$\int_{\Omega^c} \nabla\bar{\Phi}(x).\nabla\Psi(x)dx = -\int_{\Omega^c} \nabla\tilde{\Phi}_c.\nabla\Psi(x)dx.$$

We use standard P_1 finite elements to compute the potential Φ.
An unstructured mesh composed of tetrahedrons is introduced.
The infinite boundary condition is troublesome. Since we cannot mesh the space up to infinity, a fictitious sphere Γ_s centred in $O(0,0,0)$ with radius R_∞ is introduced. Instead of using finite elements coupled with integral equations, infinite elements are used.
Let $\mathcal{O}$ be the open set delimited by the surface of the satellite and Γ_s.

O. Chanrion has solved the Laplace equation (9.1) in a two-dimensional axisymmetric frame by using infinite elements ([13]) on the boundary of the computational domain and finite elements inside the computational domain. Indeed, the shape functions for infinite elements decrease like $1/r_s$ where r_s is the distance between the origin and a point of the mesh. The infinite element method consists in using the linear shape functions associated to the segment

of the sphere Γ_s. These linear shape functions are multiplied by $\frac{R_\infty}{r}$.

Our aim is to solve the Laplace equation in $\mathbb{R}^3$ for any geometry of the satellite.
In the next section, we introduce different methods found in the literature. Then, we present a new approach of infinite element for the resolution of the Laplace equation in the whole space.

9.2 Different methods used in problems with infinite domains

Robin condition

On the infinite boundary Γ_s, we put a Robin condition, which is written as

$$\frac{\partial \Phi}{\partial n} + \frac{1}{R_\infty}\Phi = 0. \tag{9.2}$$

This condition is appropriate to the sphere case and is a classical method for the resolution of problems with infinite domain.
Inside $\mathcal{O}$, we use P_1 finite elements. On the boundary of $\mathcal{O}$, we also use finite tetrahedrons which are composed of a triangle T on Γ_s and the point O.

The variational formulation writes as

$$\int_{\mathcal{O}} \nabla\Phi.\nabla\Psi \; dx - \frac{1}{R_\infty}\int_{\partial\mathcal{O}} \Phi \; \Psi \; d\gamma = 0, \quad \Psi \in H^1(O).$$

The terms in the elementary stiffness matrix write as,

$$\int_{finite \;\; tetrahedron} \nabla\lambda_i.\nabla\lambda_j \; dV = \frac{1}{R_\infty}\int_T \lambda_i \; \lambda_j \; dS,$$

where λ_i is the shape function associated to the vertices A_i and T is the face of the finite tetrahedron which is on the boundary of the computational domain $\mathcal{O}$.
When the satellite is a sphere, an analytical solution to the Laplace equation is known,

$$\Phi(r) = \Phi_c \frac{R}{r},$$

where R is the radius of the satellite. This solution satisfies (9.2) and behaves like $\frac{1}{r}$ at infinity. This asymptotic behaviour of Φ is really specific to the sphere frame.

Let us introduce the different infinite element methods met in the literature.

The infinite element method has been introduced in order to treat problems in exterior domains. It consists in generalizing finite elements in unbounded domains. More precisely, shape functions are defined by piece on elementary volumes, and extended at infinity.

Boundary Element Method (BEM)

G. Beer and J.O. Watson studied the boundary element method which can be used in problems with infinite domains ([6]).

The boundary element method seems to be adapted to the analysis of problems involving infinite domains, when the problem surface can be discretized and the conditions at infinity are automatically satisfied by the fundamental solution. However, in some cases, one encounters problems in which the surface to be discretized also extends to infinity. In that case, these problems can be solved by truncating the boundary element mesh at a large distance, away from the zone of interest. The disadvantage of such a scheme is that a large number of boundary elements may be used for modelling the remote surface and that an unknown error may be introduced if the truncation occurs too close to the zone of interest.
This method is precise but expensive to implement.

Infinite element method

In [24], K. Gerdes and L. Demkowicz focus on the convergence study for infinite element discretizations of the Laplace equation in exterior domains. Their approximation applies to separable geometries only, combining an *hp*-finite element discretization on the boundary of the domain with a spectral-like representation in the radial direction.
An *hp*-infinite element is obtained by extending the curvilinear triangle given on the fictitious sphere, in the radial direction.

The implementation of the element stiffness matrix seems to be difficult.

In [9] and [8], P. Bettess presented an infinite element method consisting in extending a finite element at infinity. The shape function for infinite elements is written as a product of the finite element shape function by a decay function. The role of the decay function is to ensure that the behaviour of the element at infinity corresponds to the requested infinite boundary condition.
If the parent finite element shape function is written as $P_i(\xi, \eta)$, where ξ and η are the local coordinates, and the decay function is $f_i(\xi, \eta)$, where the subscript denotes the node number, then

$$N_i(\xi, \eta) = P_i(\xi, \eta) \times f_i(\xi, \eta),$$

where $f_i(\xi, \eta)$ must be unity at its own node, i.e. $f_i(\xi_i, \eta_i) = 1$.
So N_i must tend to the far field value at infinity. There is no requirement that the decay function takes any special value at other nodes.
Similar considerations apply in three dimensions.
The ξ coordinate would normally be in the radial direction, away from the domain of interest, and is usually simply a constant multiplied by r, the radial coordinate.
An infinite element is obtained by distorting isoparametric elements.

In the next section, we introduce a new infinite element method which deals with the resolution of the Laplace equation.

9.3 A new approach of infinite element

In our study, we introduce a new method which consists in building infinite elements from P_1 finite elements in the following way.
Start from a finite element $OA_1A_2A_3$, where $A_1A_2A_3$ is a flat triangle on the fictitious sphere Γ_s. We then extend the face (O, A_1, A_2), (O, A_2, A_3), (O, A_3, A_1) until infinity. The point O is sent to infinity. There is a bijection which sends the tetrahedron $OA_1A_2A_3$ to the infinite element, on the other side of the face (A_1, A_2, A_3) (see picture 9.1).
If $\lambda_1,\ \lambda_2,\ \lambda_3$ and λ_0 are the barycentric coordinates with respect to the points $A_1,\ A_2,\ A_3$ and O, the point with barycentric coordinates λ_i' such that

$$\lambda_i' = \lambda_i \ \frac{R_\infty^2}{r^2},\ i \in \{1, 2, 3\}$$

belongs to this infinite element.
This transformation can be written as

$$\begin{aligned} \lambda'_0 &= -\frac{\lambda_0}{1-\lambda_0}, \\ \lambda'_i &= \frac{\lambda_i}{(1-\lambda_0)^2}, \quad i = 1, 2, 3, \end{aligned}$$

where

$$r^2 = R_\infty^2 (1-\lambda_0)^2.$$

We take λ'_i as shape functions for infinite elements.

Let K be the infinite volume between the face A_1, A_2, A_3 and the extension of the 3 faces with the outside of the sphere Γ_s.
Picture 9.1 explains this infinite element method.

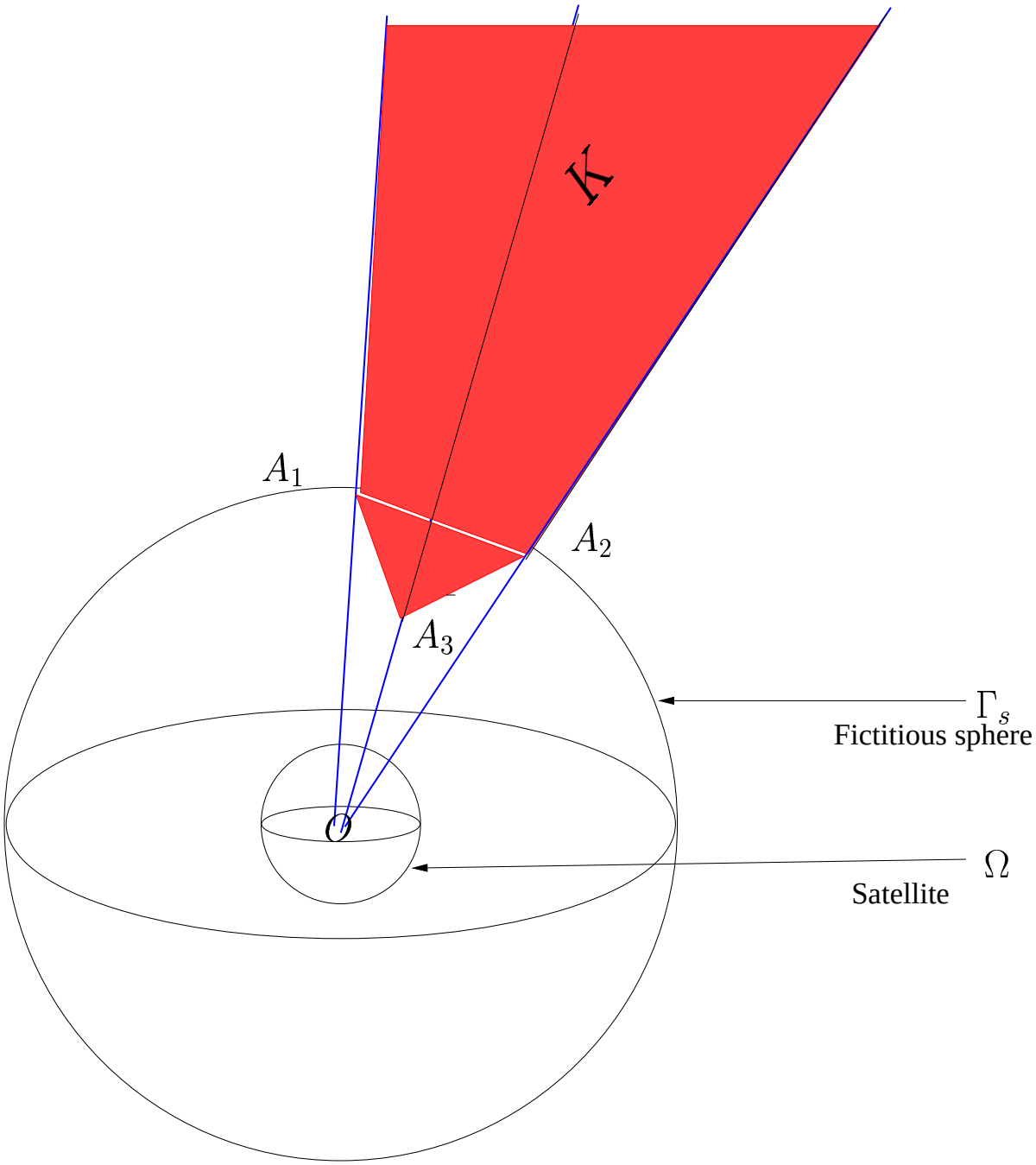

Figure 9.1: An infinite element

T.Z. Boulmezaoud presented a similar method at the numerical congress CANUM 2003 ([10]).

I presented this new infinite element method, implemented in december 2002 at the numerical congress CANUM 2004, independently of [10]. S. Clerc presented this method at the workshop in simulation of plasmas in may 2003, independently of [10].

9.3.1 Computation of the terms in the elementary stiffness matrix

For the computation of the term $\int_K \nabla\lambda_i'.\nabla\lambda_j'\ dV,\ i,j \in \{1,..,3\}$, we consider a frame of coordinates centered at O, with the axis (O,x_1) orthogonal to the triangle $T = A_1A_2A_3$ of Γ_s.
Let y a point in T. An homothetic transformation with center y and ratio $\lambda > 0$ is performed. This gives

$$x = (\lambda R_\infty, \lambda y), \quad \lambda \in [1, +\infty[, \quad y \in T. \tag{9.3}$$

Thanks to the change of variable (9.3), the term $\int_K \nabla\lambda_i'.\nabla\lambda_j'\ dV$ writes as

$$\int_K \nabla\lambda_i'(x).\nabla\lambda_j'(x)\ dV = \int_{\lambda\in[1,+\infty[} \lambda^2 R_\infty \int_{y\in T} \nabla\lambda_i'(\lambda y).\nabla\lambda_j'(\lambda y)\ dy\ d\lambda.$$

Since the function $\lambda_i'(x) = \dfrac{\lambda_i(x)}{(1-\lambda_0(x))^2}$ is homogeneous of degree -1, the vector function

$$\nabla\lambda_i'(x) = \frac{\nabla\lambda_i(x)}{(1-\lambda_0)^2} + \frac{2\lambda_i(x).\nabla\lambda_0(x)}{(1-\lambda_0)^3}$$

is homogeneous of degree -2,
Then $\nabla\lambda_i'(x).\nabla\lambda_j'(x)$ is homogeneous of degree -4.
So,

$$\nabla\lambda_i'(\lambda y).\nabla\lambda_j'(\lambda y) = \lambda^{-4}\ \nabla\lambda_i'(y).\nabla\lambda_j'(y).$$

Moreover,

$$\begin{aligned}\int_K \nabla\lambda_i'(x).\nabla\lambda_j'(x)\ dV &= R_\infty \int_{\lambda\in[1,+\infty[} \lambda^{-2} \int_{y\in T} \nabla\lambda_i'(y).\nabla\lambda_j'(y)\ dy\ d\lambda \\ &= R_\infty \int_{y\in T} \nabla\lambda_i'(y).\nabla\lambda_j'(y)\ dy \\ &= R_\infty \int_{y\in T} (\nabla\lambda_i + 2\lambda_i.\nabla\lambda_0)(\nabla\lambda_j + 2\lambda_j.\nabla\lambda_0)(y)\ dS,\end{aligned}$$

because $\lambda_0(y) = 0$ for $y \in T$.
Finally, we obtain

$$\begin{aligned}\int_K \nabla\lambda_i'.\nabla\lambda_j'\ dV &= R_\infty\ \text{area}(T)\nabla\lambda_i.\nabla\lambda_j + 4R_\infty\ \nabla\lambda_0.\nabla\lambda_0 \int_T \lambda_i\lambda_j\ dS \\ &+ 2R_\infty\ \nabla\lambda_i.\nabla\lambda_0 \int_T \lambda_j\ dS + 2R_\infty\ \nabla\lambda_0.\nabla\lambda_j \int_T \lambda_i\ dS,\end{aligned}$$

with $\nabla\lambda_0 = \dfrac{n}{R_\infty}$, n being the normal vector to the face $(A_1A_2A_3)$.

The numerical method consists in using finite elements inside the computational domain $\mathcal{O}$, and infinite elements on the boundary of $\mathcal{O}$.
The expression of the approximate solution by finite and infinite elements is

$$\Phi_h(t,x,v) = \sum_{i\in\mathcal{O}} \phi_i\Phi_i(x,v) + \sum_{i\in\Gamma_s} \phi_i\Phi_i^{inf}(x,v).$$

The problem to be solved then writes as the following global linear system,

$$A\ \Phi = B(\Phi_c), \tag{9.4}$$

where $\Phi = (\Phi_i)_i$ is a vector with N components where N is the number of points of the considered mesh. B is the right-hand side of (9.4). It depends on Φ_c. The linear system (9.4) is solved by a conjugate gradient method.
The matrix A is a positive symmetric matrix. Indeed, the bilinear form associated to this matrix is symmetric and coercive.

9.4 Numerical results

In order to test the infinite element method, the following two cases where analytical solutions are available, are studied.

9.4.1 Case of a sphere

We assume that the satellite is a sphere with radius $R = 1\ m$. The potential of the exact solution is $\Phi(r) = \dfrac{\Phi_c}{r}$.
The numerical values are

$$R_\infty = 25\ m,\ \Phi_c := \Phi(R = 1) = -25000\ V,\ n_0 = 10^6\ m^{-3},\ kT_e = 10^4\ eV.$$

A mesh of an eight of a sphere is considered. The whole sphere is then obtained by symmetry arguments.
Recall that there is no dielectric and that the reemission effect is neglected.
From a numerical point of view, we study the convergence of the infinite element method and compare it to the Robin condition. The error in norm L^2 is analyzed.

Case of infinite elements

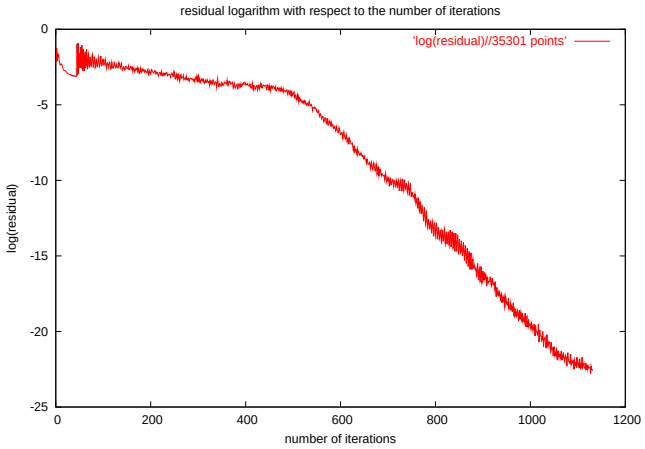

Figure 9.2: Residual curve for the infinite element method

The curve on Picture 9.2 represents the residual of the conjugate gradient with respect to the number of iterations in a semi-logarithmic scale. The residual decreases, so that the conjugate gradient converges.

The curve on Picture 9.3 represents the potential $\Phi(r)$ obtained numerically with respect to the radius r in a semi-logarithmic scale, by using the infinite element method. The potential of the exact solution is also plotted.

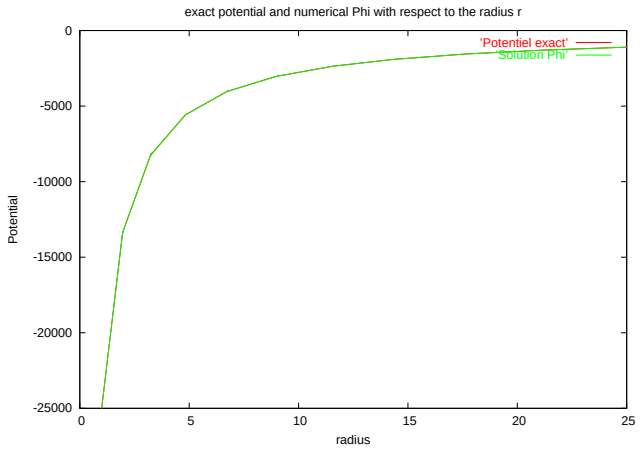

Figure 9.3: Potential with respect to the radius

The two curves overlap and the potential decreases at infinity.
Then, the problem is well conditioned by using the infinite elements.

The Robin condition :

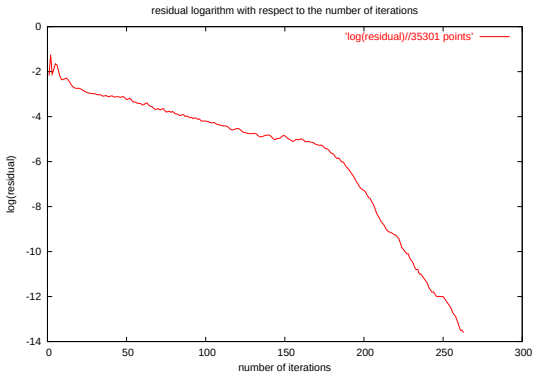

Figure 9.4: Residual curve with the Robin condition

The same curves are drawn by using the Robin condition on the boundary of $\mathcal{O}$ instead of the infinite elements.

The two methods differ from each other by the terms of tangential gradients which are very weak for a spherical geometry. We remark a difference of convergence between the two methods.

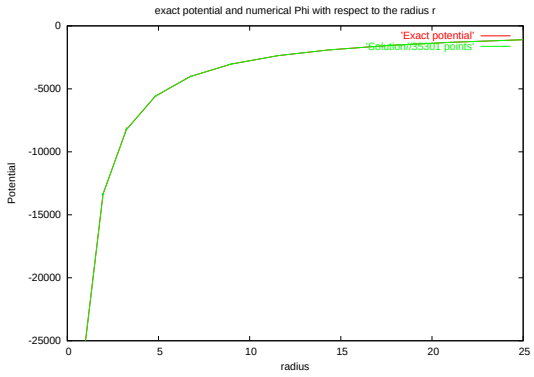

Figure 9.5: Potential with respect to the radius

Error curve in L^2 norm

The error in L^2 norm is plotted with respect to the number of points of the mesh in logarithmic scale, i.e. for any meshes.

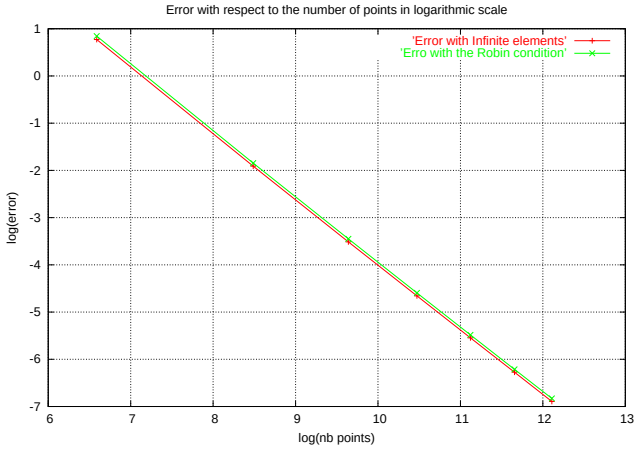

Figure 9.6: Error in L^2 norm with the Robin condition and the infinite element method

Picture 9.6 represents the error with respect to the number of points of a mesh. The green curve is the error with the Robin condition and the red curve is the error using infinite elements.

We note that the error is the same for the infinite element method and

for the Robin condition for all meshes, because the Robin condition is well adapted to the case of a sphere.

9.4.2 Case of two sources

We consider two sources localized in $(0.5, 0, 0)$ and $(-0.5, 0, 0)$. For the satellite, the mesh of section 9.4.1 is kept. The sources are inside the sphere with radius $R = 1$. We impose the potential of the exact solution as a Dirichlet condition on the surface of the sphere with radius 1. The exact solution is

$$\Phi(r) = \frac{1}{4\pi} \sum_{i=1}^{2} \frac{1}{r_i},$$

where r_i is the distance between the sources and the points of the mesh. The L^2 error with respect to the radius of the sphere Γ_s for different meshes in logarithmic scale is represented in picture 9.7. The error in L^2 norm decreases and is given by the following quadrature formula (for a P_2 function, with 5 points),

$$\begin{aligned}\int_K |\Phi_{exact} - \Phi_{approximated}|^2 dx\, dy\, dz \\ = \frac{Vol(K)}{20} \sum_{i=1}^{4} |\Phi_{exact} - \Phi_{approximated}|^2(a_i) + \\ + \frac{4}{5} Vol(K) |\Phi_{exact} - \Phi_{approximated}|^2(a_5),\end{aligned}$$

where a_i, $i = 1, .., 4$ are the 4 vertices of the considered tetrahedron and $a_5 = \frac{1}{4}(a_1 + a_2 + a_3 + a_4)$ its center of gravity.

In Picture 9.7 the L^2 errors for the infinite element method and the Robin condition are plotted. This is done for different radii of the fictitious sphere Γ_s and for different meshes in logarithmic scale. Indeed, for a given mesh, R_∞ is given for different values. The errors obtained by using infinite elements and the Robin condition are computed. The errors for thin and coarse meshes are also computed.

The pink curve represents the error for infinite elements with a mesh having 35 301 points. The blue curve represents the error for infinite elements with a mesh having 4 851 points. The orange curve corresponds to the error for the Robin condition with a mesh having 35 301 points. We note that the error is

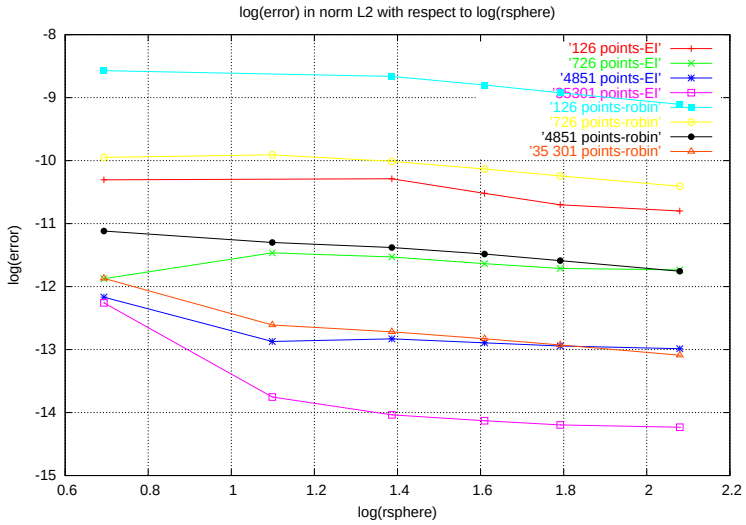

Figure 9.7: Error curves for infinite elements and for Robin

the same for these two curves.
The green curve corresponds to the error for infinite elements with a mesh having 726 points and the black curve is the error for the Robin condition with a mesh having 4 851 points. We also note that the error is the same for these two curves.
The red curve represents the error for infinite elements with a mesh having 126 points and the yellow curve is the error for the Robin condition with a mesh having 726 points. Th error is the same for these two curves. Finally the turquoise curve is the error for Robin method with a mesh having 126 points.

We notice that for a given mesh, the error for infinite elements is smaller than the error for the Robin condition. For example, with a mesh having 35 301 points, the pink curve for infinite elements is below the orange curve for the Robin condition.

For reaching an error equal to 3.34×10^{-5}, the infinite elements method requires a mesh with 126 points, whereas the Robin condition requires a mesh with 726 points. In all the cases, the infinite element method is the best. It can be easily checked on tables 9.1 and 9.2 which represent the error for the infinite elements and for the Robin condition.

The Robin condition.

Mesh / R_∞	126 points	726 points	4 851 points	35 301 points
2	$1,893.10^{-4}$	$4,778.10^{-5}$	$1,484.10^{-5}$	$7,000.10^{-6}$
3	$1,944.10^{-4}$	$4,977.10^{-5}$	$1,237.10^{-5}$	$3,338.10^{-6}$
4	$1,729.10^{-4}$	$4,484.10^{-5}$	$1,142.10^{-5}$	$2,994.10^{-6}$
5	$1,508.10^{-4}$	$3,974.10^{-5}$	$1,030.10^{-5}$	$2,684.10^{-6}$
6	$1,332.10^{-4}$	$3,560.10^{-5}$	$9,266.10^{-6}$	$2,433.10^{-6}$
8	$1,109.10^{-4}$	$3,020.10^{-5}$	$7,836.10^{-6}$	$2,067.10^{-6}$

Table 9.1: Error with the Robin condition

Infinite elements.

Mesh / R_∞	126 points	726 points	4 851 points	35 301 points
2	$3,346.10^{-5}$	$6,960.10^{-6}$	$5,191.10^{-6}$	$4,748.10^{-6}$
3	$4,087.10^{-5}$	$1,048.10^{-5}$	$2,571.10^{-6}$	$1,063.10^{-6}$
4	$3,405.10^{-5}$	$9,822.10^{-6}$	$2,677.10^{-6}$	$8,018.10^{-7}$
5	$2,697.10^{-5}$	$8,843.10^{-6}$	$2,515.10^{-6}$	$7,296.10^{-7}$
6	$2,249.10^{-5}$	$8,198.10^{-6}$	$2,391.10^{-6}$	$6,826.10^{-7}$
8	$2,041.10^{-5}$	$8,009.10^{-6}$	$2,290.10^{-6}$	$6,580.10^{-7}$

Table 9.2: Error with the infinite elements

Moreover, we plotted in picture 9.8 the potential on the boundary of the domain $\mathcal{O}$ by using infinite elements and the Robin condition. We notice that the solutions obtained with infinite elements are more precise than the solutions obtained with the Robin condition.

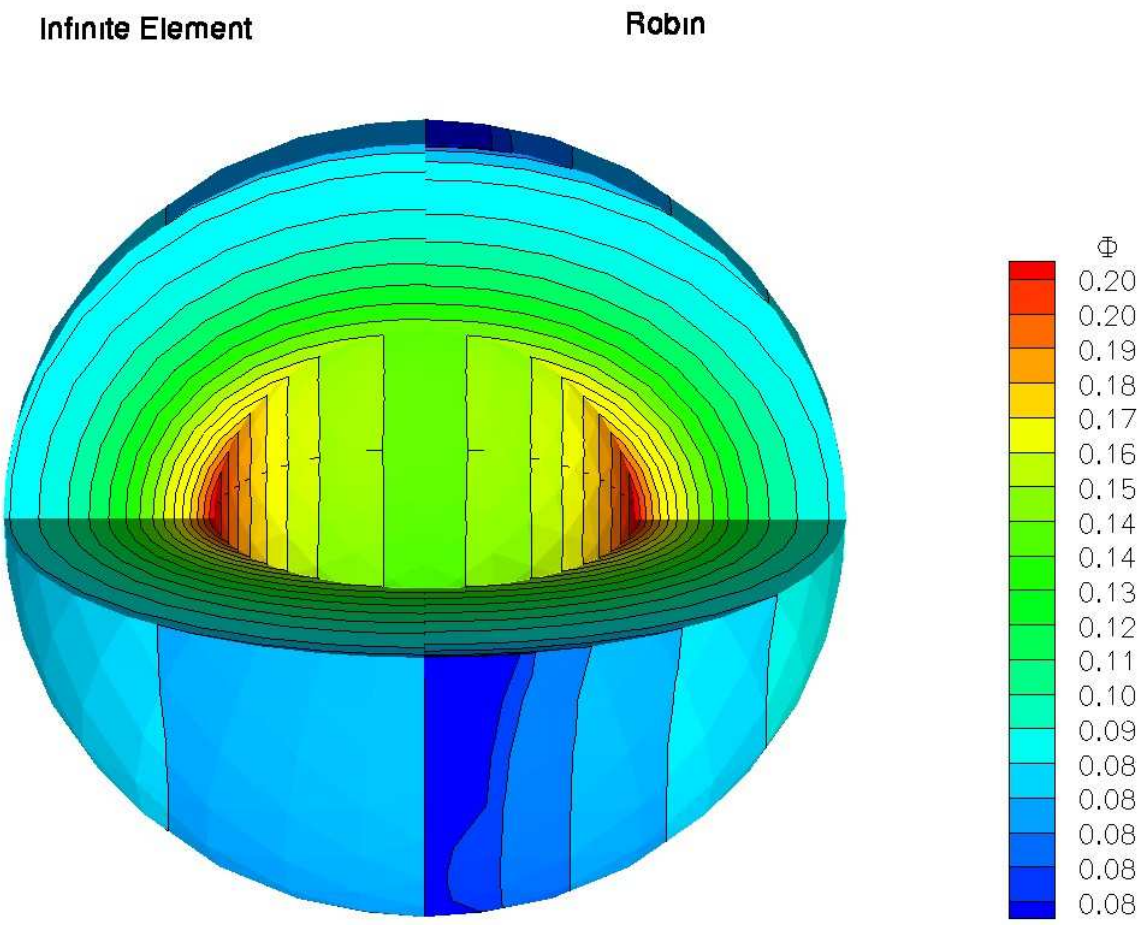

Figure 9.8: Potential Φ on the fictitious sphere

Chapter 10

The coupling with the Vlasov equation

Contents

10.1 The back-trajectories method 111

10.2 Numerical approximation for the ion and the electron currents at the surface of the satellite 114

10.2.1 The ion current 115

10.2.2 The electron current 116

The potential Φ being computed, a back-trajectories particle method is used to solve the Vlasov equation in $\mathbb{R}^3$ for any geometry of the satellite. Then, we compute the distribution function for ions and electrons and also the ion and the electron currents received by the surface of the satellite.

10.1 The back-trajectories method

Recall the method introduced by O. Chanrion in [13].
The Vlasov equation implies that the distribution function of the particles is constant along their trajectories, i.e.

$$f_{i/e}(X(t), V(t)) = constant, \quad t \geq 0.$$

The backtrajectories method consists in following the trajectories of the particles in the reverse sense with an opposite velocity, i.e. going back.

The trajectory of a particle is defined by its position X and its velocity V, and satisfies the following equations,

$$\begin{aligned}
&\frac{\partial X(t)}{\partial t} = V(t), \quad t \geq 0, \\
&\frac{\partial V(t)}{\partial t} = \kappa_{i/e} \ \nabla_x \Phi, \\
&X(0) = X_0, \ V(0) = V_0,
\end{aligned}$$

where $\kappa_i = -\mu$ and $\kappa_e = 1$.

We define $\mathcal{T}_{i/e}^{direct}(X_0, V_0)$, the trajectory from $X(0) = X_0$ and $V(0) = V_0$.

We define the back-trajectories $\mathcal{T}_{i/e}^{back}(X_f, V_f)$ reaching the final point (X_f, V_f) by

$$\begin{aligned}
&\frac{\partial X(t)}{\partial t} = -V(t), \quad t \geq 0, \\
&\frac{\partial V(t)}{\partial t} = -\kappa_{i/e} \ \nabla_x \Phi, \\
&X(0) = X_f, \ V(0) = V_f.
\end{aligned}$$

The Liouville theorem implies that the distribution function of the particles is a Maxwellian along all the trajectories which come from infinity and 0 elsewhere. The conservation of the total energy gives

$$V(t)^2 + \frac{2q_{i/e}\Phi(X(t))}{m_{i/e}} = V_f^2 + \frac{2q_{i/e}\Phi(X_f)}{m_{i/e}}.$$

Consider a trajectory such that $\lim_{t\to\infty; X(t)\in\mathcal{T}_{i/e}^{back}(X_f,V_f)} \|X(t)\| = +\infty$. Then $\Phi(X(t)) = 0$ and,

$$V(t) = \sqrt{V_f^2 + \frac{2q_{i/e}}{m_{i/e}}\Phi(X_f)}.$$

Hence,

$$\begin{cases}
f_{i/e}(X_f, V_f) = g_{i/e}\Big(\sqrt{V_f^2 + \dfrac{2q_{i/e}}{m_{i/e}}\Phi(X_f)}\Big), & \lim\limits_{t\to\infty; X(t)\in\mathcal{T}_{i/e}^{back}(X_f,V_f)} \|X(t)\| = +\infty, \\
f_{i/e}(X_f, V_f) = 0 \quad \text{else.}
\end{cases}$$

Let $\nu_{i/e}^{inf}(X_f)$ be the set of velocities V_f such that

$$\lim_{t\to\infty; X(t)\in T_{i/e}^{back}(X_f,V_f)} \|X(t)\| = +\infty,$$

for a given X_f.
So,

$$f_{i/e}(X_f,V_f) = g_{i/e}\Big(\sqrt{V_f^2 + \frac{2q_{i/e}}{m_{i/e}}\Phi(X_f)}\Big)\ \mathbb{1}_{\{V_f\ \in\ \nu_{i/e}^{inf}(X_f)\}},$$

i.e.

$$\begin{aligned} f_e(X_f,V_f) &= g_e\Big(\sqrt{V_f^2 - \frac{2e}{m_e}\Phi(X_f)}\Big), \quad V_f.\gamma_\Omega > 0,\ V_f \in \nu_{i/e}^{inf}(X_f), \\ f_i(X_f,V_f) &= g_i\Big(\sqrt{V_f^2 + \frac{2e}{m_i}\Phi(X_f)}\Big), \quad \|V_f\| \geq \sqrt{\frac{-2e\Phi(X_f)}{m_i}} := v_{min},\ V_f \in \nu_{i/e}^{inf}(X_f). \end{aligned}$$

Remark 10.1.1
In the case of ions, when the potential is negative, the conservation of the total energy imposes that the velocity norm $\|V_f\|$ must be greater or equal to v_{min} if $V_f \in \nu_{i/e}^{inf}(X_f)$.

In order to compute the characteristic function $\mathbb{1}_{\{V_f\ \in\ \nu_{i/e}^{inf}(X_f)\}}$, we discretize the velocity space in spherical coordinates with V_γ (modulus), θ_γ, ϕ_γ (angles between the velocities and the normal vector γ to the surface of the satellite). The velocity V_f is taken as the mild value on the mesh cell in the velocity space. We numerically follow the particle trajectory. If this particle trajectory goes out through the fictitious sphere Γ_s, we consider that this particle comes from infinity and

$$\mathbb{1}_{\{V_f\ \in\ \nu_{i/e}^{inf}(X_f)\}} = 1.$$

If this particle comes from a boundary of the satellite, then

$$\mathbb{1}_{\{V_f\ \in\ \nu_{i/e}^{inf}(X_f)\}} = 0.$$

Why is this backtrajectories method interesting ?

The standard algorithm takes into account all the trajectories coming from infinity without distinction of those arriving on the satellite. Since we are

only interested by those arriving on the satellite (without reemission effects), it is no use computing the trajectories of particles which will never reach the satellite.
On the contrary, the back-trajectories algorithm only takes into account the trajectories coming from infinity and arriving on the satellite. By doing so, more prcision can be done in the zone where more precision is required.
The scheme 10.1 explains the difference between the direct and back-trajectories algorithms.

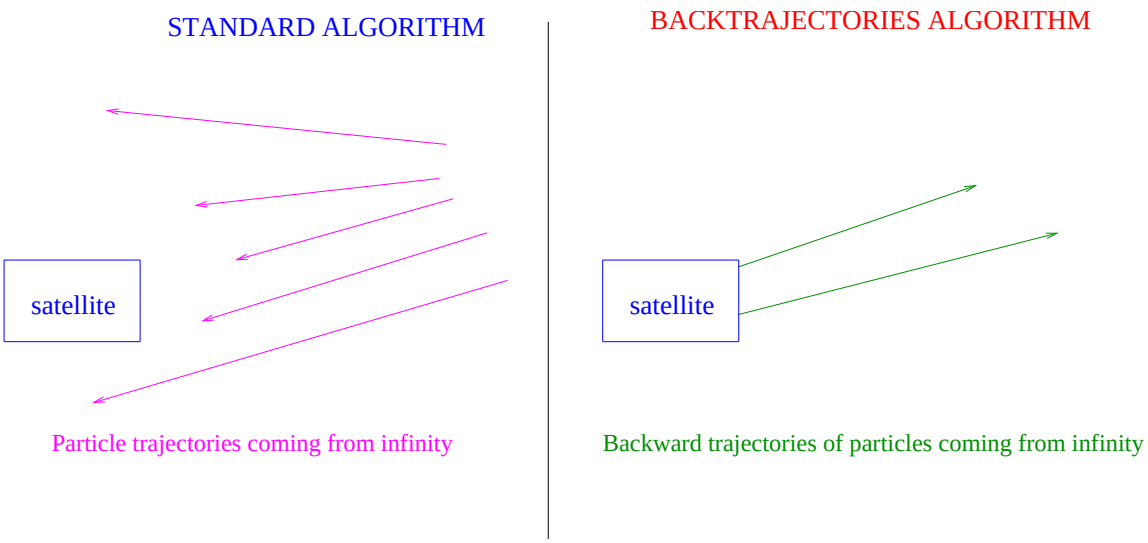

Figure 10.1: Standard algorithm and backtrajectories algorithm

10.2 Numerical approximation for the ion and the electron currents at the surface of the satellite

For a given point X_f on the surface of the satellite with a normal vector γ_Ω (directed inside the satellite), the currents (non dimensionless) received are

$$
\begin{aligned}
J_e(V_f) &= -\int_{V_f\in\mathbb{R}^3;V_f.\gamma_\Omega>0} e\ (V_f.\gamma_\Omega) f_e(X_f,V_f)\ dV_f,\\
J_i(V_f) &= \int_{V_f\in\mathbb{R}^3;V_f.\gamma_\Omega>0} e\ (V_f.\gamma_\Omega) f_i(X_f,V_f)\ dV_f.
\end{aligned}
$$

10.2.1 The ion current

The ion current writes as

$$
J_i(V_f) = e\, n_0 \left(\frac{m_i}{2\pi k T_e}\right)^{\frac{3}{2}} \exp\left(\frac{-e\Phi}{kT_e}\right) \int_{V_f\in\mathbb{R}^3;V_f\in\nu_i^{inf}(X_f)} (V_f.\gamma_\Omega)\ \exp\Big(-\frac{m_i V_f^2}{2kT_e}\Big)\ dV_f.
$$

By passing in spherical coordinates with V_γ (modulus), θ_γ, ϕ_γ (angles between the velocities and the normal vector γ to the surface of the satellite), we obtain that

$$
\begin{aligned}
J_i(V_f) = e\ n_0\ \left(\frac{m_i}{2\pi k T_e}\right)^{\frac{3}{2}} \exp\left(\frac{-e\Phi}{kT_e}\right) \int_{v_{min}}^{+\infty}\int_{-\frac{\pi}{2}}^{\frac{\pi}{2}}\int_{-\frac{\pi}{2}}^{\frac{\pi}{2}} V_\gamma^3 |\sin(\theta_\gamma)|\cos(\theta_\gamma)\times\\
\times \exp\Big(-\frac{m_i V_\gamma^2}{2kT_e}\Big)\ \mathbb{1}_{\{\nu_i^{inf}(r,\theta,\phi)\}}\ dV_\gamma d\theta_\gamma d\phi_\gamma.
\end{aligned}
$$

The discretization of the velocity space in spherical coordinates leads to

$$
\begin{aligned}
J_i \simeq e\ n_0\ \left(\frac{m_i}{2\pi k T_e}\right)^{\frac{3}{2}} \exp\left(\frac{-e\Phi}{kT_e}\right) \sum_{i_r=1}^{N_r}\sum_{i_\theta=1}^{N_\theta}\sum_{i_\phi=1}^{N_\phi} \int_{Vmod_1}^{Vmod_2}\int_{\theta_1}^{\theta_2}\int_{-\frac{\pi}{2}+\frac{i_\phi-1}{N_\phi}\pi}^{-\frac{\pi}{2}+\frac{i_\phi}{N_\phi}\pi} V_\gamma^3\times\\
\times \exp\Big(-\frac{m_i V_\gamma^2}{2kT_e}\Big) |\sin(\theta_\gamma)|\cos(\theta_\gamma)\ \mathbb{1}_{\{\nu_i^{inf}(r,\theta,\phi)\}}\ d\theta_\gamma\ d\phi_\gamma\ dV_\gamma,
\end{aligned}
$$

where

$$\begin{aligned}
V_i^{th} &= \sqrt{\frac{kT_e}{m_i}} \\
v_{min} &= \sqrt{\frac{-2e\Phi}{m_i}}, \\
v_{max} &= 5\ V_i^{th}, \\
Vmod_1 &= \frac{i_r - 1}{N_r}(v_{max} - v_{min}) + v_{min}, \\
Vmod_2 &= \frac{i_r}{N_r}(v_{max} - v_{min}) + v_{min}, \\
\theta_1 &= -\frac{\pi}{2} + \frac{i_\theta - 1}{N_\theta}\pi, \\
\theta_2 &= -\frac{\pi}{2} + \frac{i_\theta}{N_\theta}\pi.
\end{aligned}$$

10.2.2 The electron current

The electron current writes as

$$J_e(V_f) = -\ e\ n_0 \left(\frac{m_e}{2\pi kT_e}\right)^{\frac{3}{2}} \exp\left(\frac{e\Phi}{kT_e}\right) \int_{V_f \in \mathbb{R}^3; V_f.\gamma_\gamma > 0} (V_f.\gamma_\Omega)\ \exp\Big(-\frac{m_e V_f^2}{2kT_e}\Big)\ dV_f.$$

Passing in spherical coordinates,

$$\begin{aligned}
J_e(V_f) = -e\ n_0 \left(\frac{m_e}{2\pi kT_e}\right)^{\frac{3}{2}} \exp\left(\frac{e\Phi}{kT_e}\right) \int_0^{+\infty} \int_{-\frac{\pi}{2}}^{\frac{\pi}{2}} \int_{-\frac{\pi}{2}}^{\frac{\pi}{2}} V_\gamma^3 |\sin(\theta_\gamma)| \cos(\theta_\gamma) \times \\
\times \exp\Big(-\frac{m_e V_\gamma^2}{2kT_e}\Big)\ \mathbb{1}_{\{\nu_i^{inf}(r,\theta,\phi)\}}\ dV_\gamma d\theta_\gamma d\phi_\gamma.
\end{aligned}$$

By discretizing the velocity space and performing similar computations as for J_i, we obtain

$$\begin{aligned}
J_e \simeq -e\ n_0 \left(\frac{m_e}{2\pi kT_e}\right)^{\frac{3}{2}} \exp\left(\frac{e\Phi}{kT_e}\right) \sum_{i_r=1}^{N_r} \sum_{i_\theta=1}^{N_\theta} \sum_{i_\phi=1}^{N_\phi} \int_{Vmod_1}^{Vmod_2} \int_{\theta_1}^{\theta_2} \int_{-\frac{\pi}{2}+\frac{i_\phi - 1}{N_\phi}\pi}^{-\frac{\pi}{2}+\frac{i_\phi}{N_\phi}\pi} V_\gamma^3 \times \\
\times \exp\Big(-\frac{m_e V_\gamma^2}{2kT_e}\Big) |\sin(\theta_\gamma)| \cos(\theta_\gamma)\ \mathbb{1}_{\{\nu_i^{inf}(r,\theta,\phi)\}}\ d\theta_\gamma\ d\phi_\gamma\ dV_\gamma,
\end{aligned}$$

where

$$
\begin{aligned}
V_e^{th} &= \sqrt{\frac{kT_e}{m_e}}, \\
v_{min} &= 0, \\
v_{max} &= 5\ V_e^{th}, \\
Vmod_1 &= \frac{i_r - 1}{N_r}(v_{max} - v_{min}) + v_{min}, \\
Vmod_2 &= \frac{i_r}{N_r}(v_{max} - v_{min}) + v_{min}, \\
\theta_1 &= -\frac{\pi}{2} + \frac{i_\theta - 1}{N_\theta}\pi, \\
\theta_2 &= -\frac{\pi}{2} + \frac{i_\theta}{N_\theta}\pi.
\end{aligned}
$$

Chapter 11

Analytical computations of the charge density in the whole space for a sphere

Contents

11.1 Computations of the electron and ion densities . 121

11.1.1 Electron density 121

11.1.2 Trapping case 125

11.1.3 Untrapping case 133

11.2 The Charge density and the asymptotic behaviour 133

11.2.1 Trapping case 135

11.2.2 Untrapping case 137

11.3 Curves 139

11.3.1 Untrapping case 139

11.3.2 Trapping case 140

In order to understand why we neglect the charge density near the satellite, we are interested in the charge around a sphere. In this case, we are able to compute an analytical expression of the charge density ρ in the whole space. The aim of this chapter is to compute the charge density ρ around a sphere with radius R for a given potentiel field Φ.
When there is no reemission, the potential Φ is monotonous, so that there is no potential barrier.

When there is a potential barrier, we can perform similar computations but they are more complicated.
The potential Φ is assumed to be negative, so that the ions are attracted and the electrons are repulsed. The case where $\Phi > 0$ is similar.
Denote by v_r (resp. $v_\perp$) the radial (resp. perpendicular) component of the particle velocity. Let $r_0 \geq R$. The space charge ρ is given by

$$\rho(r_0, \Phi(r_0)) = \frac{e}{\epsilon_0}(n_e(r_0, \Phi(r_0)) - n_i(r_0, \Phi(r_0))).$$

The particle trajectories can easily be parametrized from the conservation of the total energy and the momentum. More precisely, by writing the conservation of the total energy and momentum, we obtain

$$\begin{cases} \frac{1}{2}v_r^2(r) + \frac{1}{2}v_\perp^2(r) \ + \frac{q_{i/e}}{m_{i/e}} \ \Phi(r) = \frac{1}{2}v_r^2(r_0) + \frac{1}{2}v_\perp^2(r_0) \ + \frac{q_{i/e}}{m_{i/e}} \ \Phi(r_0), \\ v_\perp^2(r_0) = \frac{R^2}{r_0^2} \ v_\perp^2(r). \end{cases}$$

A relation between the radius and the square of the radial velocity is obtained,

$$v_r^2(r) = -\frac{r_0^2}{r^2} \ v_{\perp_0}^2 - \frac{2q_{i/e}\Phi(r)}{m_{i/e}} + v_{r_0}^2 + v_{\perp_0}^2 + \frac{2q_{i/e}\Phi(r_0)}{m_{i/e}}. \qquad (11.1)$$

When there is no potential barrier, a particle can reach the radius r if and only if $v_r^2(r) > 0$ as this point. By using this argument for $r = R$ and $r = \infty$, five types of trajectories are determined depending on their starting and final points. They can be described as,

- $v_r^2(R) > 0$ and $v_r^2(\infty) > 0$. For
  - $v_r(R) > 0$, it corresponds to the satellite-infinity trajectories, denoted by $S \to \infty$,
  - $v_r(R) < 0$, it corresponds to the infinity-satellite trajectories, denoted by $\infty \to S$,
- $v_r^2(R) < 0$ and $v_r^2(\infty) < 0$, then it corresponds to trapped ions which orbit around the satellite without meet it,
- $v_r^2(R) > 0$ and $v_r^2(\infty) < 0$, then it corresponds to the satellite-satellite trajectories, denoted by $S \to S$,

- $v_r^2(R) < 0$ and $v_r^2(\infty) > 0$, then it corresponds to the infinity-infinity trajectories, denoted by $\infty \to \infty$.

Only the trajectories of the second and the last type correspond to the trajectories of the particles coming from infinity, so that their distribution function is not equal to 0. They will be the only ones of interest for the explicit computation of the densities.

11.1 Computations of the electron and ion densities

11.1.1 Electron density

We have the following result.

Lemma 11.1.1
Assume that the satellite is a sphere of radius R. Then the electron density writes as

$$n_e(r_0, \Phi(r_0)) = n_0 \ \exp(\frac{e\Phi(r_0)}{kT}) - \frac{n_0}{2} \ \exp(\frac{e\Phi(r_0)}{kT}) \Big[1 - erf\sqrt{\frac{e}{kT}(\Phi(r_0) - \Phi(R))}\Big]$$
$$+ \frac{n_0}{2} \ \exp(\frac{e\Phi(r_0)}{kT}) \ \exp\Big(\frac{e}{kT} \ \frac{(\Phi(r_0) - \Phi(R))}{(\frac{r_0^2}{R^2} - 1)}\Big) \sqrt{1 - \frac{R^2}{r_0^2}}$$
$$\times \Big[1 - erf\sqrt{\frac{r_0^2}{r_0^2 - R^2} \ \frac{e}{kT}(\Phi(r_0) - \Phi(R))}\Big].$$

Proof of lemma 11.1.1.

The velocity diagram for the electrons is represented in picture 11.1.

The electron density at r_0 is

$$n_e(r_0, \Phi(r_0)) = \int_{v \in I\!R^3} 1\!\!1_{\{f_e \neq 0\}} \ g_e\Big(\sqrt{v_{r_0}^2 + v_{\perp_0}^2 - \frac{2e}{m_e}\Phi(r_0)}\Big) \ d^3v,$$

where g_e is the Maxwellian defined by

$$g_e(v) = n_0\Big(\frac{m_e}{2\pi kT}\Big)^{\frac{3}{2}} exp\Big(-\frac{1}{2}\frac{m_e v^2}{kT}\Big).$$

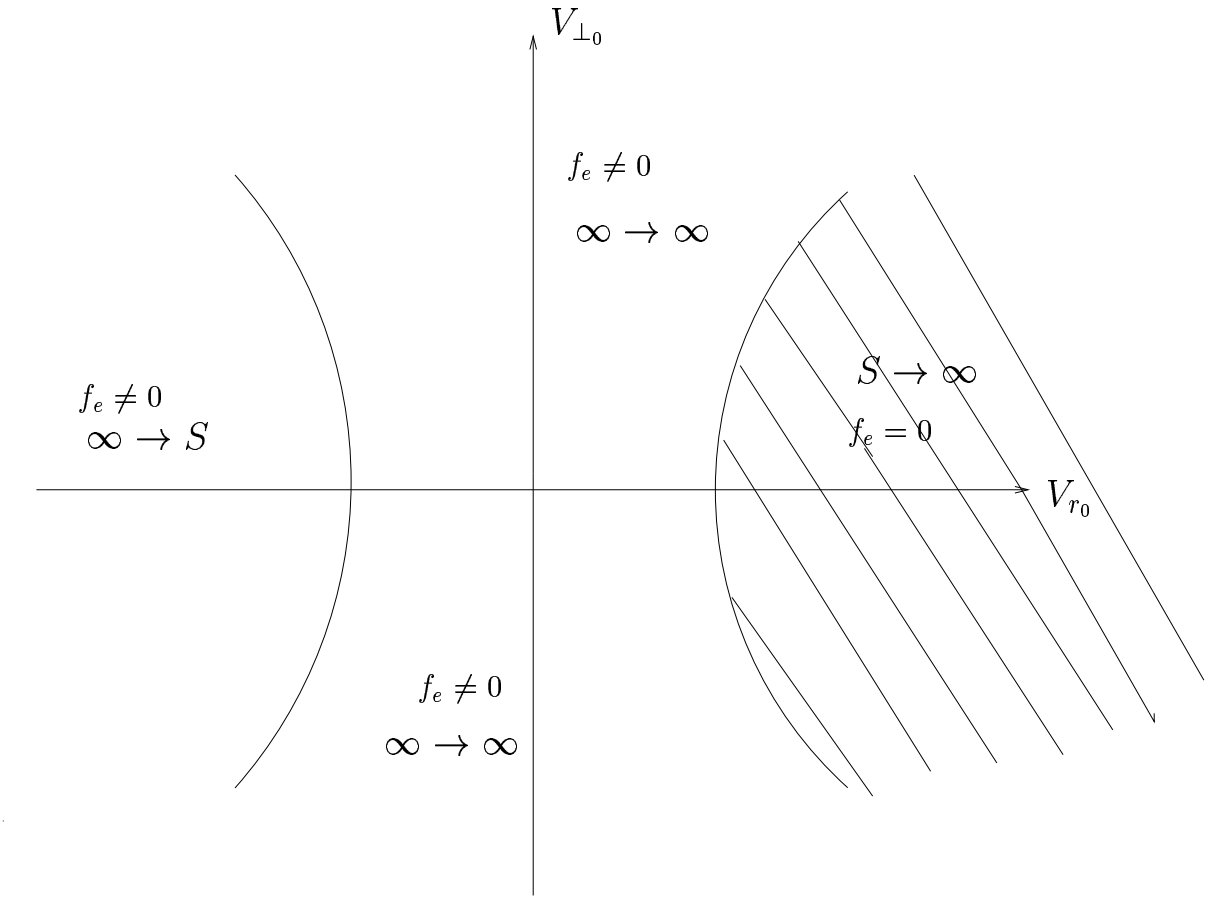

Figure 11.1: Velocity diagram for electrons

The electron distribution function f_e is not zero when

$$\left\{ \begin{array}{c} \text{either } v_{r_0} \leq 0, \\ \text{or} \left\{ \begin{array}{l} v_{r_0}^2 + \Big(1 - \dfrac{r_0^2}{R^2}\Big) v_{\perp_0}^2 + \dfrac{2e}{m_e}(\Phi(R) - \Phi(r_0)) < 0, \\ 0 \leq v_{r_0} \leq \sqrt{-\dfrac{2e}{m_e}(\Phi_c - \Phi(r_0))}. \end{array} \right. \end{array} \right. \tag{11.2}$$

The electron density becomes

$$n_e(r_0, \Phi(r_0)) = \int_{v \in I\!R^3} g_e\Big(\sqrt{v^2 - \frac{2e}{m_e}\Phi(r_0)}\Big)\ d^3v - \int_{\mathcal{J}} g_e\Big(\sqrt{v_{r_0}^2 + v_{\perp_0}^2 - \frac{2e}{m_e}\Phi(r_0)}\Big)\ d^3v,$$

where

$$\mathcal{J} = \Big\{ v \in I\!R^3;\ v_{r_0}^2 + \Big(1 - \frac{r_0^2}{R^2}\Big) v_{\perp_0}^2 + \frac{2e}{m_e}(\Phi(R) - \Phi(r_0)) > 0 \text{ and } v_{r_0} > \sqrt{-\frac{2e}{m_e}(\Phi_c - \Phi(r_0))} \Big\}.$$

Then

$$\begin{aligned} n_e(r_0, \Phi(r_0)) &= n_0 \Big(\frac{m_e}{2\pi kT}\Big)^{\frac{3}{2}} \exp(\frac{e\Phi(r_0)}{kT}) \int_{v \in I\!R^3} \exp(-\frac{1}{2}\frac{m_e}{kT} v^2)\ d^3v \\ &\quad - n_0 \Big(\frac{m_e}{2\pi kT}\Big)^{\frac{3}{2}} \exp(\frac{e\Phi(r_0)}{kT}) \int_{\mathcal{J}} \exp(-\frac{1}{2}\frac{m_e}{kT} v_{r_0}^2)\ \exp(-\frac{1}{2}\frac{m_e}{kT} v_{\perp_0}^2)\ dv_{r_0} d^2 v_{\perp_0} \\ &\quad = A - B, \end{aligned}$$

with

$$\begin{aligned} A &= n_0 \Big(\frac{m_e}{2\pi kT}\Big)^{\frac{3}{2}} \exp(\frac{e\Phi(r_0)}{kT}) \int_{v \in I\!R^3} \exp(-\frac{1}{2}\frac{m_e}{kT} v^2)\ d^3v, \\ B &= n_0 \Big(\frac{m_e}{2\pi kT}\Big)^{\frac{3}{2}} \exp(\frac{e\Phi(r_0)}{kT}) \int_{\mathcal{J}} \exp(-\frac{1}{2}\frac{m_e}{kT} v_{r_0}^2)\ \exp(-\frac{1}{2}\frac{m_e}{kT} v_{\perp_0}^2)\ dv_{r_0} d^2 v_{\perp_0}. \end{aligned}$$

Passing in spherical coordinates,

$$A = n_0\ \exp(\frac{e\Phi(r_0)}{kT}). \tag{11.3}$$

Computations of B.

$$B = n_0\Big(\frac{m_e}{2\pi kT}\Big)^{\frac{3}{2}} \exp(\frac{e\Phi(r_0)}{kT}) \int_{\sqrt{-\frac{2e}{m_e}(\Phi(R)-\Phi(r_0))}}^{\infty} \exp(-\frac{1}{2}\frac{m_e}{kT}v_{r_0}^2) \times \int_{\mathcal{I}} \exp(-\frac{1}{2}\frac{m_e}{kT}v_{\perp_0}^2)\ d^2v_{\perp_0}\ dv_{r_0},$$

where

$$\mathcal{I} = \Big\{ v_{\perp_0} \in I\!R^2; |v_{\perp_0}| < \sqrt{\frac{v_{r_0}^2 + \frac{2e}{m_e}(\Phi(R)-\Phi(r_0))}{\Big(\frac{r_0^2}{R^2}-1\Big)}} \Big\}.$$

Passing in polar coordinates with respect to $v_{\perp_0}$, B writes as

$$B = 2\pi\ n_0\Big(\frac{m_e}{2\pi kT}\Big)^{\frac{3}{2}} \exp(\frac{e\Phi(r_0)}{kT}) \int_{\sqrt{-\frac{2e}{m_e}(\Phi(R)-\Phi(r_0))}}^{\infty} \exp(-\frac{1}{2}\frac{m_e}{kT}v_{r_0}^2)\ U(v_{r_0})\ dv_{r_0},$$

where

$$U(v_{r_0}) = \int_0^{\sqrt{\frac{v_{r_0}^2+\frac{2e}{m_e}(\Phi(R)-\Phi(r_0))}{\left(\frac{r_0^2}{R^2}-1\right)}}} |v_{\perp_0}|\ \exp(-\frac{1}{2}\frac{m_e}{kT}|v_{\perp_0}|^2)\ d|v_{\perp_0}|.$$

The change of variables $u = \sqrt{\frac{m_e}{2kT}}\ |v_{\perp_0}|$ in $U(v_{r_0})$ leads to

$$U(v_{r_0}) = \frac{kT}{m_e}\ \Big[1 - \exp\Big(-\frac{m_e}{2kT}\ \frac{v_{r_0}^2 + \frac{2e}{m_e}(\Phi(R)-\Phi(r_0))}{\Big(\frac{r_0^2}{R^2}-1\Big)}\Big)\Big].$$

Thus

$$B = 2\pi\ n_0\Big(\frac{m_e}{2\pi kT}\Big)^{\frac{3}{2}}\Big(\frac{kT}{m_e}\Big) \exp(\frac{e\Phi(r_0)}{kT})\ \Big[A_1 - \exp\Big(\frac{e}{kT}\ \frac{\Phi(r_0)-\Phi(R)}{(\frac{r_0^2}{R^2}-1)}\Big)\ A_2\Big],$$

with

$$A_1 = \int_{\sqrt{-\frac{2e}{m_e}(\Phi(R)-\Phi(r_0))}}^{+\infty} \exp(-\frac{1}{2}\frac{m_e}{kT}v_{r_0}^2)\ dv_{r_0},$$

$$A_2 = \int_{\sqrt{-\frac{2e}{m_e}(\Phi(R)-\Phi(r_0))}}^{+\infty} \exp\Big(-\frac{m_e}{2kT}v_{r_0}^2(1+\frac{R^2}{r_0^2-R^2})\Big)\ dv_{r_0}.$$

So,

$$B = \frac{n_0}{2}\ \exp(\frac{e\Phi(r_0)}{kT})\Big[1 - erf\sqrt{\frac{e}{kT}(\Phi(r_0) - \Phi(R))}\Big] - \frac{n_0}{2}\ \exp(\frac{e\Phi(r_0)}{kT})$$
$$\times \exp\Big(\frac{e}{kT}\ \frac{(\Phi(r_0) - \Phi(R))}{(\frac{r_0^2}{R^2} - 1)}\Big)\sqrt{1 - \frac{R^2}{r_0^2}}\ \Big[1 - erf\sqrt{\frac{r_0^2}{r_0^2 - R^2}\ \frac{e}{kT}(\Phi(r_0) - \Phi(R))}\Big]. \tag{11.4}$$

(11.3) and (11.4) lead to the result. □

Remark 11.1.1 *When* $r_0 \to R$,

$$n_e(r_0, \Phi(r_0)) \to n_e(R) := \frac{n_0}{2}\ \exp(\frac{e\Phi(R)}{kT}).$$

We focus now on ions. Contrary to the electrons, we have a circle and an hyperbola for the ion velocities. There are two different cases : the case where four points of intersection between the circle and the hyperbole exist and the case where there is no point of intersection.

11.1.2 Trapping case

We have the following result

Lemma 11.1.2
Assume that the satellite is a sphere of radius R. Then the ion density is

$$n_i(r_0, \Phi(r_0)) = n_0\Big[\frac{1}{\sqrt{\pi}}\sqrt{\frac{-e\Phi(r_0)}{kT}} + \frac{1}{2}\ \exp(\frac{-e\Phi(r_0)}{kT})\ \Big(1 - erf\sqrt{\frac{-e\Phi(r_0)}{kT}}\Big)$$
$$+ \frac{1}{2}\ \exp(\frac{-e\Phi(r_0)}{kT})\ \exp\Big(\frac{e}{kT}\ \frac{\Phi(R) - \Phi(r_0)}{(\frac{r_0^2}{R^2} - 1)}\Big)\ \times\ \sqrt{1 - \frac{R^2}{r_0^2}}$$
$$+\ \frac{1}{\sqrt{\pi}}\ \sqrt{\frac{e}{kT}\ \Big(\frac{R^2}{r_0^2}\ \Phi(R) - \Phi(r_0)\Big)}$$
$$-\ \frac{1}{2}\ \sqrt{1 - \frac{R^2}{r_0^2}}\ \exp(\frac{-e\Phi(r_0)}{kT})\ \exp\Big(-\frac{e}{kT}\ \frac{\Phi(r_0) - \Phi(R)}{(\frac{r_0^2}{R^2} - 1)}\Big)\ \times$$
$$\times\ erf\sqrt{\frac{e}{kT}\ \frac{r_0^2}{r_0^2 - R^2}\ \Big(\frac{R^2}{r_0^2}\ \Phi(R) - \Phi(r_0)\Big)}\Big],\ when\ \frac{R^2}{r_0^2}\ \Phi(R) > \Phi(r_0).$$

Proof of the lemma.

The ion density at r_0 is

$$n_i(r_0, \Phi(r_0)) = \int_{v \in I\!R^3} 1\!\!1_{\{f_i \neq 0\}}\ g_i\Big(\sqrt{v_{r_0}^2 + v_{\perp_0}^2 + \frac{2e}{m_i}\Phi(r_0)}\Big)\ d^3v,$$

The ion distribution function f_i is not vanish when

$$\begin{cases} v_{r_0}^2 + \Big(1 - \dfrac{r_0^2}{R^2}\Big) v_{\perp_0}^2 + \dfrac{2e}{m_e}(\Phi(r_0) - \Phi(R)) < 0, \\ \text{and } v_{r_0}^2 + v_{\perp_0}^2 + \dfrac{2e}{m_i}\Phi(r_0) > 0 \text{ and } v_{r_0} \geq 0,\ r_0 \geq R. \end{cases} \tag{11.5}$$

Let $\mathcal{C}$ be the circle with equation

$$v_{r_0}^2 + v_{\perp_0}^2 + \frac{2e}{m_i}\Phi(r_0) = 0,$$

and $\mathcal{H}$ the hyperbola with equation

$$v_{r_0}^2 + \Big(1 - \frac{r_0^2}{R^2}\Big) v_{\perp_0}^2 + \frac{2e}{m_i}(\Phi(r_0) - \Phi(R)) = 0.$$

The coordinates of the 4 points of intersection of the circle $\mathcal{C}$ and the hyperbola $\mathcal{H}$ are

$$\begin{aligned} v_{r_0} &= \pm\sqrt{\frac{2e}{m_i}\ \Big(\frac{R^2}{r_0^2}\ \Phi(R) - \Phi(r_0)\Big)}, \quad \text{when } \frac{R^2}{r_0^2}\ \Phi(R) > \Phi(r_0), \\ v_{\perp_0} &= \pm\sqrt{-\frac{2e}{m_i}\ \frac{R^2}{r_0^2}\ \Phi(R)}. \end{aligned}$$

The velocity diagram for ions is the following

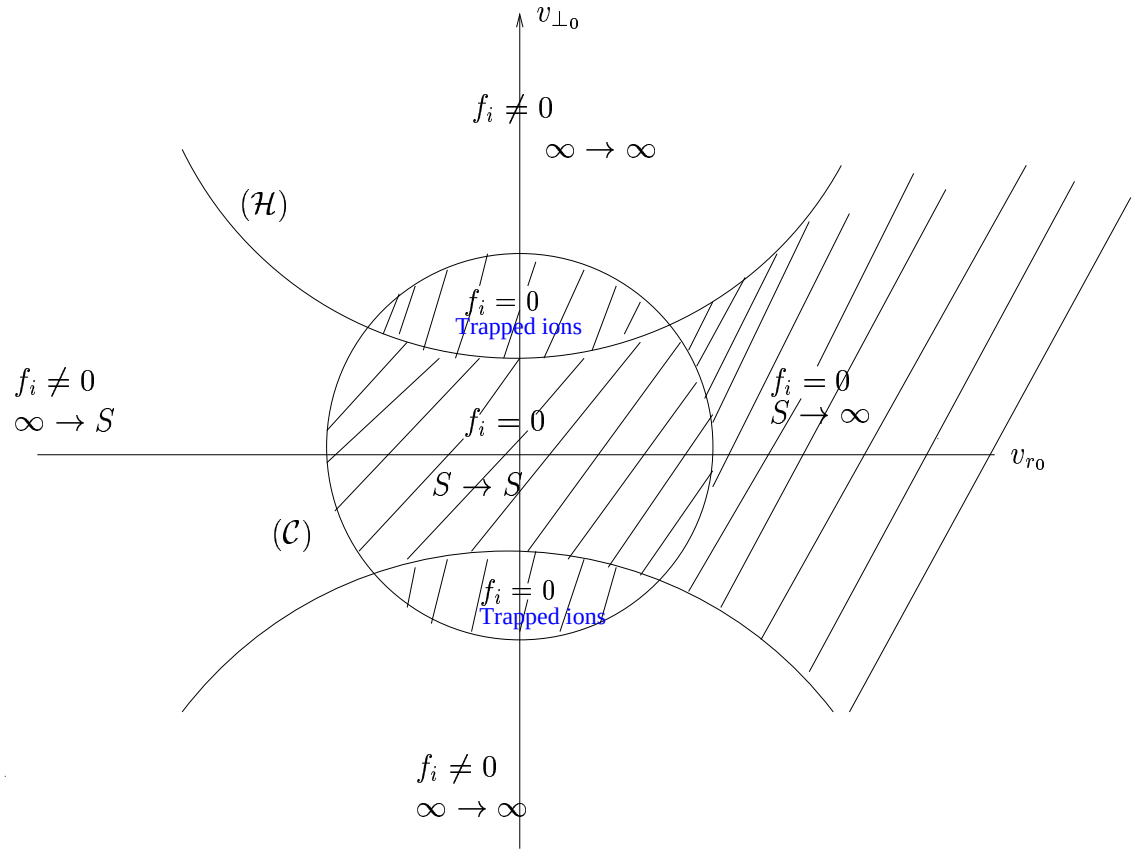

Figure 11.2: Velocity diagram for ions

The ion density at r_0 is

$$\begin{aligned} n_i(r_0, \Phi(r_0)) &= \int_{v \in I\!R^3;\ v^2 + \frac{2e}{m_i}\Phi(r_0) > 0} g_i\Big(\sqrt{v^2 + \frac{2e}{m_i}\Phi(r_0)}\Big)\ d^3v \\ &\quad - \int_{\mathcal{G}} g_i\Big(\sqrt{v_{r_0}^2 + v_{\perp_0}^2 + \frac{2e}{m_i}\Phi(r_0)}\Big)\ d^3v, \\ &= A - B, \end{aligned}$$

with

$$\begin{aligned} \mathcal{G} = \Big\{ v \in I\!R^3;\ & v_{r_0}^2 + \Big(1 - \frac{r_0^2}{R^2}\Big) v_{\perp_0}^2 + \frac{2e}{m_e}(\Phi(r_0) - \Phi(R)) > 0, \\ & v_{r_0}^2 + v_{\perp_0}^2 + \frac{2e}{m_i}\Phi(r_0) > 0, \quad v_{r_0} \geq 0 \Big\}, \end{aligned}$$

and

$$\begin{aligned} A &= \int_{v \in I\!R^3;\ v^2 + \frac{2e}{m_i}\Phi(r_0) > 0} g_i\Big(\sqrt{v^2 + \frac{2e}{m_i}\Phi(r_0)}\Big)\ d^3v, \\ B &= \int_{\mathcal{G}} g_i\Big(\sqrt{v_{r_0}^2 + v_{\perp_0}^2 + \frac{2e}{m_i}\Phi(r_0)}\Big)\ d^3v = C + D. \end{aligned}$$

Here,

$$\begin{aligned} C &= \int_{\mathcal{Q}} g_i\Big(\sqrt{v^2 + \frac{2e}{m_i}\Phi(r_0)}\Big)\ d^3v, \\ D &= \int_{\mathcal{R}} g_i\Big(\sqrt{v^2 + \frac{2e}{m_i}\Phi(r_0)}\Big)\ d^3v, \end{aligned}$$

with

$$\mathcal{Q} = \Big\{ v \in I\!R^3; \quad v_{r_0}^2 + \Big(1 - \frac{r_0^2}{R^2}\Big) v_{\perp_0}^2 + \frac{2e}{m_e}(\Phi(r_0) - \Phi(R)) > 0,$$

$$v_{r_0} \geq \sqrt{\frac{-2e\Phi(r_0)}{m_i}} \geq 0 \Big\},$$

$$\mathcal{R} = \Big\{ v \in I\!R^3; \quad v_{r_0}^2 + \Big(1 - \frac{r_0^2}{R^2}\Big) v_{\perp_0}^2 + \frac{2e}{m_e}(\Phi(r_0) - \Phi(R)) > 0,$$

$$\sqrt{\frac{2e}{m_i}\,\Big(\frac{R^2}{r_0^2}\,\Phi(R) - \Phi(r_0)\Big)} \leq v_{r_0} \leq \sqrt{\frac{-2e\Phi(r_0)}{m_i}},$$

$$v_{\perp_0}^2 \geq -v_{r_0}^2 - \frac{2e}{m_i}\Phi(r_0) > 0 \Big\}$$

The picture 11.3 explains the sets $\mathcal{Q}$ and $\mathcal{R}$.

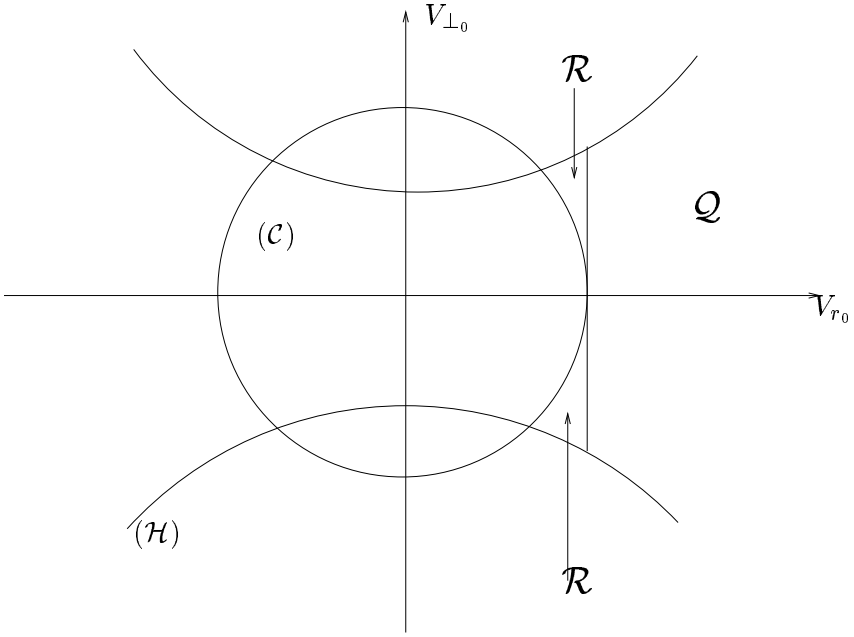

Figure 11.3: The sets $\mathcal{Q}$ and $\mathcal{R}$

Passing in spherical coordinates,

$$A \;=\; 4\pi\; n_0\; \Big(\frac{m_i}{2\pi kT}\Big)^{3/2}\; \exp(-\frac{e\Phi(r_0)}{kT})\; A_1,$$

where

$$\begin{aligned} A_1 \;&=\; \int_{\sqrt{-\frac{2e\Phi(r_0)}{m_i}}}^{+\infty} \;\; |v|^2\; \exp(-\frac{1}{2}\frac{m_i}{kT}v^2)\; d|v| \\ &=\; \Big(\frac{2kT}{m_i}\Big)^{3/2}\Big[\frac{1}{2}\sqrt{-\frac{e\Phi(r_0)}{kT}}\exp(\frac{e\Phi(r_0)}{kT}) + \frac{\sqrt{\pi}}{4}\Big(1 - erf\sqrt{-\frac{e\Phi(r_0)}{kT}}\Big)\Big], \end{aligned}$$

and

$$erf(x) = \frac{2}{\sqrt{\pi}}\int_0^x e^{-t^2}\; dt.$$

Then

$$A = 2\; n_0\; \Big[\frac{1}{\sqrt{\pi}}\;\sqrt{-\frac{e\Phi(r_0)}{kT}} + \frac{1}{2}\;\exp(-\frac{e\Phi(r_0)}{kT})\;\Big(1 - erf\sqrt{\frac{-e\Phi(r_0)}{kT}}\Big)\Big]. \quad (11.6)$$

Computations of C.

C can be written as

$$C = \int_{\mathcal{Q}} g_i\Big(\sqrt{v_{r_0}^2 + v_{\perp_0}^2 + \frac{2e}{m_i}\Phi(r_0)}\Big)\; d^3v,$$

Passing in spherical coordinates,

$$\begin{aligned} C \;&=\; 2\pi\; n_0\; \Big(\frac{m_i}{2\pi kT}\Big)^{3/2} \exp(\frac{-e\Phi(r_0)}{kT}) \int_{\sqrt{\frac{-2e\Phi(r_0)}{m_i}}}^{+\infty} \;\; \exp(-\frac{1}{2}\frac{m_i}{kT}v_{r_0}^2) \\ &\times\; \int_0^{\sqrt{\frac{v_{r_0}^2 + \frac{2e}{m_i}(\Phi(r_0)-\Phi(R))}{\left(\frac{r_0^2}{R^2}-1\right)}}} \;\; |v_{\perp_0}|\; \exp\Big(-\frac{1}{2}\frac{m_i}{kT}\;|v_{\perp_0}|^2\Big)\; d|v_{\perp_0}|\; dv_{r_0} \\ &=\; 2\pi\; n_0\; \Big(\frac{m_i}{2\pi kT}\Big)^{3/2} \exp(\frac{-e\Phi(r_0)}{kT}) \int_{\sqrt{\frac{-2e\Phi(r_0)}{m_i}}}^{+\infty} \;\; \exp(-\frac{1}{2}\frac{m_i}{kT}v_{r_0}^2)\; A_2\; dv_{r_0}, \end{aligned}$$

with

$$\begin{aligned} A_2 \;&=\; \int_0^{\sqrt{\frac{v_{r_0}^2 + \frac{2e}{m_i}(\Phi(r_0)-\Phi(R))}{(\frac{r_0^2}{R^2}-1)}}} \;\; |v_{\perp_0}|\; \exp\,(-\frac{1}{2}\frac{m_i}{kT}\;v_{|\perp_0}|^2)\; d|v_{\perp_0}| \\ &=\; \Big(\frac{kT}{m_i}\Big)\;\Big[1 - \exp\Big(-\frac{m_i}{kT}\;\frac{v_{r_0}^2 + \frac{2e}{m_i}(\Phi(r_0)-\Phi(R))}{(\frac{r_0^2}{R^2}-1)}\Big)\Big]. \end{aligned}$$

Thus

$$C = 2\pi n_0 \Big(\frac{m_i}{2\pi kT}\Big)^{3/2} \Big(\frac{kT}{m_i}\Big) \exp(\frac{-e\Phi(r_0)}{kT}) \Big[A_3 - \exp\Big(\frac{e}{kT}\ \frac{\Phi(R)-\Phi(r_0)}{(\frac{r_0^2}{R^2}-1)}\Big)\ A_4\Big],$$

with

$$\begin{aligned} A_3 &= \int_{\sqrt{\frac{-2e\Phi(r_0)}{m_i}}}^{+\infty} \exp(-\frac{1}{2}\frac{m_i}{kT} v_{r_0}^2)\ dv_{r_0}, \\ A_4 &= \int_{\sqrt{\frac{-2e\Phi(r_0)}{m_i}}}^{+\infty} \exp\Big(-\frac{1}{2}\frac{m_i}{kT}\ v_{r_0}^2\ (\frac{r_0^2}{r_0^2-R^2})\Big)\ dv_{r_0}. \end{aligned}$$

Finally,

$$\begin{aligned} C = n_0\ \Big[\frac{1}{2}\ \exp(\frac{-e\Phi(r_0)}{kT})\ \Big(1 - erf\sqrt{\frac{-e\Phi(r_0)}{kT}}\Big) - \frac{1}{2}\exp(\frac{-e\Phi(r_0)}{kT}) \\ \times \exp\Big(\frac{e}{kT}\ \frac{\Phi(R)-\Phi(r_0)}{(\frac{r_0^2}{R^2}-1)}\Big)\sqrt{1-\frac{R^2}{r_0^2}}\ \Big(1 - erf\sqrt{\frac{r_0^2}{r_0^2-R^2}\times\frac{-e\Phi(r_0)}{kT}}\Big)\Big] \end{aligned} \tag{11.7}$$

Computations of D.

It holds that

$$\begin{aligned} D = n_0\ \Big(\frac{m_i}{2\pi kT}\Big)^{3/2} \exp(\frac{-e\Phi(r_0)}{kT}) \int_{\sqrt{\frac{2e}{m_i}\ (\frac{R^2}{r_0^2}\ \Phi(R)-\Phi(r_0))}}^{\sqrt{\frac{-2e\Phi(r_0)}{m_i}}} \exp(-\frac{1}{2}\frac{m_i}{kT} v_{r_0}^2) \\ \times \int_{\mathcal{R}} \exp(-\frac{1}{2}\frac{m_i}{kT} v_{\perp_0}^2)\ d^2 v_{\perp_0}\ dv_{r_0}, \end{aligned}$$

Passing in polar coordinates with respect to $v_{\perp_0}$, we obtain

$$D = 2\pi n_0 \Big(\frac{m_i}{2\pi kT}\Big)^{3/2} \exp(\frac{-e\Phi(r_0)}{kT}) \int_{\sqrt{\frac{2e}{m_i}\ (\frac{R^2}{r_0^2}\ \Phi(R)-\Phi(r_0))}}^{\sqrt{\frac{-2e\Phi(r_0)}{m_i}}} \exp(-\frac{1}{2}\frac{m_i}{kT} v_{r_0}^2) U(v_{r_0})\ dv_{r_0},$$

where

$$\begin{aligned} U(v_{r_0}) &= \int_{\sqrt{-v_{r_0}^2 - \frac{2e}{m_i}\Phi(r_0)}}^{\sqrt{\frac{v_{r_0}^2 + \frac{2e}{m_i}(\Phi(r_0)-\Phi(R))}{(\frac{r_0^2}{R^2}-1)}}} |v_{\perp_0}|\ \exp(-\frac{1}{2}\frac{m_i}{kT} v_{\perp_0}^2)\ dv_{\perp_0}, \\ &= \frac{kT}{m_i}\Big[\exp(\frac{e\Phi(r_0)}{kT} + \frac{1}{2}\frac{m_i}{kT} v_{r_0}^2) - \exp\Big(-\frac{1}{2}\frac{m_i}{kT}\ \frac{v_{r_0}^2 + \frac{2e}{m_i}(\Phi(r_0)-\Phi(R))}{(\frac{r_0^2}{R^2}-1)}\Big)\ \Big]. \end{aligned}$$

Then

$$D = n_0 \left(\frac{m_i}{2\pi kT}\right)^{3/2} 2\pi \exp(\frac{-e\Phi(r_0)}{kT}) \left(\frac{kT}{m_i}\right) \times [V(r_0) - W(r_0)],$$

with

$$V(r_0) = \int_{\sqrt{\frac{2e}{m_i}(\frac{R^2}{r_0^2}\ \Phi(R)-\Phi(r_0))}}^{\sqrt{\frac{-2e\Phi(r_0)}{m_i}}} \exp(-\frac{1}{2}\frac{m_i}{kT}v_{r_0}^2) \quad \exp(\frac{e\Phi(r_0)}{kT} + \frac{1}{2}\frac{m_i}{kT}v_{r_0}^2)\ dv_{r_0}$$

$$W(r_0) = \int_{\sqrt{\frac{2e}{m_i}(\frac{R^2}{r_0^2}\ \Phi(R)-\Phi(r_0))}}^{\sqrt{\frac{-2e\Phi(r_0)}{m_i}}} \exp(-\frac{1}{2}\frac{m_i}{kT}v_{r_0}^2) \quad \exp\Big(-\frac{1}{2}\frac{m_i}{kT}\ \frac{v_{r_0}^2 + \frac{2e}{m_i}(\Phi(r_0)-\Phi(R))}{(\frac{r_0^2}{R^2}-1)}\Big)\ dv_{r_0}.$$

So,

$$V(r_0) = \exp(\frac{e\Phi(r_0)}{kT})\Big[\sqrt{-\frac{2e}{m_i}\Phi(r_0)} - \sqrt{\frac{2e}{m_i}\ \Big(\frac{R^2}{r_0^2}\Phi(R) - \Phi(r_0)\Big)}\ \Big].$$

Performing the change of variables $u = \sqrt{\frac{1}{2}\frac{m_i}{kT}\frac{r_0^2}{r_0^2 - R^2}}\ v_{r_0}$ in $W(r_0)$, we obtain

$$W(r_0) = \frac{1}{2}\sqrt{\frac{2\pi kT}{m_i}\Big(1-\frac{R^2}{r_0^2}\Big)}\ \exp\Big(-\frac{e}{kT}\ \frac{\Phi(r_0)-\Phi(R)}{(\frac{r_0^2}{R^2}-1)}\Big)$$
$$\times \Big[erf\sqrt{-\frac{e\Phi(r_0)}{kT}\ \frac{r_0^2}{r_0^2-R^2}} - erf\sqrt{\frac{e}{kT}\ \frac{r_0^2}{r_0^2-R^2}\ \Big(\frac{R^2}{r_0^2}\ \Phi(R)-\Phi(r_0)\Big)}\ \Big].$$

Thus,

$$\begin{aligned} D = n_0 \Big[&\frac{1}{\sqrt{\pi}}\sqrt{\frac{-e\Phi(r_0)}{kT}} - \frac{1}{\sqrt{\pi}}\sqrt{\frac{e}{kT}\ \Big(\frac{R^2}{r_0^2}\Phi(R)-\Phi(r_0)\Big)} \\ &- \frac{1}{2}\sqrt{1-\frac{R^2}{r_0^2}}\exp\Big(-\frac{e\Phi(r_0)}{kT} - \frac{e}{kT}\frac{\Phi(r_0)-\Phi(R)}{(\frac{r_0^2}{R^2}-1)}\Big) erf\sqrt{-\frac{e\Phi(r_0)}{kT}\ \frac{r_0^2}{r_0^2-R^2}} \\ &+ \frac{1}{2}\sqrt{1-\frac{R^2}{r_0^2}}\ \exp\Big(-\frac{e\Phi(r_0)}{kT} - \frac{e}{kT}\frac{\Phi(r_0)-\Phi(R)}{(\frac{r_0^2}{R^2}-1)}\Big) \\ &\times erf\sqrt{\frac{e}{kT}\ \frac{r_0^2}{r_0^2-R^2}\ \Big(\frac{R^2}{r_0^2}\Phi(R)-\Phi(r_0)\Big)}\ \Big]. \end{aligned} \tag{11.8}$$

Since $n_i(r_0, \Phi(r_0)) = A - C - D$, and thanks to (11.6)-(11.7)-(11.8) that

$$n_i(r_0,\Phi(r_0)) = n_0\Big[\frac{1}{\sqrt{\pi}}\sqrt{\frac{-e\Phi(r_0)}{kT}} + \frac{1}{2}\ \exp(\frac{-e\Phi(r_0)}{kT})\ \Big(1 - erf\sqrt{\frac{-e\Phi(r_0)}{kT}}\Big)$$
$$+ \frac{1}{2}\ \exp(\frac{-e\Phi(r_0)}{kT})\ \exp\Big(\frac{e}{kT}\ \frac{\Phi(R)-\Phi(r_0)}{(\frac{r_0^2}{R^2}-1)}\Big)\ \times\ \sqrt{1-\frac{R^2}{r_0^2}}$$
$$+\ \frac{1}{\sqrt{\pi}}\sqrt{\frac{e}{kT}\ \Big(\frac{R^2}{r_0^2}\ \Phi(R) - \Phi(r_0)\Big)} -\ \frac{1}{2}\sqrt{1-\frac{R^2}{r_0^2}}\ \exp(\frac{-e\Phi(r_0)}{kT})$$
$$\times\ \exp\Big(-\frac{e}{kT}\ \frac{\Phi(r_0)-\Phi(R)}{(\frac{r_0^2}{R^2}-1)}\Big)\ erf\sqrt{\frac{e}{kT}\ \frac{r_0^2}{r_0^2-R^2}\ \Big(\frac{R^2}{r_0^2}\ \Phi(R) - \Phi(r_0)\Big)}\Big].$$

□

11.1.3 Untrapping case

The diagram 11.4 is used to locate the velocities where f_i is not zero. The computations for getting the untrapped ion density are similar as the computations for the trapped ion density. They lead to the following formula.

Lemma 11.1.3
Assume that the satellite is a sphere of radius R. Then the ion density is

$$n_i(r_0,\Phi(r_0)) = n_0\Big[\frac{1}{\sqrt{\pi}}\sqrt{-\frac{e\Phi(r_0)}{kT}} + \frac{1}{2}\ \exp(-\frac{e\Phi(r_0)}{kT})\Big(1 - erf\sqrt{-\frac{e\Phi(r_0)}{kT}}\Big)\Big]$$
$$+\ \frac{n_0}{2}\ \exp(-\frac{e\Phi(r_0)}{kT})\sqrt{1-\frac{R^2}{r_0^2}}\ \exp\Big(-\frac{e}{kT}\ \frac{(\Phi(r_0)-\Phi(R))}{(\frac{r_0^2}{R^2}-1)}\Big).$$

11.2 The Charge density and the asymptotic behaviour

In this section, we deal with the charge density for trapped ions, untrapped ions and their asymptotic behaviour. The asymptotic behaviour of ρ will be used in chapter 12.

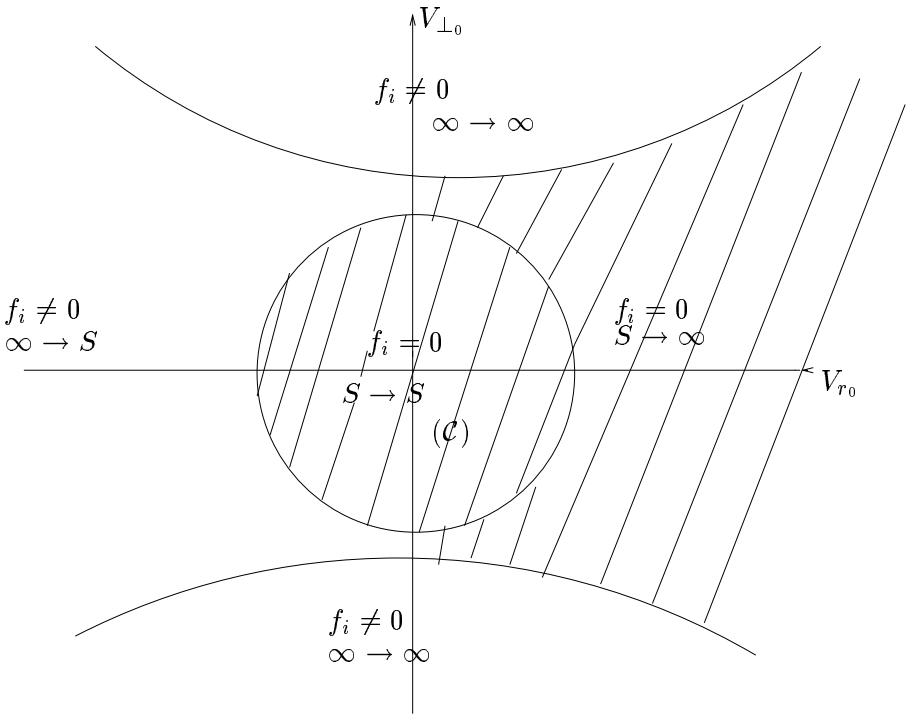

Figure 11.4: Velocity diagram for the ions

11.2.1 Trapping case

Thanks to Lemmas 11.1.1 and 11.1.2, the space charge ρ in the whole space writes as

$$\begin{aligned}
\rho(r_0,\Phi) = \frac{e\ n_0}{\epsilon_0}\Big[&\frac{1}{2}\exp(\frac{e\Phi}{kT})\Big(1 - erf\sqrt{\frac{e}{kT}(\Phi-\Phi(R))}\\
&+\exp\Big(\frac{e}{kT}\ \frac{(\Phi-\Phi(R))}{(\frac{r_0^2}{R^2}-1)}\Big)\sqrt{1-\frac{R^2}{r_0^2}}\\
&\times\Big(1 - erf\sqrt{\frac{r_0^2}{r_0^2-R^2}\ \frac{e}{kT}(\Phi-\Phi(R))}\Big)\Big)\\
&-\frac{1}{\sqrt{\pi}}\sqrt{\frac{-e\Phi}{kT}} - \frac{1}{2}\ \exp(\frac{-e\Phi}{kT})\ \Big(1 - erf\sqrt{\frac{-e\Phi}{kT}}\Big)\\
&-\frac{1}{2}\ \exp(\frac{-e\Phi}{kT})\ \exp\Big(\frac{e}{kT}\ \frac{\Phi(R)-\Phi}{(\frac{r_0^2}{R^2}-1)}\Big)\ \sqrt{1-\frac{R^2}{r_0^2}}\\
&-\ \frac{1}{\sqrt{\pi}}\ \sqrt{\frac{e}{kT}\ \Big(\frac{R^2}{r_0^2}\ \Phi(R)-\Phi\Big)}\\
&+\ \frac{1}{2}\ \sqrt{1-\frac{R^2}{r_0^2}}\ \exp(\frac{-e\Phi}{kT})\ \exp\Big(-\frac{e}{kT}\ \frac{\Phi-\Phi(R)}{(\frac{r_0^2}{R^2}-1)}\Big)\\
&\times\ erf\sqrt{\frac{e}{kT}\ \frac{r_0^2}{r_0^2-R^2}\ \Big(\frac{R^2}{r_0^2}\ \Phi(R)-\Phi\Big)}\Big]
\end{aligned} \tag{11.9}$$

When $r_0 \to +\infty$ and for a given Debye length λ_d, the potential Φ such that

$$\rho(r_0,\Phi) = 0,$$

is an asymptotic solution. Indeed, the dimensionless Poisson equation when $r_0 \to +\infty$ and for a given Debye length λ_d writes as

$$\begin{cases} \dfrac{\lambda_d^2}{L^2}\ \Delta_{\tilde{x}}\tilde{\Phi} = \tilde{\rho}, \quad \tilde{x}\in\Omega^c, \\ \tilde{\Phi} = \tilde{\Phi}_c \ \text{ on } \Gamma_{c-v}, \\ \tilde{\Phi}\to 0 \ \text{ at infinity}, \end{cases} \tag{11.10}$$

where the dimensionless quantities are

$$\tilde{x} = \frac{x}{L},\ \eta = \frac{L}{\lambda_d},\ \lambda_d = \sqrt{\frac{\epsilon_0\ kT_e}{n_0\ e^2}}.$$

Here, L is the reference length of the region of the space that we interest.

Since L is larger than the Debye length at infinity, the term $\frac{\lambda_d^2}{L^2}\ \Delta_{\tilde{x}}\tilde{\Phi}$ vanishes and $\tilde{\rho}(\tilde{\Phi}) \to 0$.

The asymptotic behaviour for ρ when Φ is small and $r_0 \to \infty$ is studied as follows.

The following approximations are used.

(i) $\Phi(r_0)$ is negligible with respect to $\Phi(R)$ in the term $\exp\Big(\frac{e}{kT}\ \frac{(\Phi - \Phi(R))}{(\frac{r_0^2}{R^2} - 1)}\Big)$,

(ii) $erf\sqrt{x} \sim \frac{2}{\sqrt{\pi}}\sqrt{x}$ when $x \to 0$.

Let $\phi = -\frac{e\Phi(r_0)}{kT},\ \phi_c = -\frac{e\Phi(R)}{kT}$.

Performing an expansion of the space charge ρ when ϕ is small and $r_0 \to \infty$, we obtain after some computations that

$$\rho(r_0,\phi) = -e\ n_0\Big[\frac{1}{\sqrt{\pi}}\Big(-\frac{R^2}{r_0^2}\ \phi_c + \phi\Big)^{3/2} + 2\Big(\phi - \frac{R^2}{2r_0^2}\ \phi_c\Big) + \frac{1}{2}\frac{R^2}{r_0^2}\ \phi_c\ erf\sqrt{\phi_c}\Big] + o\Big(\phi, \frac{1}{r_0^2}\Big),$$

when $\frac{R^2}{r_0^2}\ \phi_c < \phi$.

Notice that there is no analytical solution ϕ to $\rho(r_0,\phi) = 0$.

11.2.2 Untrapping case

Thanks to Lemmas 11.1.1 and 11.1.3, the space charge ρ in the whole space writes as

$$\begin{aligned}\rho(r_0,\Phi) = \frac{e}{\epsilon_0}\frac{n_0}{2}\Big[&\exp(\frac{e\Phi}{kT})\Big(1 - erf\sqrt{\frac{e}{kT}(\Phi(r_0)-\Phi(R))}\\ &+ \exp\Big(\frac{e}{kT}\ \frac{(\Phi(r_0)-\Phi(R))}{(\frac{r_0^2}{R^2}-1)}\Big)\sqrt{1-\frac{R^2}{r_0^2}}\\ &\times\Big(1 - erf\sqrt{\frac{r_0^2}{r_0^2-R^2}\ \frac{e}{kT}(\Phi(r_0)-\Phi(R))}\Big)\Big)\\ &- \frac{2}{\sqrt{\pi}}\ \sqrt{-\frac{e\Phi}{kT}} - \exp(-\frac{e\Phi}{kT})\Big(1 - erf\sqrt{-\frac{e\Phi}{kT}}\Big)\\ &- \exp(-\frac{e\Phi}{kT})\sqrt{1-\frac{R^2}{r_0^2}}\ \exp\Big(-\frac{e}{kT}\ \frac{(\Phi-\Phi(R))}{(\frac{r_0^2}{R^2}-1)}\Big)\Big]\end{aligned} \tag{11.11}$$

J.F. Roussel in [37], I.B. Bernstein and I.N. Rabinowitz in [7], M.J.M. Parrot, L.R.O. Storey, L.W. Parker and J.G. Laframboise in [33] and [29] assumed without proving it that the potential Φ decreases as $\frac{1}{r^2}$ at infinity in the trapping case. This is proved by the following lemma.

Lemma 11.2.1
For r_0 large enough and for a potential Φ small enough, we are in the untrapping case and Φ behaves like $\frac{\Phi(R)\ R^2}{2\ r_0^2}$.

Proof.

As before, when $r_0 \to +\infty$ and for a given Debye length λ_d, the potential Φ such that

$$\rho(r_0,\Phi) = 0,$$

is a asymptotic solution.
For this purpose, the asymptotic behaviour of ρ when Φ is small and $r_0 \to \infty$ is studied as follows.

The same approximations as for the trapping case are used here.

Linearizing the space charge when Φ is small and $r_0 \to \infty$ lead to

$$\rho(r_0,\Phi) = \frac{e\ n_0}{\epsilon_0}\Big[- \frac{e\ \Phi(R)\ R^2}{kT\ r_0^2}\Big(1 - \frac{1}{2} erf\sqrt{-\frac{e\ \Phi(R)}{kT}}\Big) + 2\ \frac{e\Phi}{kT}\Big] + o\Big(\frac{1}{r_0^2},\Phi\Big), \tag{11.12}$$

when $\dfrac{e\Phi(r_0)}{kT} > \dfrac{e\Phi(R)R^2}{kT\ r_0^2}$. □

Consequently,

- Trapping case : if $\dfrac{R^2}{r_0^2}\ \Phi(R) > \Phi$, then

$$\rho(r_0,\Phi) = -\frac{e\ n_0}{\epsilon_0}\Big[\frac{1}{\sqrt{\pi}}\Big(\frac{R^2}{r_0^2}\ \frac{e\Phi(R)}{kT} - \frac{e\Phi}{kT}\Big)^{3/2} + 2\Big(- \frac{e\Phi}{kT} + \frac{R^2}{r_0^2}\ \frac{e\Phi(R)}{kT}\Big) - \frac{1}{2}\frac{R^2}{r_0^2}\ \frac{e\Phi(R)}{kT}\ erf\sqrt{-\frac{e\Phi(R)}{kT}}\Big] + o\Big(\frac{1}{r_0^2},\Phi\Big).$$

- Untrapping case : if $\dfrac{R^2}{r_0^2}\ \Phi(R) < \Phi$, then

$$\rho(r_0,\Phi) = \frac{e\ n_0}{\epsilon_0}\Big[-\frac{e\ \Phi(R)\ R^2}{kT\ r_0^2}\Big(1-\frac{1}{2} erf\sqrt{-\frac{e\ \Phi(R)}{kT}}\Big)+2\ \frac{e\Phi}{kT}\Big]+o\Big(\frac{1}{r_0^2},\Phi\Big).$$

Notice that in the trapping case, there is no analytical solution Φ to $\rho(r_0,\Phi) = 0$. Therefore, the untrapping case is obtained at infinity. More precisely, the solution of $\rho(r_0,\Phi) = 0$ at infinity is

$$\Phi(r_0) \sim \frac{\Phi(R)\ R^2}{2\ r_0^2}\Big(1 - \frac{1}{2} erf\sqrt{-\frac{e\ \Phi(R)}{kT}}\Big), \tag{11.13}$$

when Φ is small and $r_0 \to \infty$.

For small r_0, we have

$$\Phi(r_0) < \frac{\Phi(R)R^2}{r_0^2}, \tag{11.14}$$

and there are trapped ions. The condition (11.14) is satisfied in the case where there are trapped ions because for r_0 small, the dimensionless Poisson equation

gives that ρ is neglected (see chapter 8). Moreover, the solution of the Laplace equation,

$$\begin{cases} \Delta\Phi = 0, \quad \text{in } \Omega^c \\ \Phi = \Phi_c \quad \text{on} \quad \Gamma_{c-v}, \\ \Phi \to 0 \quad \text{at infinity} \end{cases}$$

is

$$\Phi(r_0) = \frac{\Phi_c R}{r_0}.$$

11.3 Curves

In this section, we draw the curve of ρ with respect to the radius in order to see its asymptotic behaviour.
The following numerical values are taken,

$kT = 10^4\ eV,\ \Phi_c := \Phi(R) = -25000\ V,\ n_0 = 10^6\ m^{-3},\ R = 1\ m,\ \lambda_d = 743\ m.$

11.3.1 Untrapping case

The exact potential for a sphere is $\Phi = \Phi(R)\ \dfrac{R}{r_0}$.

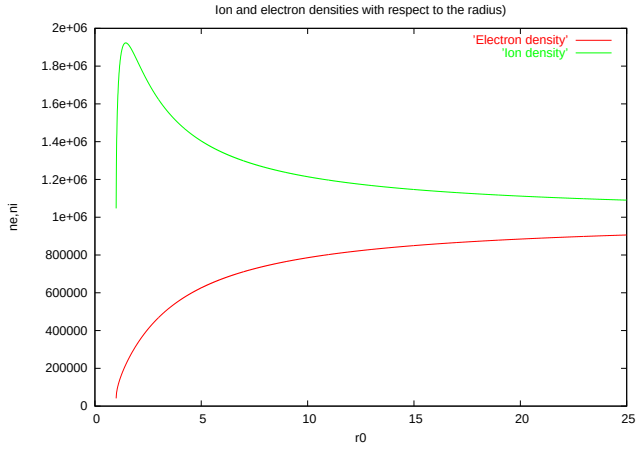

Figure 11.5: Ions and electrons densities

Picture 11.5 represents the ion (red curve) and electron (green curve) densities with respect to the radius (we are close to the satellite because $\lambda_d = 743$ and $R_\infty = 25$. We notice that the ion density presents a maximum before

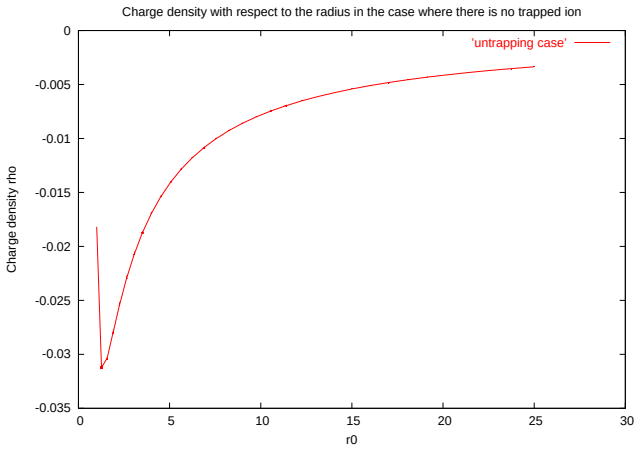

Figure 11.6: Space charge

tending to its value at infinity, whereas the electron density strictly increases to its value at infinity (case of a sphere charged negatively).

The curve in Picture 11.6 is the space charge ρ plotted with respect to the radius.

11.3.2 Trapping case

We plot here the analytical curve of ρ as well as the densities of ions and electrons with respect to the radius.

Picture 11.7 represents the trapped ion (green curve) and the electron (red curve) densities with respect to the radius. We notice that the ion density presents a maximum before tending to its value at infinity, whereas the electron density strictly increases to its value at infinity (case of a sphere charged negatively).

Picture 11.8 is the space charge ρ plotted with respect to the radius. The minimum of ρ for trapped ions is lower than the minimum of ρ in the previous case.

In the next chapter, we solve the Vlasov-Poisson system by taking into account the right-hand side ρ computed analytically before.

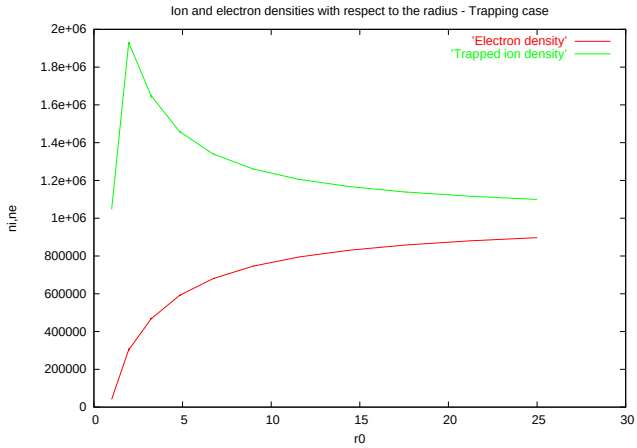

Figure 11.7: Ions and electrons densities

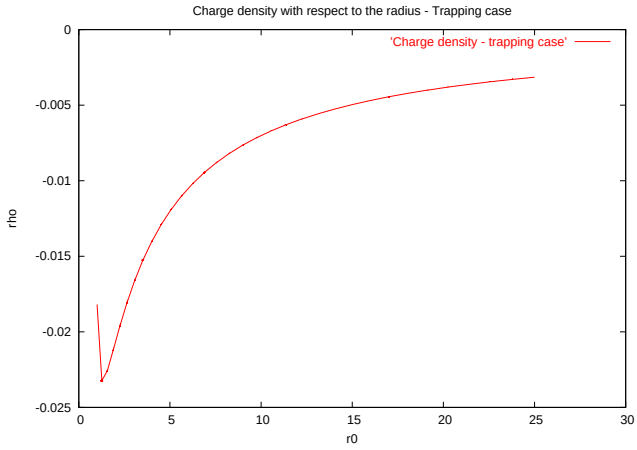

Figure 11.8: Space charge

Chapter 12

Solution of the stationary Vlasov-Poisson system

Contents

12.1 Solution of the Poisson equation 143

12.2 A new approach for the solution of the Poisson equation 144

12.3 Conclusion 148

In this chapter, we solve the Vlasov-Poisson system in the whole space for a sphere.

12.1 Solution of the Poisson equation

We keep the analytical expression of ρ found in chapter 11 in the right-hand side of the Poisson equation. To compute the potential Φ, the following system is solved,

$$\begin{cases} \Delta\Phi_{k+1}(r_0) = \rho(\Phi_k(r_0)), \quad r_0 > R, \\ \Phi_{k+1}(r_0) = \Phi_{k+1}(R) \text{ on } \Gamma_{c-v}, \\ \Phi_{k+1} \to 0 \text{ at infinity.} \end{cases} \tag{12.1}$$

At the first iteration, we solve

$$\begin{cases} \Delta\Phi_0(r_0) = 0, \quad r_0 > R, \\ \Phi_0 = \Phi_c \text{ on } \Gamma_{c-v}, \\ \Phi_0 \to 0 \text{ at infinity}, \end{cases} \tag{12.2}$$

which has a solution $\Phi_0(r) = \dfrac{\Phi_c\ R}{r}$.
At the second iteration, the problem to be solved is the following

$$\begin{cases} \Delta\Phi_1(r_0) = \rho(\Phi_0), \quad r_0 > R, \\ \Phi_1 = \Phi_c \quad \text{on } \Gamma_{c-v}, \\ \Phi_1 \to 0 \text{ at infinity}, \end{cases}$$

but this problem is not well posed because the decrease of the space charge ρ when $r_0 \to \infty$ is not fast enough to solve it.
Indeed, the asymptotic behaviour of ρ at infinity does not behave like $\dfrac{1}{r_0}$. The asymptotic development shows that if Φ behaves like $\dfrac{1}{r_0}$, then ρ behaves like $\dfrac{1}{r_0}$.

So, we introduce a new approach based on a relaxation method for the resolution of the Poisson equation.

12.2 A new approach for the solution of the Poisson equation

Let

$$f = \frac{e\ \Phi(r)}{kT}, \quad f_b = \frac{e\ \Phi_c}{kT}.$$

As recalled before, the resolution of the system (12.1) gives a solution which does not tend fast enough to zero when $r_0 \to \infty$.
To deal with this problem, we build a one-dimensional algorithm which takes into account the behaviour of ρ at infinity.
So, we solve the following relaxated three-dimensional spherical symmetry

equation with respect to the radial coordinate r.

$$\begin{cases} \dfrac{1}{r^2}\dfrac{d}{dr}\Big(r^2\dfrac{d}{dr}f^{k+1}(r)\Big) - \dfrac{2}{\lambda_d^2}\ f^{k+1}(r) = \rho(f^k(r)) - \dfrac{2}{\lambda_d^2}\ f^k(r), \\ f^{k+1}(R=1) = f_b, \\ \dfrac{\partial f^{k+1}}{\partial r} + \dfrac{1}{L}f^{k+1} = 0, \end{cases} \tag{12.3}$$

where L is the length of the mesh. It can be taken as equal to many Debye lengths.

The coefficient 2 in the term $\dfrac{2}{\lambda_d^2}\ f^{k+1}(r)$ comes from the asymptotic behaviour of ρ (for the case of a sphere). The following numerical values are taken

$$kT = 10^4\ eV,\ \Phi_c = -25000\ V,\ n_0 = 10^6\ m^{-3},\ R = 1\ m,\ f_b = -2.5.$$

The value $f_b = -2.5$ is closed to the equilibrium floating potential.
We use a finite difference method and we put the Robin condition at $r = L$. At the first iteration, we solve,

$$\begin{cases} \dfrac{1}{r^2}\dfrac{d}{dr}\Big(r^2\dfrac{d}{dr}f^0(r)\Big) - \dfrac{2}{\lambda_d^2}\ f^0(r) = 0, \\ f^0(1) = f_b, \\ \dfrac{\partial f^0}{\partial r} + \dfrac{1}{L}f^0 = 0. \end{cases} \tag{12.4}$$

The analytical solution is

$$f^0(r) = f_b\ \frac{e^{-\frac{\sqrt{2}}{\lambda_d}(r-1)}}{r}.$$

We plot on a same picture the numerical solution $f(r)$, the exact solution $f^0(r)$ to the Laplace equation (12.4) with relaxation, as well as the curve $\dfrac{f_b}{r}$ and $\dfrac{f_b}{2\ r^2}$ with respect to the radius r in logarithmic scale. We take different values for Debye length. We recall that $\dfrac{f_b}{r}$ is the solution to the Laplace equation (12.2) without the space charge and without relaxation and $\dfrac{f_b}{2\ r^2}$ is the solution to

$\rho(r, f(r)) = 0$ at infinity (see chapter 11).

- Case $\lambda_d = 100\ m$.

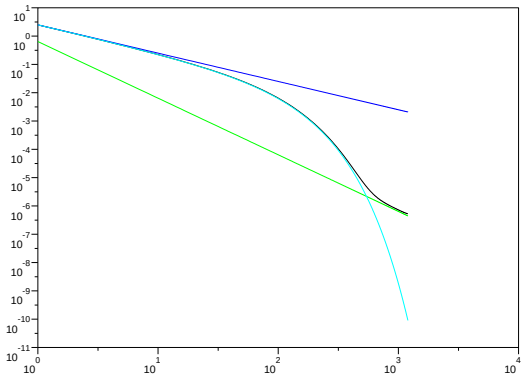

Figure 12.1: Numerical solution to the Poisson equation for $\lambda_d = 100\ m$

The black curve represents the solution f with respect to r. The blue curve is the function $r \to \frac{f_b}{r}$, which is the analytical solution of the Laplace equation without relaxation and without space charge ρ. The green curve is the function $r \to \frac{f_b}{2\ r^2}$ which is the solution of the equation (11.13) at infinity (case of untrapped ions) and the turquoise curve represents the function $f^0(r)$.

- Case $\lambda_d = 743\ m$.

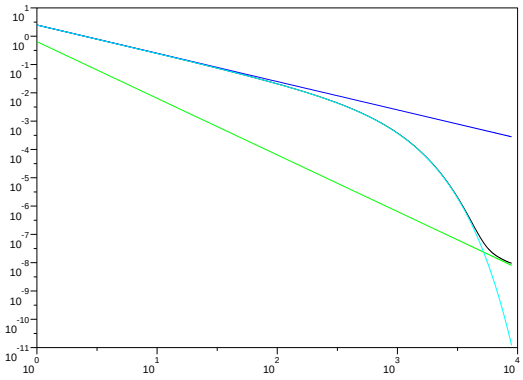

Figure 12.2: Numerical solution to the Poisson equation for $\lambda_d = 743\ m$

- Case $\lambda_d = 1\ m$.

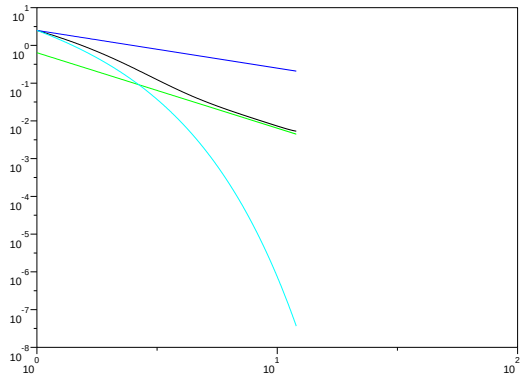

Figure 12.3: Numerical solution to the Poisson equation for $\lambda_d = 1\ m$

We notice that near the satellite, f is tangent to the solution $r \to \dfrac{f_b}{r}$ to the Laplace equation without relaxation. Moreover, f satisfies $-f(r) + \dfrac{f_b}{r^2} > 0$. At infinity, f behaves like the asymptotic solution $\dfrac{f_b}{2r^2}$.

As expected, there are trapped ions near the satellite (r small) i.e in the sheath and the space charge ρ is negligible, so that we solve the Laplace equation in the sheath.
There are untrapped ions at infinity and ρ is not negligible, so that we solve the equation $\rho(\Phi) = 0$ in the presheath.
Consequently, there is a transition between the trapping region and the untrapping region. The intersection between the curves $f^0(r)$ and $\frac{fb}{2r^2}$ gives the length of this transition. We notice on pictures 12.1-12.3 that the transition is over than one Debye length.

12.3 Conclusion

In this second part of the thesis, we have started to simplify the model of Vlasov-Poisson. We have neglected the space charge in the Poisson equation near the satellite, i.e. in the sheath.

For the resolution of the Laplace equation, we have used a finite element method inside the computational domain and infinite elements at infinity. The example of two localized points is a good validation of our choice for infinite element method to the computation of the potential.

In chapter 11, we have assumed that there is no potential barrier for the computation of the space charge. Numerical results show that this hypothesis is valid. As long as ρ has the same sign, no potential barrier can appear. Next, we have studied the asymptotic behaviour of ρ at infinity. By using the behaviour of ρ, we have built a new algorithm for the solution of the system of Vlasov-Poisson in the whole space and showed that it converges after 50 iterations.

Two zones of the space have been determined : the sheath (domain around the satellite) where there are trapped ions and the presheath where there is no trapped ions.
The space charge ρ is negligible in the sheath and not in the presheath.
In conclusion, we solve the Laplace equation in the sheath and the equation $\rho(\Phi) = 0$ in the presheath.

Part III

General conclusion and perspectives

Chapter 13

Part 1

In the first part of this thesis, we have studied a quantum kinetic homogeneous equation describing the Compton effect. This phenomenon takes place when photons interact with electrons. We have proven a local existence theorem for this equation.

One of the interesting perspectives of the quantum Boltzmann equation is the study of the formation and the evolution of Bose-Einstein condensates, a phenomenon that we briefly describe in this chapter.

13.1 Description of Bose-Einstein condensates

The Bose-Einstein condensate is a gaseous superfluid phase highlighted in 1920. Physicists like Satyendra Nath Bose and Albert Einstein were interested in the behaviour of matter at absolute zero. In 1924, Satyendra Nath Bose showed that it was possible to describe the light by the statistical evolution of a gas of particles, the photons. Albert Einstein generalized this theory to other entities. He highlighted the original behaviour of Bosons at very low temperatures. They have a collective behaviour and are in the same quantum state.

In 1995, an american team succeeded in confining thousands of atoms during a few minutes. Temperatures of the order of micro-kelvins were reached, which led to a Nobel price in 1997.

13.2 The first condensate

In 1995, one american team of Colorado, led by Eric Cornell and Carl Wieman, succeeded in obtaining during a few seconds the first Bose-Einstein condensate. It was constitued by around ten thousands atoms of Rubidium precooled by a laser. Next, they were again cooled by evaporation in a magnetic trap. So they reached a very low temperature close to absolute zero.

The rubidium was condensated in June 1995, then the lithium by a Houston team, then the sodium by MITT team.
Finally, many physicists succeeded in 1997 in producing a laser effect with the atoms. They first formed a condensate and next extracted a part of the condensated atomes.

13.3 Bose-Einstein condensates from a mathematical point of view

The Bose-Einstein condensates belong to the measure solutions studied in this thesis in the sense that they are recognized by a possible Dirac at 0 in the Lebesgue decomposition of these measures. In order to study them more precisely, it is convenient to separate this Dirac at zero energy from the rest of the solution. So, we can describe their evolution by coupling two equations. The Gross-Pitaevskii equation is a Schrödinger equation for the wave function of the condensates, whereas a quantum Boltzmann equation describes the distribution function of the part which is not condensated. W. Bao, L. Pareschi and P.A. Markowich studied this problem in [3].

Chapter 14

Part 2

In the second part of the thesis, we have solved the Vlasov-Poisson system by taking account the space charge in the whole space with a one-dimensional numerical model, in the case where there is no reemission. The obtained results are satisfying. Indeed, we can determine in which part of the plasma the trapped ions are. They are in the sheath. In the presheath, there are untrapped ions and the potential behaves like $1/r^2$ at infinity.

The first interesting perspective would be to numerically solve the Poisson equation, taking into account the space charge in the whole space with a three-dimensional model and for any geometry of the satellite. Indeed, the back-trajectories algorithm can be used not only to compute the currents but also to compute the space charge in the whole space. Then, using the algorithm of chapter 10, we can ensure the coupling of the Vlasov and Poisson equations. This point leads to an article in process.

The second interesting perspective would be to consider a more general distribution function of ion and electron. As an example, we can describe the plasma by a sum of two Maxwellians with hot and cold particles.

The third interesting perspective would be to take into account the reemission effect and the space charge in the resolution of the $3D$ Vlasov-Poisson system.

The last point is to take into account the artificial source plasma on the satellite in the resolution of the $3D$ Vlasov-Poisson system.

Bibliography

[1] H. Andreasson. Regularity of the gain term and strong L^1 convergence to equilibrium for the relativistic Boltzmann equation. *SIAM J. Math. Anal.*, 27(5):1386–1405, 1996.

[2] L. Arkeryd. On the strong L^1 trend to equilibrium for the Boltzmann equation. *Stud. Appl. Math.*, 87:283–288, 1992.

[3] W. Bao, L. Pareschi, and P.A. Markowich. Quantum kinetic theory : modelling and numerics for Bose-Einstein condensation. *Model. Simul. Sci. Eng. technol.*, pages 287–320, 2004.

[4] C. Bardos and P. Degond. Global existence for the Vlasov-Poisson equation in 3 space variables wit small initial data. *Ann. Inst. Henri Poincare*, 2:101–118, 1985.

[5] J. Batt, H. Berestycki, P. Degond, and B. Perthame. Some families of solutions of the Vlasov-Poisson system. *Arch. Rational Mech. Anal.*, 104:79–103, 1988.

[6] G. Beer and J.O. Watson. Infinite boundary elements. *Int. J. Num. Meth. Ing.*, 28:1233–1247, 1989.

[7] I.B. Bernstein and I.N. Rabinowitz. Theory of electrostatic probes in a low-density plasma. *Phys. Fluids*, 2(2), 1959.

[8] P. Bettess. Infinite elements. *International journal for numerical methods in engineering*, 11:53–64, 1977.

[9] P. Bettess. *Infinite elements.* Penshaw Press, 1992.

[10] T.Z. Boulmezaoud. Inverted finite elements : a new method for solving elliptic problems in unbounded domains. *preprint*, 2003.

[11] R. E. Caflish and C. D. Levermore. Equilibrium for radiation in a homogeneous plasma. *Phys. Fluids*, 29:748–752, 1986.

[12] M. Chane-Yook and A. Nouri. On a quantum kinetic equation linked to the Compton effect. *submitted*, 2003.

[13] O. Chanrion. *Simulation de l'influence de la propulsion plasmique sur la charge electrostatique d'un satellite en milieu magnetosphérique.* Thèse de doctorat, ENPC, 2001.

[14] S. Clerc, S. Brosse, and M. Chane-Yook. Sparcs : an advanced software for spacecraft charging analyses. *8th. Spacecraft Charging Tech. Conf., Huntsville, Alabama*, 2003.

[15] G. Cooper. Compton Fokker-Planck equation for hot plasma. *Phys. Rev*, D3:2412–2416, 1974.

[16] F. Demengel. Espaces de fonctions à dérivées mesure et théorème de compacité. *C. R. Acad. Sc. Paris*, 302(4), 1986.

[17] F. Demengel and R. Temam. Convex Functions of a measure and Applications. *Indiana Math. J.*, 33(5):673–709, 1984.

[18] R. Diperna and P.L. Lions. Solutions globales d'équations du type Vlasov-Poisson. *C.R. Acad. Sci. Paris*, 307-1:655–658, 1990.

[19] H. Dreicer. Kinetic theory of an electron-photon gas. *Phys. Fluids*, 7:735–753, 1964.

[20] M. Dudynski and M. Elkiel-Jezewska. Global existence proof for relativistic Bolzmann equation. *Journal of Statistical Physics*, 66(3/4), 1992.

[21] M. Escobedo and S. Mischler. Equation de Boltzmann quantique homogène : existence et comportement asymptotique. *C. R. Acad. Sci. Paris*, 329(I):593–598, 1999.

[22] M. Escobedo and S. Mischler. On a quantum Boltzmann equation for a gas of photons. *J. Math. Pures Appl.*, 80(5):471–515, 2001.

[23] M. Escobedo, S. Mischler, and M.A. Valle. Homogeneous Boltzmann equation for quantum and relativistic particles. *Electronic Journal of Differential Equations*, Monograph,4:85 pp, 2003.

[24] K. Gerdes and L. Demkowicz. Solution of 3d-Laplace and Helmholtz equations in exterior domains using hp-infinite elements. *Comput. Methods Appl. Mech. Engrg.*, 137:239–273, 1996.

[25] R.T. Glassey. *The Cauchy problem in kinetic theory.* SIAM, Philadelphia, 1996.

[26] R.T. Glassey and W.A. Strauss. Asymptotic stability of the relativistic Maxwellian. *Publ. Res. Inst. Math. Sciences, Kyoto University*, 29(2), 1993.

[27] S. R. Groot, W. A. Van Leeuwen, and Ch. G. Weert. *Relativistic Kinetic Theory.* North Holland Publishing Company, 1980.

[28] A. S. Kompaneets. The establishment of thermal equilibrium between quanta and electrons. *Soviet Physics JETP*, 1957.

[29] J.G. Laframboise. *Theory of spherical and cylindrical Langmuir probes in a collionless, Maxwellian plasma at rest.* Institute for Aerospace studies, University of Toronto, 1966.

[30] P.L Lions and B. Perthame. Régularité des solutions du système de Vlasov-Poisson en dimension 3. *C. R. Acad. Sci. Paris*, 311(I), 1990.

[31] X. Lu. A modified boltzmann equation for Bose-Einstein particles : isotropic solutions and long-time behavior. *Journal of Statistical Physics*, 98(5-6), 1999.

[32] V. Ougarov. *Théorie de la relativité restreinte.* Mir-Moscou, 2ème édition edition, 1976.

[33] M.J.M. Parrot, L.R.O. Storey, L.W. Parker, and J.G. Laframboise. Theory of cylindrical and spherical Langmuir probes in the limit of vanishing Debye number. *Phys. Fluids*, 25(12), 1982.

[34] D. Payan. *Charge électrostatique par électrons de haute énergie.* Cepadues Editions, Novembre 1990.

[35] K. Pfaffelmoser. Global classical solutions of the Vlasov-Poisson system in three dimension for general initial data. *Journal of Differential Equation*, 95-1:281–303, 1992.

[36] F. Poupaud. Solutions stationnaires des équations de Vlasov-Poisson. *C.R. Acad. Sci. Paris*, 311-1:307–312, 1990.

[37] J F. Roussel. Modelling of spacecraft plasma environment interactions. *ONERA/DESP Toulouse*, 1990.

[38] R.H. Stuewer. The Compton effect : Transition to quantum mechanics. *Ann. Phys. (Leipzig)*, 9(11–12):975–989, 2000.

[39] B. Wennberg. Stability and exponential convergence for the Boltzmann equation. *Arch. Rational Mech. Anal.*, 130, 1995.

[40] Ya. B. Zel'dovich and E. V. Levich. Bose condensation and shock waves in photon spectra. *Sov. Phys JETP*, 28:1287–1290, 1969.

Résumé

On s'est intéressé dans ce travail à l'étude de deux équations cinétiques.
La première est une équation cinétique quantique homogène décrivant l'effet Compton. Ce phénomène se produit lorsque les photons entrent en collision avec les électrons. Le noyau dans l'intégrale de collision présente une forte singularité en l'énergie nulle. Un résultat d'existence locale en temps d'une solution entropique au problème de Cauchy est obtenu pour de petites valeurs initiales.
La deuxième est une équation de Vlasov couplée avec l'équation de Poisson. Le système de Vlasov-Poisson modélise les interactions entre plasma et satellite. Plus précisément, on s'intéresse au phénomène de charge électrostatique d'un satellite en orbite géostationnaire. Les particules, essentiellement des ions et des électrons, sont décrites suivant une approche cinétique. On considère le cas où la dynamique des ions et des électrons obéit à une équation de Vlasov et où le potentiel est donné par l'équation de Poisson. Le but est d'étudier ce problème dans un cadre $3D$ dans tout l'espace. Une méthode particulaire pour la résolution de l'équation de Vlasov est couplée à une méthode d'éléments finis et infinis pour la partie Poisson.

Mots-clés : Equation de Boltzmann quantique, effet Compton, système de Vlasov-Poisson, méthode d'éléments finis et infinis, méthode des back-trajectories, phénomène de charge électrostatique

On a quantum kinetic linked to the Compton effect - Modelling and 3D simulation of the satellite charge in magnetospheric plasma

Abstract

This work deals with the study of two kinetic equations.
The first equation describes the interaction between photons and electrons, called the Compton effect. The kernel in the collision integral presents a strong singularity at energy zero. Existence results to the Cauchy problem are obtained for initial data small enough and locally in time.
The second equation is the Vlasov equation coupled with the Poisson equation. The Vlasov-Poisson system represents the interaction between the satellite and the magnetospheric plasma. More precisely, we are interested in the charge phenomenon of a satellite in geostationary orbit. The particles, mainly ions and electrons are described following a kinetic approach. The evolution of their distribution functions are ruled by the Vlasov equation which is coupled with the Poisson equation for the potential. The aim is to solve Vlasov-Poisson in a three-dimensional frame in the whole space. One particle method for the Vlaov equation resolution is coupled with a finite/infinite element method for the resolution of the Poisson equation.

Keywords : Quantum Boltzmann equation, Compton effect, Vlasov-Poisson system, finite and infinite element methods, back-trajectory method, electrostatic charging phenomenon

CMI, LATP, Université de Provence & INRIA Sophia Antipolis, projet CAIMAN.